



**TOWARDS A COMPREHENSIVE ASSESSMENT OF  
EXPOSURE TO SEA-LEVEL RISE AT CONTINENTAL SCALE**

**Dissertation**

**zur Erlangung des Doktorgrades der Mathematisch-  
Naturwissenschaftlichen-Fakultät der Christian-  
Albrechts-Universität zu Kiel**

**vorgelegt von  
Lena Reimann**

**Kiel, 2021**



**Cover page**

The Mediterranean region based on GHS-POP 2015 (Schiavina et al. 2019)

**Erster Gutachter: Prof. Dr. Athanasios T. Vafeidis**

**Zweiter Gutachter: Prof. Dr. Bryan Jones**

**Tag der mündlichen Prüfung: 23. April 2021**

gez. Prof. Dr. Frank Kempken



## ACKNOWLEDGMENTS

---

I have – finally – completed my PhD research, which has been a very intense, yet rewarding chapter in my life. I have learned incredibly much during this time and would like to thank everyone who has supported me along this journey.

First of all, I would like to thank you, Nassos, for taking me on as a PhD student. You gave me the opportunity to start a career in academia although I was a ‘high-risk candidate’. I enjoyed working with and learning from you, and I feel very well equipped for the next step in my career. Thanks to you, I could present my work at many international conferences that helped me build a scientific network. Also, I won’t forget the great time you showed us in Athens, from having dinner with a beautiful view over the city to crazy car rides with lots of honking and swearing (the Greek way).

I would also like to thank my second advisor, Bryan, who has done a great job welcoming me to New York. It was a pleasure learning from you – I very much enjoyed our white board brainstorming sessions as well as the conferences, workshops, and particularly the writing retreat I could join. Also, thanks for inviting me to your home and family, and the best Thanksgiving ever!

Special thanks also go to the Fulbright Commission that has supported my six-month research visit at the CUNY Institute for Demographic Research. During this time, I was able to gain first insights into research at a US university and collaborate with leading researchers in the field of demographic research. I would particularly like to thank Prof. Deborah Balk for her warm welcome, the classical music, and for showing me the best Indian lunch places.

Further, many thanks to my co-authors Jan-Ludolf Merkens, Sally Brown, Jochen Hinkel, Richard S.J. Tol, Theodore Nikolettopoulos, Bryan, and Nassos for their input, support, and feedback. Jorid Höffken and Nora Bieker, I would like to thank you for your help with all the data work.

Thank you also to my colleagues at the Coastal Risks and Sea-Level Rise research group. I really enjoyed working with you, discussing ideas, and exchanging travel stories. Special thanks go to my office mates Henrike (you supported me from Day 1), Tobias (I enjoyed being your secretary, especially when your dad called), and Bente (you became a close friend and I still owe you some vouchers). Thanks also to my other colleagues: Jan (I enjoyed the running practice with you although you overtook me about a hundred times), Claudia (thanks for a great time in Greece), Joshua (I am always happy to share my Brötchen or nuts with you), Sara (for keeping me company when it got late at the office), Leigh (for your Aussie charm), Barbara, Sunna, Jana, and Maureen.

Furthermore, I want to thank my friends who have supported me (and haven’t left me) during the last years: Julia and Frania, my climbing (and sauna, hiking, walking) friends, who distracted me from work and kept me sane. Catharina, we have been friends since we started our studies in Kiel (over 12 years!). Addi and Consti, thanks for many years of friendship and numerous relaxing evenings in Kiel’s Kneipen.

Außerdem möchte ich meiner Familie danken, die mich immer darin bestärkt hat, dass ich alles erreichen kann, was ich mir vornehme: insbesondere meiner Tante Gila, die schon vor der 1. Klasse an meine akademische Karriere geglaubt hat („der Professor“). Ich möchte auch Susanne, Hannes, Nici und Lasse danken, die mich vor über 15 Jahren als Mitglied in die Familie Lucas aufgenommen haben und mir die ein oder andere neue Sichtweise auf die Dinge eröffnet haben.

Ganz besonderer Dank gilt euch, Mama und Papa. Ohne euch wäre ich jetzt nicht hier. Ihr habt mich immer unterstützt, auch wenn ihr euch das ein oder andere Mal darüber gewundert habt, warum ich diesen Weg eingeschlagen habe. Ich bin stolz darauf eure Tochter zu sein. Das Gleiche gilt auch meiner Schwester Julia. Ich weiß, dass du dich immer um mich sorgst und stolz auf mich bist.

Mein größter Dank gilt aber dir, Jonas. Ohne dich hätte ich dieses Projekt wahrscheinlich nie gestartet (auch wenn du das abstreitest). Du hast mir das Selbstvertrauen gegeben, das ich gebraucht habe, hast mit mir auf unzähligen Reisen neue Energie getankt und warst immer für mich da, auch wenn wir 6000 km voneinander entfernt waren. Du diskutierst mit mir meine Ideen und Probleme, liest alle meine Texte gegen und erträgst meine Launen. Danke!

## SUMMARY

---

Coastal areas are increasingly at risk from coastal hazards due to sea-level rise (SLR), which will accelerate in the 21<sup>st</sup> century driven by anthropogenic climate change. Future coastal risks are not only driven by the amount of SLR, but also by a high concentration of population and assets in locations potentially exposed to SLR-related hazards. The uncertainty related to future SLR and socioeconomic development can be explored with the SSP-RCP scenario framework, which consists of physical scenarios (RCPs – Representative Concentration Pathways) and socioeconomic scenarios (SSPs – Shared Socioeconomic Pathways), and is increasingly used in coastal risk assessments at continental to global scales. Thus far, such assessments have primarily focused on characterizing future changes in SLR-related hazards in a spatially explicit manner, while research on the spatial representation of variables to characterize exposure (e.g. population, assets, infrastructure) to those hazards has been limited, in particular with regard to exploring plausible future changes under the SSPs. Previous work that has characterized exposure spatially has used global-scale data, modeling approaches, and scenario assumptions when assessing coastal risks at continental scale. Therefore, this thesis advances the spatial representation of exposure to SLR-related hazards at continental scale to facilitate assessment of future coastal risks in an integrated manner. It focuses on two exposure variables, i.e. population and cultural assets, using the Mediterranean region as a study area.

First, the global-scale SSP narratives are extended to the Mediterranean region, by including regional drivers of socioeconomic development, additionally differentiating northern versus southern and eastern countries of the region. The extended narratives are interpreted to develop spatial population projections for each SSP until 2100, accounting for the uncertainty related to future rural-urban and inland-coastal migration. Results show that the population potentially exposed to SLR-related hazards ranges from 34.1 million (SSP1) to 96.2 million (SSP3) in 2100, with marked differences across the Mediterranean. Comparison of these results with results based on the global SSPs shows a deviation of as much as 15% in the exposed population (SSP1), thereby spanning a wider range of uncertainty regarding population exposure. As this approach does not account for urban sprawl, a gravity-based modeling approach is developed, which allows for modeling urban sprawl as well as rural-urban and inland-coastal migration. The spatial population projections produced with this approach result in 51.3 million (SSP4) to 107.8 million (SSP3) people potentially exposed to SLR-related hazards in 2100. The results of the two approaches differ substantially, thereby stressing the need to consider the strengths and weaknesses of both approaches in future work.

For more comprehensive coastal risk assessments, additional exposure variables need to be considered. Therefore, a spatial database of cultural assets, an exposure variable not commonly analyzed due to a lack of high-resolution spatial data, is assembled by producing spatial representations (i.e. polygons) of 49 UNESCO World Heritage Sites (WHS) located in low-lying coastal areas of the Mediterranean. A first application of the database in a continental-scale assessment shows that, already under current conditions, 75% and 85% of the WHS are at risk from coastal flooding and erosion, respectively. Both risks will increase until 2100, depending on the SLR scenario considered, with considerable differences between WHS and across the Mediterranean basin due to spatially varying characteristics of both risks. The results

show that awareness regarding SLR-related risks posed to WHS is low and that adaptation is urgently needed to preserve WHS in the future.

This thesis offers an important contribution to characterizing exposure to SLR-related hazards at continental scale, thereby facilitating the integrated assessment of coastal risks, accounting for future uncertainties in physical as well as socioeconomic processes. The results of this thesis stress the importance to explore different migration processes in spatial population projections; characterize additional exposure variables not commonly analyzed; and account for regional characteristics when assessing coastal risks at continental scale. Future work can extend the developed data and modeling approaches and can contribute to harmonizing data and modeling approaches that have gradually increased in recent years, to further advance coastal risk assessments at continental scale.



## ZUSAMMENFASSUNG

---

In Folge des sich im 21. Jahrhundert durch den anthropogenen Klimawandel beschleunigenden Meeresspiegelanstiegs sind Küstengebiete vermehrt Küstengefahren ausgesetzt. Zukünftige Küstenrisiken werden nicht nur von der Höhe des Meeresspiegelanstiegs bestimmt, sondern auch von einer hohen Dichte an Bevölkerung und Vermögenswerten in gefährdeten Gebieten. Die mit der zukünftigen Entwicklung des Meeresspiegelanstiegs und der sozioökonomischen Entwicklung einhergehende Unsicherheit kann mit Hilfe des SSP-RCP Szenario Konzepts, das aus physischen Szenarien (RCPs – Representative Concentration Pathways) und sozioökonomischen Szenarien (SSPs – Shared Socioeconomic Pathways) besteht, untersucht werden; es findet vermehrt Anwendung in der Analyse von Küstenrisiken auf kontinentaler bis globaler Ebene. Bisher lag der Fokus solcher Studien auf der räumlichen Modellierung zukünftiger physischer Gefährdungen in Folge des Meeresspiegelanstiegs, während die Modellierung von Bevölkerung und Vermögenswerten in gefährdeten Gebieten wenig Berücksichtigung fand, insbesondere bezüglich der zukünftigen Entwicklung basierend auf den SSPs. Bisherige Arbeiten, die die zukünftige Entwicklung berücksichtigen, basieren auf globalen Daten, Modellierungsansätzen und Szenario Annahmen, auch wenn Risiken auf kontinentaler Ebene analysiert werden. Daher entwickelt diese Arbeit die räumliche Modellierung von Bevölkerung und Vermögenswerten weiter, um eine integrierte Analyse zukünftiger Küstenrisiken auf kontinentaler Ebene zu gewährleisten. Der Fokus liegt auf zwei Variablen, der Bevölkerung und Kulturgütern, die für das gewählte Untersuchungsgebiet, dem Mittelmeerraum, modelliert werden.

In einem ersten Schritt werden die globalen SSP Erzählstränge für den Mittelmeerraum erweitert, indem regionale Faktoren der sozioökonomischen Entwicklung ergänzt werden und zusätzlich zwischen nördlichen versus südlichen und östlichen Ländern unterschieden wird. Mit Hilfe der erweiterten Erzählstränge werden für jedes SSP bis 2100 räumliche Bevölkerungsprojektionen erstellt, die die Unsicherheit zukünftiger Land-Stadt und Inland-Küste Migrationsbewegungen abbilden. Die in 2100 potenziell betroffene Küstenbevölkerung liegt zwischen 34,1 Mio. (SSP1) und 96,2 Mio. (SSP3) und weist deutliche Unterschiede zwischen einzelnen Ländern auf. Ein Vergleich der Ergebnisse mit Projektionen basierend auf den globalen SSPs zeigt eine Abweichung der gefährdeten Bevölkerung von bis zu 15 % (SSP1), wodurch eine größere Bandbreite der Unsicherheit im Hinblick auf die gefährdete Bevölkerung abgebildet wird. Da dieser Modellierungsansatz das Flächenwachstum von Städten nicht abbildet, wird ein gravitationsbasierter Modellansatz entwickelt, der sowohl urbanes Flächenwachstum als auch Land-Stadt und Inland-Küste Migrationsbewegungen berücksichtigt. Die räumlichen Bevölkerungsprojektionen basierend auf diesem Ansatz führen zu 51,3 Mio. (SSP4) bis 107,8 Mio. (SSP3) Menschen in gefährdeten Küstengebieten in 2100. Da die Ergebnisse beider Modellansätze beträchtliche Unterschiede aufweisen, sollten die Stärken und Schwächen beider Ansätze in zukünftigen Studien berücksichtigt werden.

Für eine ganzheitliche Analyse von Küstenrisiken ist die Berücksichtigung weiterer Variablen nötig. Daher wird eine räumliche Datenbank von Kulturgütern, einer Variable, deren Analyse aufgrund fehlender hochauflösender Daten wenig üblich ist, entwickelt, indem räumliche Repräsentationen (d.h. Polygone) von 49 UNESCO Weltkulturerbestätten in tiefliegenden

Küstengebieten des Mittelmeerraums erstellt werden. Eine erste Anwendung der Datenbank in einer kontinentalen Gefährdungsanalyse zeigt, dass bereits unter aktuellen klimatischen Bedingungen je 75 % und 85 % der Stätten hochwasser- bzw. erosionsgefährdet sind. Diese Gefahren werden bis 2100 je nach Meeresspiegelanstiegsszenario und Weltkulturerbestätte zunehmen, da Küstenhochwasser und -erosion unterschiedliche räumliche Muster aufweisen. Aktuell ist das Bewusstsein bezüglich der Gefährdung von Weltkulturerbestätten durch den Meeresspiegelanstieg vergleichsweise gering und Anpassungsmaßnahmen sind dringend nötig um unser kulturelles Erbe zukünftig zu erhalten.

Diese Arbeit leistet einen wichtigen Beitrag zur Modellierung von Bevölkerung und Kulturgütern in potenziell vom Meeresspiegelanstieg betroffenen Gebieten und ermöglicht daher die integrierte Analyse von Küstenrisiken auf kontinentaler Ebene, insbesondere unter Berücksichtigung zukünftiger physischer und sozioökonomischer Unsicherheiten. Die Ergebnisse unterstreichen den Mehrwert dessen verschiedene Migrationsbewegungen in räumliche Bevölkerungsprojektionen zu integrieren; weitere, weniger übliche Variablen in Gefährdungsanalysen einzubeziehen; und regionale Unterschiede bei der Analyse von Küstenrisiken auf kontinentaler Ebene zu berücksichtigen. Künftige Studien können die entwickelten Daten und Modellierungsansätze erweitern und zur Harmonisierung neuer Daten und Modellansätze beitragen, um so die integrierte Analyse von Küstenrisiken auf kontinentaler Ebene weiter voranzutreiben.

# TABLE OF CONTENTS

---

Acknowledgments .....	i
Summary .....	iii
Zusammenfassung .....	v
Table of Contents .....	vii
List of Figures .....	ix
List of Tables.....	x
Abbreviations .....	xi
<b>1 INTRODUCTION.....</b>	<b>1</b>
1.1 COASTAL RISKS IN A CHANGING CLIMATE.....	1
1.1.1 Sea-level rise and its physical impacts.....	1
1.1.2 Socioeconomic development in the coastal zone.....	2
1.1.3 Framework for assessing coastal risks .....	3
1.2 CURRENT PRACTICE IN COASTAL RISK ASSESSMENTS .....	4
1.2.1 Assessing sea-level rise-related hazards .....	6
1.2.2 Assessing exposure and vulnerability .....	10
1.3 RESEARCH NEEDS AND THESIS OUTLINE .....	14
1.3.1 Research needs .....	15
1.3.2 Objectives and thesis outline .....	16
<b>2 REGIONALIZED SHARED SOCIOECONOMIC PATHWAYS: NARRATIVES AND SPATIAL POPULATION PROJECTIONS FOR THE MEDITERRANEAN COASTAL ZONE .....</b>	<b>19</b>
2.1 INTRODUCTION .....	20
2.2 MATERIAL AND METHODS .....	21
2.2.1 Narrative development.....	21
2.2.2 Gridded population projections.....	23
2.3 RESULTS .....	25
2.3.1 Mediterranean coastal SSP narratives.....	25
2.3.2 Mediterranean population projections .....	28
2.4 DISCUSSION .....	30
2.5 CONCLUSION .....	32
<b>3 ACCOUNTING FOR INTERNAL MIGRATION IN SPATIAL POPULATION PROJECTIONS – A GRAVITY-BASED MODELING APPROACH USING THE SHARED SOCIOECONOMIC PATHWAYS 35</b>	
3.1 INTRODUCTION .....	36
3.2 METHODS .....	38
3.2.1 Modeling approach .....	38
3.2.2 Calibration.....	39
3.2.3 Validation.....	40
3.2.4 Population projections .....	41
3.3 RESULTS .....	41

3.4	DISCUSSION .....	45
3.5	CONCLUSION .....	48
<b>4</b>	<b>MEDITERRANEAN UNESCO WORLD HERITAGE AT RISK FROM COASTAL FLOODING AND EROSION DUE TO SEA-LEVEL RISE.....</b>	<b>51</b>
4.1	INTRODUCTION .....	52
4.2	RESULTS .....	53
4.2.1	UNESCO World Heritage in coastal areas .....	53
4.2.2	Flood risk .....	54
4.2.3	Erosion risk .....	56
4.3	DISCUSSION .....	58
4.4	METHODS .....	63
4.4.1	General framework .....	63
4.4.2	UNESCO World Heritage data processing.....	64
4.4.3	Flood risk .....	64
4.4.4	Erosion risk .....	66
4.4.5	Code availability .....	68
4.5	DATA AVAILABILITY.....	68
<b>5</b>	<b>CONCLUSIONS AND OUTLOOK.....</b>	<b>69</b>
5.1	MAIN ACHIEVEMENTS AND FINDINGS .....	69
5.1.1	Downscaling global-scale data and modeling approaches to the continental scale .....	69
5.1.2	Developing spatial population projections that account for internal migration processes.....	70
5.1.3	Advancing the spatial representation of exposure variables not commonly used in coastal risk assessments.....	71
5.2	RECOMMENDATIONS FOR FURTHER RESEARCH .....	72
	APPENDICES .....	79
	Appendix A.....	81
	Appendix B.....	91
	Appendix C.....	101
	List of references .....	109
	Erklärung.....	133

## LIST OF FIGURES

---

<b>Figure 1.1</b> Components of the IPCC risk framework included in this thesis to assess coastal risks (adapted from Oppenheimer et al. 2014).....	4
<b>Figure 2.1</b> Selected population grids. Population per grid cell for the base year 2010 and each SSP in 2100. Pixel size = 30 arcsec .....	28
<b>Figure 2.2</b> LECZ population for each country group and each SSP in 2100 in comparison to the base year 2010. a) Number gives the total population count, b) Growth represents the growth of the LECZ population relative to the base year 2010. ....	29
<b>Figure 2.3</b> Mediterranean LECZ population in 2100 in Jones and O’Neill 2016 and Merkens et al. 2016 compared to our regionalized SSPs .....	31
<b>Figure 3.1</b> Scatter plots of the total population, urban populations, and rural populations, along with R2 and the Root Mean Squared Error (RMSE). Blue line represents the perfect fit.....	40
<b>Figure 3.2</b> Population per grid cell in the baseline (2010) and for each SSP in 2100. Resolution: 30 arc seconds (WGS84).....	42
<b>Figure 3.3</b> Urban population density in each SSP and geographical region. (a) In 2100 compared to 2010, (b) development 2010-2100 in coastal versus inland locations. Coastal = Low Elevation Coastal Zone (see SM3.3; McGranahan et al 2007). Please note different scales of the y-axes....	43
<b>Figure 3.4</b> Coastal population in each SSP and geographical region. (a) In 2100 compared to 2010, (b) development 2010-2100, differentiating urban versus rural populations. Coastal = Low Elevation Coastal Zone (see SM3.3; McGranahan et al 2007). Please note different scales of the y-axes....	44
<b>Figure 3.5</b> Mediterranean coastal population in 2100 based on Merkens et al 2016, Reimann et al 2018, Jones and O’Neill 2016 (downscaled projections of Gao 2017), and the approach used in this study. Coastal = Low Elevation Coastal Zone, based on MERIT DEM (Yamazaki et al 2017).....	47
<b>Figure 4.1</b> UNESCO cultural World Heritage sites located in the Mediterranean Low Elevation Coastal Zone (LECZ). All sites are shown with their official UNESCO ID and name. The map also shows extreme sea levels per coastal segment based on the Mediterranean Coastal Database (Wolff et al. 2018a) under the high-end sea-level rise scenario in 2100.....	54
<b>Figure 4.2</b> Temporal evolution of the flood risk indicators at each World Heritage site, averaged across the Mediterranean region. Results are shown from 2000 to 2100 for RCP2.6, RCP4.5, RCP8.5 and the high-end (HE) scenario. a) Mean area flooded (in %), b) mean flood depth (in m), c) mean flood risk index.....	55
<b>Figure 4.3</b> Flood risk index at each World Heritage site under current and future conditions. a) In 2000 and b) in 2100 under the high-end sea-level rise scenario.....	56
<b>Figure 4.4</b> Temporal evolution of two erosion risk indicators at each World Heritage site, averaged across the Mediterranean region. Results are shown from 2000 to 2100 for RCP2.6, RCP4.5, RCP8.5 and the high-end (HE) scenario. a) Mean distance from the coastline (in m), b) mean erosion risk index .....	57
<b>Figure 4.5</b> Erosion risk index at each World Heritage site under current and future conditions. a) In 2000 and b) in 2100 under the high-end sea-level rise scenario.....	58
<b>Figure 4.6</b> Examples of potential adaptation tipping points for the flood risk index and the erosion risk index. Both graphs show points in time when a World Heritage site may exceed a certain risk threshold with the respective amount of sea-level rise under the high-end scenario. Point labels show the official UNESCO ID of the sites affected. a) Flood risk index threshold of 6.5, b) erosion risk index threshold of 7.5 .....	59

## LIST OF TABLES

---

<b>Table 1.1</b> Methods and data of selected coastal flood assessments at continental to global scales (in chronological order) .....	9
<b>Table 1.2</b> Data and methods of selected coastal exposure and vulnerability assessments at continental to global scales (in chronological order) .....	14
<b>Table 2.1</b> Characteristics of each Mediterranean coastal SSP element in each SSP and geographical region, with the modification factors of rural ( $GD^R$ ) and urban ( $GD^U$ ) growth differences.....	26
<b>Table 4.1</b> Scale values used for the components of the flood risk index and the erosion risk index....	66

## ABBREVIATIONS

---

ABM	Agent-Based Modeling
AIS	Antarctic Ice Sheet
AR5	5 <sup>th</sup> Assessment Report
CBA	Cost-Benefit Analysis
CIESIN	Center for International Earth Science Information Network
CoDEC	Coastal Dataset for the Evaluation of Climate Impact
CSI	Coastal Sensitivity Index
CVI	Coastal Vulnerability Index
DCESL	DINAS-COAST ESL
DDF	Depth-Damage Function
DEM	Digital Elevation Model
DIVA	Dynamic Interactive Vulnerability Assessment
EbA	Ecosystem-based Adaptation
ERI	Erosion Risk Index
ESL	Extreme Sea Levels
EU	European Union
FLOPROS	FLOod PROtection Standards
GD	Growth Difference
GDP	Gross Domestic Product
GHSL	Global Human Settlement Layer
GIA	Glacial Isostatic Adjustment
GIS	Geographic Information System
GMSLR	Global Mean Sea Level Rise
GPW	Gridded Population of the World
GRUMP	Global Rural-Urban Mapping Project
GSHHG	Global, Self-consistent, Hierarchical, High-resolution Geography
GTSR	Global Tide and Surge Reanalysis
HE	High-End
IAM	Integrated Assessment Model
IAV	Impacts, Adaptation, and Vulnerability
ICZM	Integrated Coastal Zone Management
IPCC	Intergovernmental Panel on Climate Change
IQR	Interquartile Range
IUCN	International Union for the Conservation of Nature
LECZ	Low Elevation Coastal Zone
MAE	Mean Absolute Error
MCD	Mediterranean Coastal Database
MERIT	Multi-Error-Removed Improved-Terrain
MIP	Model Intercomparison Project
MOSE	MOdulo Sperimentale Elettromeccanico/Experimental Electromechanical Module
OSM	OpenStreetMap

OUV	Outstanding Universal Value
RAE	Relative Absolute Error
RCP	Representative Concentration Pathway
RMSE	Root Mean Square Error
RSLR	Relative Sea Level Rise
SEDAC	Socioeconomic Data and Applications Center
SLR	Sea-Level Rise
SPA	Shared Policy Assumption
SRES	Special Report on Emissions Scenarios
SROCC	Special Report on the Ocean and Cryosphere in a Changing Climate
SRTM	Shuttle Radar Topography Mission
SSP	Shared Socioeconomic Pathway
TSM	Total Suspended Matter
UHI	Urban Heat Island
UNESCO	United Nations Educational, Scientific and Cultural Organization
VLM	Vertical Land Motion
WDPA	World Database on Protected Areas
WHS	World Heritage Site
WMAPE	Weighted Mean Absolute Percentage Error
WUP	World Urbanization Prospects



# 1 INTRODUCTION

---

## 1.1 COASTAL RISKS IN A CHANGING CLIMATE

Climate change caused by anthropogenic greenhouse gas emissions results in globally rising temperatures (IPCC 2013). Coastal areas will be disproportionately affected by climate change due to two main drivers, 1) rising sea levels and 2) high densities of population and assets in locations potentially exposed to hazards related to sea-level rise (SLR). In this section, the current state of knowledge regarding the drivers of coastal risks is discussed, focusing on SLR and its physical impacts in coastal locations first, before turning to socioeconomic development in the coastal zone. Third, the risk framework used throughout this thesis for assessing future SLR-related coastal risks is presented.

### 1.1.1 Sea-level rise and its physical impacts

Higher temperatures due to climate change lead to globally rising sea levels, driven primarily by the melting of glaciers and ice sheets and the thermal expansion of warming ocean waters. The contribution of these drivers to global mean SLR (GMSLR) has increased since the beginning of the 20<sup>th</sup> century, leading to an acceleration of GMSLR. While in the period 1901-1990, GMSL rose by approximately 1.4mm yr<sup>-1</sup>, the rate of GMSLR increased to 3.2mm yr<sup>-1</sup> from 1993-2015. This rate is expected to further accelerate, in particular in the second half of the 21<sup>st</sup> century, depending on the amount of future warming, which in turn depends on the development of greenhouse gas emissions in the coming years. Therefore, the *likely* range in GMSLR in 2100 relative to 1986-2005 lies between 0.29 and 1.1m, depending on the scenario (see Box 1 and section 1.2.1 for more detail). However, SLR is not globally uniform and varies regionally due to a range of drivers. These drivers include regional differences in thermal expansion of ocean waters and land ice loss due to differences in warming, differences in winds and atmospheric pressure, ocean circulation patterns, gravitational and rotational effects, and vertical land motion (VLM) due to tectonics and glacial isostatic adjustment (GIA). Therefore, regional SLR can deviate from GMSLR by +/- 30% (Oppenheimer et al. 2019).

SLR leads to a variety of physical impacts in coastal locations, which include the submergence of low-lying coastal areas, increasing coastal erosion, saltwater intrusion in surface and ground waters, changes in coastal ecosystems as well as an increase in the frequency and intensity of coastal flooding due to extreme sea levels (ESL) (Nicholls 2010, Wong et al. 2014). While most of these impacts will gradually increase with rising sea levels (Brown et al. 2013), coastal flooding due to ESL already occurs under current climatic conditions when a low atmospheric pressure system results in strong winds that coincide with high tides and waves, thereby resulting in a storm surge (Wahl 2017). Recent research has shown that a small rise in sea levels (i.e. 10 to 20cm) may lead to an exponential increase in flood frequency (Vitousek et al. 2017, Taherkhani et al. 2020). For instance, the present-day 100-year event, which has a 1%

probability of being exceeded in any given year (Wahl et al. 2017), may become an annual or more frequent event in large parts of the world by 2100 (Vousdoukas et al. 2018c). Furthermore, Arns et al. 2017 stress the importance to account for non-linear feedbacks between tides, waves, surges, and SLR in shallow coastal areas as these feedbacks may increase future coastal flood risk due to SLR.

Additionally, coastal areas are at risk from compound flooding when at least two hazards occur simultaneously (Zscheischler et al. 2018). Particularly in river deltas and estuaries, coastal flooding due to ESL can be exacerbated by fluvial flooding due to increased river discharge caused by heavy precipitation in the river catchment (Zscheischler et al. 2020). A global study assessing the dependence between ESL and high river discharge has found that dependence is significant at more than 50% of the 187 stations analyzed (Ward et al. 2018). Globally, the probability of compound flooding may increase by about 25% until 2100, with a substantially higher increase in high latitudes and a potential decrease in the subtropics (Bevacqua et al. 2020). If compound flooding is not accounted for in assessing coastal flooding due to SLR, future risk may be considerably underestimated (Moftakhari et al. 2017, Bevacqua et al. 2020).

### **1.1.2 Socioeconomic development in the coastal zone**

High population densities and urbanization levels in locations potentially exposed to the physical impacts of SLR will be key drivers of coastal risks in the future. Currently, almost one third of the global population (1.9 billion) lives within 100km from the coast at an elevation of up to 100m, which covers 9% of the global land area (Kummu et al. 2016). In 2000, 10% of the global population (634 million) and 13% of the urban population (360 million) lived in 2% of the global land area known as the Low Elevation Coastal Zone (LECZ), defined as land with an elevation of up to 10m in hydrological connection to the sea (McGranahan et al. 2007). Accordingly, about 70% of all megacities (>8 million inhabitants), which are often on or next to river deltas, are located in the LECZ (Brown et al. 2013). Further, urban areas located in the LECZ have been observed to grow at a significantly faster rate than inland areas (Seto et al. 2011). These settlement patterns are expected to further consolidate in the future due to high urbanization rates as well as the higher attractiveness of coastal locations for human settlement compared to inland locations (Nicholls et al. 2008b, Neumann et al. 2015). Therefore, the global population in the LECZ is projected to increase in the future, ranging from 830 million to almost 1.2 billion in 2100, depending on the scenario (Merkens et al. 2016).

Exposure of population and assets to SLR-related hazards further depends on the amount of SLR experienced at a specific location, known as relative SLR (RSLR) (Oppenheimer et al. 2019). In particular VLM, which includes uplift of the land surface as well as land subsidence, can have a significant effect on RSL (Shirzaei et al. 2021). While land subsidence is a natural process due to sediment compaction, it is aggravated by anthropogenic processes such as groundwater extraction and exploitation of oil or gas reservoirs (Syvitski et al. 2009, Shirzaei et al. 2021) as well as the weight of buildings (Nicholls et al. 2011). Therefore, human-induced subsidence can be the dominant driver of RSLR, particularly in delta regions (Tessler et al.

2018, Higgins 2016). This effect is currently particularly pronounced in Asian mega deltas such as the Ganges-Brahmaputra-Meghna delta where subsidence rates of  $5.9\text{mm yr}^{-1}$  and  $8.6\text{mm yr}^{-1}$  have been reported for Dhaka and Kolkata, respectively (Brown and Nicholls 2015). Further examples include Ho Chi Minh City which subsides by up to  $40\text{mm yr}^{-1}$  (Erban et al. 2014), Jakarta where subsidence rates of more than  $200\text{mm yr}^{-1}$  were measured between 1997 and 2005 (Chaussard et al. 2013), and Shanghai which has subsided about 2m in the last century (Cheng et al. 2018). As a result, the rate of RSLR experienced at these locations can exceed GMSLR by several orders of magnitude (Syvitski et al. 2009, Higgins 2016), which increases SLR-related coastal risks substantially (Tessler et al. 2018).

Coastal adaptation is an important strategy to reduce exposure and vulnerability to SLR-related hazards. The most common adaptation strategies discussed in the literature are hard or soft protection (e.g. dikes, beach nourishment), accommodation (e.g. building codes, raising houses), and retreat in the form of migration or planned relocation (Wong et al. 2014). Two additional strategies that have received increasing attention in recent years are ecosystem-based adaptation (EbA) and advancing land by building seaward and upward (Oppenheimer et al. 2019). Studies have shown that protection can effectively reduce the area and number of people flooded due to SLR and ESL (Hinkel et al. 2013b, Hinkel et al. 2014, Paprotny et al. 2018). Without adaptation, 0.2 to 4.6% of the global population may be exposed to coastal flooding annually in 2100, which can be reduced by two orders of magnitude if protection measures are gradually upgraded with rising sea levels (Hinkel et al. 2014). Further, recent cost-benefit analyses (CBA) have shown that protection measures can cost-effectively reduce coastal flood risk (Tiggeloven et al. 2020, Vousdoukas et al. 2020a) and that protection is economically robust (i.e. under a wide range of physical and socioeconomic scenarios) at 13% of the global coastline, which covers 96% of assets in the coastal floodplain (Lincke and Hinkel 2018). Similarly, beach nourishment can cost-effectively reduce the number of people that would have to migrate due to coastal erosion by about 60% until 2100 (Hinkel et al. 2013a).

### 1.1.3 Framework for assessing coastal risks

The drivers of SLR-related coastal risks described in the preceding sections can be conceptualized with the help of the Intergovernmental Panel on Climate Change (IPCC) risk framework (Figure 1.1), where climate change risks (and therefore impacts) result from the interaction of climate hazards, exposure to these hazards, and vulnerability of the exposed elements (Field 2012). Exposure refers to the presence of e.g. people, infrastructure, assets (i.e. economic, social, cultural), and ecosystems in locations potentially affected by a hazard, whereas vulnerability is determined by the sensitivity and adaptive capacity of the exposed elements (e.g. wealth, social status) that determine how severely the exposed elements are affected. Further, future coastal risks are driven by changes in the climate system as well as socioeconomic processes, which can be explored with climatic and socioeconomic scenarios (Oppenheimer et al. 2014).

As the focus of this thesis lies on coastal risks (i.e. flood risk and erosion risk), the hazards analyzed are ESL and SLR. To assess exposure to these hazards, population and cultural assets located in coastal areas are considered. To account for future changes in these risk drivers, different SLR and socioeconomic scenarios are explored (see section 1.3 for further details). The thesis does not directly assess vulnerability or the potential feedbacks of adaptation and mitigation actions and governance on exposure and vulnerability. The following section presents the current state-of-the-art in coastal risk assessments, which provides further context regarding the hazards and exposure variables explored in this thesis.

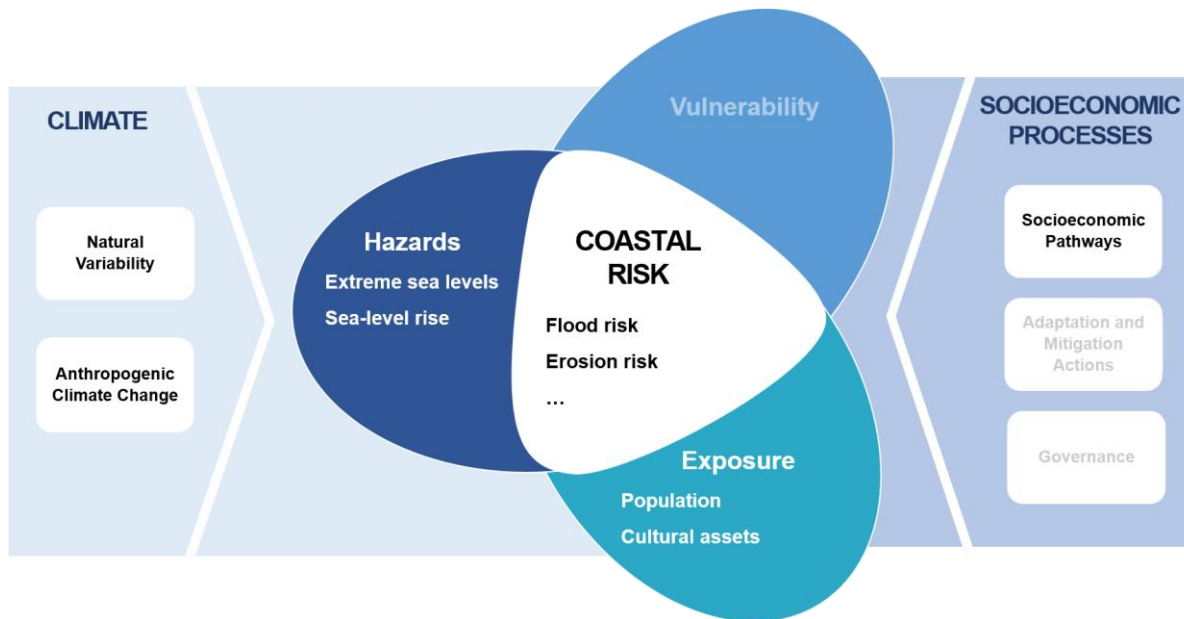


**Figure 1.1** Components of the IPCC risk framework included in this thesis to assess coastal risks (adapted from Oppenheimer et al. 2014)

## 1.2 CURRENT PRACTICE IN COASTAL RISK ASSESSMENTS

Coastal risk assessments can provide important insights into how changes in hazards, exposure, and vulnerability drive future SLR-related impacts. For such assessments, spatial data and modeling approaches are used to characterize all risk drivers in a spatially explicit manner (Toimil et al. 2020, Vousdoukas et al. 2018a). Furthermore, scenarios, both climatic and socioeconomic (Alcamo and Henrichs 2008, Moss et al. 2010), are used for exploring the uncertainty range of plausible future impacts (Toimil et al. 2020, Ward et al. 2020), as well as for estimating the dominant driver of future risk (Muis et al. 2015). The current scenario framework in climate change research, the so-called SSP-RCP scenario framework (O'Neill et al. 2020), allows for combining a range of climate scenarios (so-called Representative Concentration Pathways, RCPs) with different socioeconomic scenarios (so-called Shared Socioeconomic Pathways, SSPs) to develop fully integrated scenarios (van Vuuren et al. 2014). Box 1 provides a short description of the SSP-RCP framework.

**Box 1 The SSP-RCP scenario framework**

The development of the SSP-RCP scenario framework started with identifying a range of Representative Concentration Pathways (RCPs) based on plausible radiative forcing levels in 2100 as reported in the scientific literature (van Vuuren et al. 2011). Radiative forcing describes the amount of energy added to the earth's energy budget by anthropogenic drivers such as the concentration of greenhouse gases and aerosols in the atmosphere or changes in surface albedo, and is expressed in  $\text{Wm}^{-2}$  (relative to 1750) (Myhre et al. 2013). Four RCPs were selected, ranging from the low radiative forcing scenario RCP2.6, where radiative forcing levels peak at approximately  $3 \text{ Wm}^{-2}$  before 2100, to RCP8.5, characterized by radiative forcing levels of at least  $8.5 \text{ Wm}^{-2}$  in 2100. The two intermediate RCPs, RCP4.5 and RCP6.0 reflect a stabilization of radiative forcing levels after 2100 (Moss et al. 2010, van Vuuren et al. 2011).

As the RCPs do not include any underlying assumptions regarding socioeconomic development, the Shared Socioeconomic Pathways (SSPs) have been developed to serve this purpose. Five SSPs describe plausible alternative trends in global-scale societal development in the course of the 21<sup>st</sup> century without accounting for the potential impacts of climate change on socioeconomic development, based on their socioeconomic challenges for mitigation and adaptation (O'Neill et al. 2014). Each SSP has an underlying narrative that qualitatively describes a broad range of socioeconomic developments in the form of a story (O'Neill et al. 2017). Several key variables of socioeconomic development have been quantified with the help of the assumptions described in each SSP narrative, resulting in national-level projections of population, age, education (KC and Lutz 2017), urbanization (Jiang and O'Neill 2017), and Gross Domestic Product (GDP) (Dellink et al. 2017, Crespo Cuaresma 2017) until 2100.

To explore the uncertainty range of how plausible future socioeconomic and climatic changes drive climate change impacts, several SSPs and RCPs can be combined with each other in a scenario matrix (van Vuuren et al. 2014). Out of twenty possible combinations, 15 have been established as plausible combinations based on the results of Integrated Assessment Models (IAM) (Riahi et al. 2017, Rogelj et al. 2018). Such model runs also account for broad-scale assumptions of global mitigation and adaptation policies, so-called Shared Policy Assumptions (SPAs) (Kriegler et al. 2014), which constitute the third dimension of the scenario matrix. Recently, the matrix has been extended with three additional forcing levels (i.e. 1.9, 3.4,  $7.0 \text{ Wm}^{-2}$ ) (e.g. O'Neill et al. 2020), which have not been considered in this thesis yet.

This thesis focuses on coastal risk assessments at continental scale (Box 2). Due to the use of consistent data and modeling approaches, continental-scale risk assessments allow for comparing results across countries and regions, thereby establishing hotspots of future impacts (Ward et al. 2013, Moel et al. 2015). Continental-scale assessments can also be applied to explore the potential effectiveness of different adaptation strategies (Ward et al. 2020). The results of such assessments provide the knowledge base for global to continental frameworks such as the Sendai Framework for Disaster Risk Reduction (UNDRR 2015), the Paris Agreement on climate change (UNFCCC 2016), the European Union's (EU) Floods Directive (European Union 2007), or the Protocol on Integrated Coastal Zone Management (ICZM) in

the Mediterranean (UNEP/MAP 2008). Results can further support decision-making at international to national scales in prioritizing regions with urgent need for action and allocating funds accordingly, in particular concerning adaptation and spatial planning (McLeod et al. 2010, Ward et al. 2020). Furthermore, the re-insurance industry as well as multi-national companies use the results of these assessments to prioritize investments (Moel et al. 2015).

### **Box 2 Continental scale**

In this thesis, the term ‘continental scale’ refers to supra-national assessments as defined in Moel et al. 2015.

Accordingly, continental-scale assessments can include an entire continent (e.g. Europe) or a group of countries located in the same region and sharing a common national border, which may extend over several continents (e.g. the Mediterranean region).

The following sections discuss the current practice in continental-scale coastal risk assessments, differentiating between the assessment of SLR-related hazards as well as exposure and vulnerability to these hazards. The current literature on continental-scale coastal risk assessments is limited, with a small number of studies focusing on Europe. Therefore, global-scale assessments are also included, as similar methods and input data are used at these scales of analysis (Moel et al. 2015).

#### **1.2.1 Assessing sea-level rise-related hazards**

One standard measure to represent SLR-related coastal hazards at continental scale is delineating the LECZ. To do so, a digital elevation model (DEM) is used to determine all land with an elevation of up to 10m, followed by applying a connectivity rule to mask out low-lying land not hydrologically connected to the sea (McGranahan et al. 2007, Lichter et al. 2011). The LECZ provides a simple and inclusive measure for characterizing all land potentially affected by SLR-related hazards such as submergence, temporary flooding due to ESL, and saltwater intrusion (McGranahan et al. 2007, Balk et al. 2009), while being independent from SLR scenarios. To account for the uncertainties related to future SLR that stem from the uncertainties in the development of future greenhouse gas emissions, current coastal risk assessments explore different SLR projections. The most recent GMSLR projections are reported in the IPCC Special Report on the Ocean and Cryosphere in a Changing Climate (SROCC) (IPCC 2019), which are updated versions of those used in the IPCC’s Fifth Assessment Report (AR5) (Church et al. 2013). These projections additionally account for contributions of the Antarctic ice sheet (AIS), which were not included in previous projections due to high uncertainties in AIS dynamics, especially after 2050 (Bakker et al. 2017, Horton et al. 2018). Under RCP2.6, GMSLR in 2100 (relative to 1986-2005) is projected to be 0.43m (50<sup>th</sup> percentile), with a *likely* range (i.e. 17<sup>th</sup> to 83<sup>rd</sup> percentile) of 0.29-0.59m. Under RCP4.5, GMSLR is projected at 0.55m (*likely* range 0.39-0.72m) and 0.84m (0.61-1.1m) under RCP 8.5 (Oppenheimer et al. 2019).

The majority of current coastal risk assessments account for RSLR. If projections of GMSLR are used, these are enhanced by VLM due to GIA and natural land subsidence in river deltas

(e.g. Merkens et al. 2018, Nicholls et al. 2018). The majority of assessments use projections that account for regional SLR patterns, resulting from processes such as gravitational and rotational effects, differences in ocean circulation patterns and thermal expansion, as well as GIA (e.g. Vafeidis et al. 2019, Kulp and Strauss 2019, Athanasiou et al. 2020, Tiggeloven et al. 2020, Vousdoukas et al. 2020a, Vousdoukas et al. 2020c). These regional SLR projections are produced with the help of process-based models (e.g. Levermann et al. 2013, Hinkel et al. 2014) or with probabilistic modeling approaches that additionally account for contributions of the AIS to SLR (e.g. Kopp et al. 2014, Jackson and Jevrejeva 2016, Kopp et al. 2017). The study of Tiggeloven et al. 2020 is the only current assessment that accounts for the contribution of human-induced land subsidence due to groundwater extraction to future RSLR. Human-induced subsidence is usually not included in assessments at continental to global scales due to a lack of data and future projections (Wada et al. 2012).

### Coastal flooding

To assess coastal flooding due to ESL under alternative SLR scenarios, the amount of SLR per scenario and time step is usually added to the present-day ESL of a certain return period. The 100-year event is the most commonly used return period in such assessments (e.g. Hinkel et al. 2014, Neumann et al. 2015, Merkens et al. 2018, Vafeidis et al. 2019, Tiggeloven et al. 2020, Kirezci et al. 2020). Available datasets of present-day ESL are the DINAS-COAST ESL (DCESL) data (Vafeidis et al. 2008) and the GTSR (Global Tide and Surge Reanalysis) data (Muis et al. 2016), both of which account for the two ESL components storm surge and tides. As GTSR was modeled with a hydrodynamic modeling approach, the dataset better represents present-day ESL than DCESL (Muis et al. 2017). Further, as storm surges and wind waves are statistically dependent at large parts of the global coast (Marcos et al. 2019), recent work has accounted for wind waves as a third ESL component (Vousdoukas et al. 2018c). Thus far, two studies have produced future ESL projections by including SLR under RCP4.5 and RCP8.5 (Vousdoukas et al. 2018c, Muis et al. 2020). The Coastal Dataset for the Evaluation of Climate Impact (CoDEC) is the first ESL dataset that accounts for dynamic interactions between tides, surges, and mean sea level under current and future conditions (Muis et al. 2020). To our knowledge, CoDEC has not been used in coastal flood risk assessments yet.

To model the coastal floodplain, a static DEM-based approach similar to the one used for delineating the LECZ is widely used (e.g. Jongman et al. 2012, Neumann et al. 2015, Brown et al. 2018, Paprotny et al. 2018, Kulp and Strauss 2019, Kirezci et al. 2020). With the help of this so-called bathtub approach, all land up to the projected water level in hydrological connection to the sea is defined (Poulter and Halpin 2008, Ramirez et al. 2016). The most commonly used DEM is the Shuttle Radar Topography Mission (SRTM) DEM (Farr et al. 2007) or DEMs developed from SRTM such as the Multi-Error-Removed Improved-Terrain (MERIT) DEM (Yamazaki et al. 2017) and CoastalDEM (Kulp and Strauss 2018). While all of these (near-) global DEMs have the same horizontal resolution of 3 arc seconds (about 90m at the equator), their vertical resolution differs: SRTM DEM has a vertical resolution of 1m and the other two DEMs one of below 1m (i.e. elevation is given in decimal values). Therefore, studies using the

SRTM DEM have to interpolate linearly between elevation increments (e.g. Hinkel et al. 2014, Nicholls et al. 2018, Merkens et al. 2018, Vafeidis et al. 2019). For the US, the root mean square error (RMSE) of SRTM DEM in the LECZ has been established as 5.57m, while MERIT DEM and CoastalDEM have a RMSE of 3.14m and 3.1m, respectively (Gesch 2018). Therefore, MERIT DEM and CoastalDEM are increasingly used to assess coastal flood risk at continental to global scales.

As the bathtub approach does not account for hydrodynamic processes such as the influence of surface roughness on water flow direction, it potentially overestimates the coastal floodplain, in particular in mildly sloping terrain (Vousdoukas et al. 2016, Seenath et al. 2016). To address this limitation, recent work has developed an enhanced bathtub approach that accounts for different rates of water level attenuation for different land use classes and can be applied at continental to global scales at low computational cost (Vafeidis et al. 2019, Tiggeloven et al. 2020). Furthermore, the use of the two-dimensional hydrodynamic model LISFLOOD-FP (Bates and Roo 2000) has been explored, with applications at European scale available in the current literature (Vousdoukas et al. 2018b, Vousdoukas et al. 2020a). While LISFLOOD-FP is less computationally expensive than other hydrodynamic models such as DELFT3D (Deltares 2020), a computational facility is needed to apply it at continental scale (Vousdoukas et al. 2016). As the resolution of the underlying DEM (see DEMs above) does not resolve coastal protection measures already in place and continental-scale data on protection do not exist (Vousdoukas et al. 2018a), stylized assumptions of current protection standards such as the global database of FLOod PROtection Standards (FLOPROS) (Scussolini et al. 2016) are used.

An overview of selected coastal flood assessments along with the data and methods used to characterize the floodplain is provided in Table 1.1.



**Table 1.1** Methods and data of selected coastal flood assessments at continental to global scales (in chronological order)

Study	Scale of analysis	SLR projections* (RCPs)	Return period (dataset)	Modeling approach	DEM	Current protection standard included?
Hinkel et al. 2014	Global (DIVA)	H14 (RCP2.6, 4.5, 8.5)	100-yr (DCESL)	Bathtub	SRTM**, GLOBE***	No
Brown et al. 2018	Global (DIVA)	G17, scaled with Slangen et al. 2014 + GIA (RCP8.5 + mitigation scenarios)	100-yr (GTSR)	Bathtub	SRTM v4.1	No
Merkens et al. 2018	Global (DIVA)	C13 + SUB + GIA (RCP2.6, 4.5, 6.0, 8.5)	100-yr (GTSR)	Bathtub	SRTM v4.1	No
Kulp and Strauss 2019	Global	K14/17 (RCP2.6, 4.5, 8.5)	1-yr (GTSR)	Bathtub	SRTM v2.1, CoastalDEM	No
Vafeidis et al. 2019	Global (DIVA)	H14 (RCP4.5, 8.5)	100-yr (GTSR)	Enhanced bathtub	SRTM v4.1	No
Tiggeloven et al. 2020	Global	J16 + HSUB (RCP4.5, 8.5)	100-yr (GTSR)	Enhanced bathtub	MERIT	Yes
Vousdoukas et al. 2020a	Europe	H14 (RCP4.5, 8.5)	Different return periods (JRC)****	LISFLOO D-FP	SRTM	Yes

\* H14 = Hinkel et al. 2014, G17 = Goodwin et al. 2017, C13 = Church et al. 2013, K14/17 = Kopp et al. 2014, 2017, J16 = Jackson and Jevrejeva 2016; GIA = Glacial Isostatic Adjustment, SUB = natural subsidence in river deltas, HSUB = human subsidence due to groundwater extraction

\*\* Different versions of the SRTM DEM exist; it was not always possible to find out which version was used. As SRTM DEM has near-global coverage, it was complemented by other DEMs above 60°N for global assessments, which are not listed here.

\*\*\* Hastings and Dunbar 1999

\*\*\*\* Vousdoukas et al. 2017, 2018c

DIVA = use of the Dynamic Interactive Vulnerability Assessment (DIVA) database (Vafeidis et al. 2008)

### Coastal erosion

Previous research on continental-scale assessments of coastal erosion due to SLR has been limited. One main approach that has been employed for several decades and at different spatial scales is the Bruun rule. The Bruun rule (Bruun 1962, 1983) assumes that sandy coastlines respond to SLR by retreating landward and upward, maintaining an equilibrium profile. This two-dimensional rule is based on the assumption that all eroded sediment is deposited offshore, and neglects alongshore sediment transport. Therefore, erosion of sandy coastlines depends on two main factors, the amount of SLR and the nearshore coastal slope (Davidson-Arnott 2005, Ranasinghe and Stive 2009). Due to its modest data requirements and low computational costs, the Bruun rule offers an easy-to-use method for first-order assessments of SLR-related erosion of sandy coastlines at continental scales (Ranasinghe and Stive 2009, Athanasiou et al. 2020).

However, most applications focus on local to national scales (see Athanasiou et al. 2020 for an overview), with four continental- to global-scale studies available in the literature. Hinkel et al. 2010, 2013a applied a simplified version of the Bruun rule, assuming the same nearshore slope in all locations, under a range of SLR scenarios based on the Special Report on Emissions Scenarios (SRES) (Nakićenović 2000), both at European (Hinkel et al. 2010) and global scales (Hinkel et al. 2013a). Two recent studies extended this work: the European-scale study of Athanasiou et al. 2020 analyzed shoreline retreat due to SLR only, while the global-scale study by Vousdoukas et al. 2020c additionally accounted for past shoreline changes established in prior research (Luijendijk et al. 2018, Mentaschi et al. 2018). Both assessments accounted for spatially varying nearshore slopes (Athanasiou et al. 2019) as well as for two scenarios of RSLR based on RCP4.5 and 8.5 (Jackson and Jevrejeva 2016). Due to its simplified assumptions (e.g. equilibrium profile, not considering longshore sediment transport), the use of the Bruun rule has been criticized for several years (Cooper and Pilkey 2004, Ranasinghe and Stive 2009, Cooper et al. 2020, Vousdoukas et al. 2020b). Furthermore, as it is only applicable to sandy coastlines, it can only be used at about one third of the global coastline (Luijendijk et al. 2018).

Another method for assessing SLR-related coastal erosion is an index-based approach such as the Coastal Vulnerability Index (CVI) (Gornitz 1991) and the Coastal Sensitivity Index (CSI) (Shaw et al. 1998), both of which aim to assess the physical vulnerability of the coastline due to SLR. These indices have been applied extensively in subnational to national assessments (e.g. Thieler and Hammar-Klose 1999, Abuodha and Woodroffe 2010, López Royo et al. 2016, Mavromatidi et al. 2018). Both indices are based on similar input variables, i.e. coastal material, shoreline erosion and accretion, coastal slope, relative SLR, wave climate, and tidal range. Each variable receives a score from 1 (very low vulnerability) to 5 (very high vulnerability) which is then aggregated to one risk index per stretch of coastline. One advantage of this approach is that it can be consistently applied to the entire coastline; however, it relies on a range of input variables that may not be readily available at continental scale (Athanasiou et al. 2020).

The scarcity of continental-scale studies of SLR-related erosion in the current literature underlines the challenges related to assessing erosion at this scale of analysis as it is a phenomenon that is driven by a complex interplay of local conditions (Oppenheimer et al. 2019). These local conditions can be resolved in three-dimensional hydrodynamic models such as DELFT3D (Ranasinghe 2016), which cannot (yet) be used in continental-scale assessments due to their prohibitive computational costs (see discussion in the subsection on coastal flooding). Therefore, assessments of coastal erosion based on the two approaches described above can only be a first-order estimate of future erosion due to SLR.

### **1.2.2 Assessing exposure and vulnerability**

To assess exposure to SLR-related coastal hazards, spatially explicit hazard information, e.g. the LECZ or coastal floodplain, are intersected with spatial representations of potentially exposed elements such as population, assets, and infrastructure. To assess vulnerability of the

exposed elements, characteristics of these elements that determine how severely they are affected are included as well (Moel et al. 2015).

### Exposure

Population is by far the most-analyzed exposure variable in current coastal risk assessments at continental scale<sup>1</sup>. In the past, data of spatial population distributions were intersected with the LECZ to estimate potential exposure to SLR-related hazards (McGranahan et al. 2007, Balk et al. 2009, Lichter et al. 2011, Mondal and Tatem 2012). The spatial population data used in these assessments represented the population distribution at that time, with the data of the Global Rural-Urban Mapping Project (GRUMP) (Center for International Earth Science Information Network - Columbia University (CIESIN) et al. 2011) and LandScan (Bright et al. 2012) being the most-used population datasets<sup>2</sup>.

Recent coastal risk assessments have increasingly accounted for changes in future hazard conditions and population distributions under a range of physical (i.e. SLR) and socioeconomic scenarios. While some studies have analyzed future exposure based on the current distribution of the population only (e.g. Muis et al. 2017, Kulp and Strauss 2019), the majority of recent work accounts for future changes in population distributions. Such studies either analyze one scenario (e.g. Jongman et al. 2012, Brown et al. 2016, Vafeidis et al. 2019) or a range of plausible scenarios, primarily based on the SSPs (e.g. Hinkel et al. 2014, Neumann et al. 2015, Nicholls et al. 2018, Vousdoukas et al. 2020a). Most of these assessments apply national-level growth rates to the current population distribution, thereby assuming homogeneous population growth per country (e.g. Jongman et al. 2012, Brown et al. 2018, Lincke and Hinkel 2018, Vafeidis et al. 2019). However, this assumption neglects internal migration processes such as rural-urban and inland-coastal migration (Box 3), which result in non-uniform spatial population growth patterns (McGranahan et al. 2007, Seto et al. 2012).

To account for inland-coastal migration, Nicholls 2004 (also Nicholls et al. 2008b) and Neumann et al. 2015 used distinct growth rates for inland versus coastal locations by applying scenario-specific correction factors to the national growth rates. Merkens et al. 2016 extended this work and developed spatial population projections for the five SSPs based on the analysis of historical changes in coastal versus inland population growth patterns in each country, additionally accounting for

#### **Box 3 Migration**

In this thesis, the term ‘migration’ refers to internal migration within countries, which is considered to occur at long time scales (Hugo 2011). Furthermore, migration is the result of a decision that is driven by social, political, demographic, economic, and environmental factors, or a combination thereof (Black et al. 2011). A specific focus lies on rural-urban migration as well as inland-coastal migration.

<sup>1</sup> See McMichael et al. (2020) for a comprehensive review of population exposure assessments in coastal locations.

<sup>2</sup> See Leyk et al. (2019) for an overview of global-scale spatial population datasets available in the current literature in addition to those reported here.

rural-urban migration. A second set of SSP-based spatial population projections available in the current literature accounts for rural-urban migration as well as for spatial changes in settlement patterns (i.e. urban sprawl) (Jones and O'Neill 2016). Both sets of SSP-based spatial population projections are gradually adopted in coastal risk assessments at continental to global scales (Merkens et al. 2018, Vousdoukas et al. 2018b, Vousdoukas et al. 2020a). Further spatial population projections available at global (Murakami and Yamagata 2019) and continental scales (Lückenötter et al. 2017, Boke-Olén et al. 2017) have not been used in coastal risk assessments yet.

In addition to population exposure, several coastal risk assessments account for exposure of assets by applying national-level projections of GDP per capita to the spatial population distribution and multiplying it with a certain factor to estimate assets of every person (e.g. Hanson et al. 2011, Hallegatte et al. 2013, Hinkel et al. 2014, Lincke and Hinkel 2018). Furthermore, previous work has assessed future exposure of urban land under projections of built-up land expansion (Jongman et al. 2012, Tiggeloven et al. 2020). Recently developed SSP-based projections of urban land expansion provide the basis for similar global- (Gao and O'Neill 2020, Chen et al. 2020a) to continental-scale (Terama et al. 2019, Wolff et al. 2020) assessments. Additional exposure variables that have been analyzed in coastal risk assessments are cities (Nicholls et al. 2008a, Hanson et al. 2011, Hallegatte et al. 2013), infrastructure such as airports (Yesudian and Dawson 2021) and roads and railways (Koks et al. 2019), and cultural assets, i.e. UNESCO World Heritage sites (Marzeion and Levermann 2014). However, studies based on these variables are scarce in the current literature due to a lack of high-resolution spatial data of these variables at continental to global scales.

### Vulnerability

Current coastal risk assessments at continental to global scales account for vulnerability to a limited degree. The most common approach is the assessment of damages with the help of depth-damage functions (DDF) (Moel et al. 2015). DDF are based on the assumption that damages increase with increasing flood depth (Huizinga et al. 2017). Current studies apply DDF to different land-use types (e.g. Jongman et al. 2012, Vousdoukas et al. 2018b, Tiggeloven et al. 2020) or assets (e.g. Hallegatte et al. 2013, Hinkel et al. 2014). As DDF are assumed to remain static in time, temporal changes in vulnerability can only be accounted for to a limited degree, although vulnerability is a dynamic process that changes with socioeconomic changes (Turner et al. 2003, Jurgilevich et al. 2017). Two studies account for changes in vulnerability to a certain extent by applying the static DDF to spatially changing urban land-use types (Tiggeloven et al. 2020, Vousdoukas et al. 2020a). To characterize vulnerability of exposed populations under the uncertainty of future socioeconomic development, spatial projections of variables such as age structure, sex, and education level are needed (van Ruijven et al. 2014, Birkmann et al. 2015). Little research has focused on the spatial distribution of such variables at continental scales, with two examples at administrative unit level for Europe (Rohat 2018, Terama et al. 2019). In general, understanding of the processes that drive vulnerability is

limited, which further impedes spatially explicit vulnerability assessments at continental to global scales (Muis et al. 2015, Jongman et al. 2015, Rohat 2018).

One strategy to reduce vulnerability to SLR-related hazards is the implementation of adaptation measures (Jurgilevich et al. 2017, Pörtner et al. 2019). Several studies explore adaptation strategies and their potential to reduce exposure and damages, with a focus on hard protection (e.g. Hallegatte et al. 2013, Hinkel et al. 2014, Tiggeloven et al. 2020). These assessments are usually based on CBA to determine where protection measures can cost-effectively reduce coastal flood risk (e.g. Lincke and Hinkel 2018, Tiggeloven et al. 2020, Vousdoukas et al. 2020a) (see also section 1.1.2). Analyses of other adaptation strategies such as beach nourishment (Hinkel et al. 2010, 2013a) and retreat (Diaz 2016) are scarce in the current literature.

Table 1.2 provides an overview of selected coastal exposure and vulnerability assessments along with the data and methods used in each study. It is worth noting that all studies reviewed in this section use global-scale data and scenario assumptions that potentially inhibit their applicability at continental scales as they reflect regional characteristics to a limited degree.

**Table 1.2** Data and methods of selected coastal exposure and vulnerability assessments at continental to global scales (in chronological order)

Study	Scale of analysis	Socio-economic scenarios	Exposure variable(s) (base data)*	Modeling approach	Vulnerability assessment method
Hinkel et al. 2014	Global (DIVA)	SSPs 1,2,3,5	Population (GRUMP, LandScan); Assets	Homogenous growth; GDP/capita * 2.8	DDF** for assets; hard protection
Neumann et al. 2015	Global	Foresight scenarios (A-D)***	Population (GRUMP)	Correction factor coastal versus inland	-
Brown et al. 2018	Global (DIVA)	SSPs 1-5	Population (GRUMP)	Homogenous growth	-
Merkens et al. 2018	Global (DIVA)	SSPs 1-5	Population (GRUMP)	Comparison of homogenous growth, urban versus rural growth, Merkens et al. 2016, and Jones and O'Neill 2016	-
Vafeidis et al. 2019	Global (DIVA)	SSP2	Population (GRUMP); Assets	Homogenous growth; GDP/capita * 2.8	DDF for assets
Tiggeloven et al. 2020	Global	SSPs 1-5	Assets based on built-up land (HYDE) and GDP/capita (LandScan)	Built-up land projections based on Winsemius et al. 2016 and homogenous growth of GDP/capita	DDF for land use; hard protection
Vousdoukas et al. 2020a	Europe	SSPs 1,3,5	Assets based on land use (CORINE) and GDP/capita (Batista e Silva et al. 2013a)	Urban land use and homogenous growth of GDP/capita based on Jones and O'Neill 2016	DDF for land use; hard protection

\* GRUMP = Center for International Earth Science Information Network - Columbia University (CIESIN) et al. 2011, LandScan = Bright et al. 2012, HYDE = Klein Goldewijk et al. 2010, CORINE = Batista e Silva et al. 2013b  
\*\* DDF = Depth-Damage Function  
\*\*\* Foresight 2011  
DIVA = use of the Dynamic Interactive Vulnerability Assessment (DIVA) database (Vafeidis et al. 2008)

### 1.3 RESEARCH NEEDS AND THESIS OUTLINE

This section first establishes three key research needs that arise from the research gaps in the current practice of continental-scale coastal risk assessments, as described in the preceding sections. Second, it provides a short overview of how the remainder of the thesis is structured and explains how the research needs are addressed in each following chapter.

### 1.3.1 Research needs

The preceding sections have illustrated several research gaps in the current practice of continental-scale coastal risk assessments. Previous research has primarily focused on using and advancing different modeling approaches for characterizing coastal hazards in a spatially explicit manner by exploring the uncertainty in future changes in coastal hazards under a range of SLR scenarios (section 1.2.1). Research on the spatial representation of variables to characterize exposure and vulnerability has been less extensive, in particular regarding the use of socioeconomic scenarios (section 1.2.2). While the number of studies that account for the uncertainty in future socioeconomic development has increased in recent years, most of these studies use simplistic modeling approaches, e.g. assuming homogenous growth in population and GDP per country, thereby neglecting internal migration processes (e.g. Jongman et al. 2012, Hinkel et al. 2014, Brown et al. 2018, Vafeidis et al. 2019). Gradually, spatial modeling approaches are being developed that account for internal migration processes such as inland-coastal migration (e.g. Neumann et al. 2015, Merkens et al. 2016) and urban sprawl (Jones and O'Neill 2016). Thus far, these modeling approaches have been applied to produce spatial population projections at the global scale based on a broad set of scenario assumptions that do not necessarily reflect regional differences at continental scale in a plausible manner. Downscaling the above modeling approaches to the continental scale allows for capturing such regional differences based on a refined set of scenario assumptions. Furthermore, previous research has almost exclusively focused on the spatial distribution of population or population-based variables such as GDP per capita to characterize exposure, although other variables such as infrastructure or cultural assets in potentially exposed locations are important additional drivers of coastal risk, which are rarely accounted for in coastal risk assessments.

The imbalance in modeling practices in current coastal risk assessments summarized above raises the need for advancing spatial data and modeling approaches of exposure and vulnerability variables to facilitate the assessment of coastal risks in an integrated manner. Therefore, this thesis addresses the following key research needs (RN):

- RN1** To downscale global data and modeling approaches to the continental scale to allow for capturing regional differences across the study area
- RN2** To explore uncertainty in plausible future changes in socioeconomic development in coastal locations, particularly focusing on spatial population modeling approaches that account for important internal migration processes (i.e. inland-coastal migration, urban sprawl)
- RN3** To advance the spatial representation of exposure variables not commonly analyzed in coastal risk assessments such as cultural assets

At least two of the three research needs are addressed in each of the following three chapters, each of which has its own research objective. Chapters 2 and 4 have been published as original research articles in peer-reviewed scientific journals and Chapter 3 is currently under peer review. A short description of the objectives pursued in each chapter is provided in the next section along with the research needs addressed per chapter/objective (in parentheses).

### **1.3.2 Objectives and thesis outline**

The remainder of this thesis focuses on the Mediterranean region as a case study as it is characterized by high population densities and urbanization levels in coastal locations due to a small tidal range and steep topography in inland locations (UNEP/MAP 2017, MedECC 2020a). Further, as several ancient civilizations have developed in the region, a high number of cultural assets is located in coastal areas (Benoit and Comeau 2005, Cazenave 2014). The Mediterranean is a socioeconomically diverse region with large differences between northern, southern, and eastern parts of the region (UNEP/MAP 2016), which is reflected in e.g. varying adaptation strategies and protection standards across the region (Scussolini et al. 2016). These characteristics make the Mediterranean a suitable study region for addressing the above-stated research needs, by pursuing the following three objectives:

#### **Objective 1 To develop extended SSP narratives and spatial population projections that account for regional characteristics and inland-coastal migration**

In Chapter 2, the global SSPs are extended to the Mediterranean region by enhancing them with elements that are important drivers of socioeconomic development in the region, with a specific focus on coastal elements that drive coastal attractiveness for human settlement. The extended SSP narratives differentiate two geographical regions, the northern versus the southern and eastern Mediterranean. By interpreting the extended narratives, spatial population projections are developed that explore the uncertainty of inland-coastal migration in each SSP and both geographical regions, using and extending the modeling approach of Merkens et al. 2016. (RN1, RN2)

#### **Objective 2 To develop spatial population projections that account for regional characteristics, inland-coastal migration, and urban sprawl**

Chapter 3 presents the development of a gravity-based population downscaling model for the Mediterranean region that allows for exploring the uncertainty in inland-coastal migration as well as urban sprawl. This work refines and advances the modeling approach of Jones and O'Neill 2016. By interpreting the global SSP narratives as well as those developed in Chapter 2, spatial population projections are produced for each SSP based on distinct model assumptions in the two geographical regions. (RN1, RN2)

#### **Objective 3 To develop a spatial database of cultural assets in low-lying coastal areas and to employ this database to assess the risks of SLR-related coastal flooding and erosion to these assets**



In Chapter 4, a database that includes spatial representations of cultural assets (i.e. UNESCO World Heritage sites (WHS)) located in the Mediterranean LECZ is developed and applied in a continental-scale coastal risk assessment. Based on four SLR scenarios until 2100, a flood risk index and an erosion risk index are calculated for each WHS and time step, thereby allowing for comparing the severity of both risks at different WHS. (RN1, RN3)



## **2 REGIONALIZED SHARED SOCIOECONOMIC PATHWAYS: NARRATIVES AND SPATIAL POPULATION PROJECTIONS FOR THE MEDITERRANEAN COASTAL ZONE**

---

Existing narratives and population projections of the global-scale Shared Socioeconomic Pathways (SSPs) do not capture regional differences in socioeconomic development in the Mediterranean region. In this study, we regionalize the global SSPs to account for differences in coastal population development between northern, eastern, and southern countries of the region. First, we develop coastal SSP narratives that include region-specific elements and differentiate between geographical regions. Based on these narratives, we derive coastal population growth rates that vary for each SSP as well as between coastal, inland, rural, and urban areas. We apply these growth assumptions to observed population growth patterns in a spatially explicit manner. The Mediterranean coastal SSPs thereby reflect socioeconomic development patterns across countries as well as coastal versus inland development within countries. Our results show that coastal population in the Mediterranean increases across SSPs 2-5 by 3 to 130% until 2100 except for SSP1, where population declines by almost 20% compared to 2010. We observe considerable differences between geographical regions and countries. In the Mediterranean north, coastal population declines in SSP1, SSP3, and SSP4 and experiences the highest increase of more than 100% in SSP5. In southern and eastern Mediterranean countries, the highest increase in coastal population takes place in SSP3 and amounts to almost 180% by 2100. The regionalized SSP narratives and population projections are intended for assessing future exposure, vulnerability, and impacts of population to coastal hazards and sea-level rise but can also be of use for a wider range of Impact, Adaptation, and Vulnerability (IAV) studies.

This chapter is published as<sup>3</sup>:

Reimann, L., Merkens, J.-L., Vafeidis, A.T., 2018. Regionalized Shared Socioeconomic Pathways: narratives and spatial population projections for the Mediterranean coastal zone. *Regional Environmental Change* 18, 235-245. DOI: 10.1007/s10113-017-1189-2.

---

<sup>3</sup> Please note: For consistency throughout the thesis, the term ‘regional’ has been changed to ‘continental’ in two instances when we refer to the scale of analysis.

## 2.1 INTRODUCTION

The Shared Socioeconomic Pathways (SSPs) constitute one component of the current climate change scenario framework which has been developed by the climate change research community in recent years (Ebi et al. 2014, O'Neill et al. 2014, Riahi et al. 2017). As climate change impacts are determined by prevailing socioeconomic conditions, the research community called for a new framework which would be more useful for Impact, Adaptation, and Vulnerability (IAV) research to replace the IPCC's Special Report on Emission Scenarios (SRES) (Moss et al. 2010, Hallegatte et al. 2011, Kriegler et al. 2012).

Five basic SSPs have been developed to cover possible challenges for climate change mitigation and adaptation. The SSPs “describe plausible alternative trends in the evolution of society and natural systems over the 21<sup>st</sup> century at the level of the world and large world regions” (O'Neill et al. 2014, p 389). Each SSP consists of two dimensions: a qualitative narrative, which explores future socioeconomic developments in form of a storyline (O'Neill et al. 2017), and a quantitative dimension, which quantifies key elements of the narratives in projections for the five SSPs until 2100 (see KC and Lutz 2017 for population projections, Jiang and O'Neill 2017 for urbanization projections, and Crespo Cuaresma 2017, Dellink et al. 2017, and Leimbach et al. 2017 for GDP projections). Combining SSPs with Representative Concentration Pathways (RCPs) (van Vuuren et al. 2011a) and Shared Policy Assumptions (SPAs) (Kriegler et al. 2014), which are two further components of the scenario framework, a number of integrated climate scenarios can be developed.

As the basic SSPs have been designed for global-scale assessments, the scenario assumptions reflect developments on regional to local scale to a limited degree (Absar and Preston 2015). If regional or local processes deviate from those assumed at global scales, the use of the basic SSPs in IAV assessments could yield misleading results at regional to local scale. Therefore, decision makers may pursue measures (e.g., adaptation strategies, policies) which do not fit to the characteristics of their area of interest. For this reason, the IAV research community has called for regional and spatially explicit extensions of the basic SSPs depending on the application at hand (van Ruijven et al. 2014). Recent studies have addressed this call with either regional extensions (Absar and Preston 2015, Schweizer and Kurniawan 2016) or spatially explicit extensions (Merkens et al. 2016, Jones and O'Neill 2016) but not both.

We address this gap by (1) extending the basic SSPs to the Mediterranean region, specifically focusing on its coastal zone, and (2) developing gridded population projections. We choose the Mediterranean as it is a socioeconomically diverse region and global scenario assumptions would not necessarily reflect regional differences. Further, the Mediterranean region has experienced rapid socioeconomic growth in recent decades, especially in coastal locations where industry and services (e.g., tourism, ports, fisheries, infrastructure) are concentrated (Benoit and Comeau 2005, European Environment Agency (EEA) 2006, 2014, Piante and Ody 2015). A large share of the Mediterranean population lives in the coastal zone, being exposed to potential hazards such as coastal flooding, salt water intrusion, water scarcity, and land subsidence (Benoit and Comeau 2005, Blue Plan 2008, European Environment Agency (EEA) 2014). In the course of the century, coastal hazards are expected to exacerbate due to climate

change (European Environment Agency (EEA) 2014, Wong et al. 2014). Depending on the adaptive capacity and vulnerability of exposed population and assets, impacts will vary regionally (Hallegatte et al. 2013, Wong et al. 2014, Satta et al. 2015). The aim of this study is to develop Mediterranean coastal SSPs which yield plausible results in continental-scale IAV assessments and which can serve as a decision tool for policy makers and stakeholders. We specifically focus on possible futures of population development in coastal areas to span the range of uncertainty in future coastal population change and do not quantify other elements such as GDP, urbanization, or land use.

We follow a two-step process. First, we develop Mediterranean coastal SSP narratives by combining characteristics of the basic SSPs with coastal elements and region-specific elements that influence socioeconomic development in the coastal zone. We further differentiate between geographical regions based on the current state of socioeconomic development. In a second step, we quantify our narratives to develop gridded population projections for all Mediterranean countries. These projections reflect, in line with the narratives, regional differences across countries as well as differences in coastal versus inland population growth for rural and urban areas in each country. In section 2.2, the methods employed to develop the narratives and the population projections are explained, followed by a description of the results in section 2.3. Section 2.4 discusses the benefits of this work for IAV assessments in the Mediterranean and compares our results to previous work.

## **2.2 MATERIAL AND METHODS**

### **2.2.1 Narrative development**

We develop Mediterranean coastal SSP narratives using a qualitative approach. The basic SSP narratives by O'Neill et al. 2017 are the starting point of our Mediterranean coastal SSP narratives. To ensure consistency with the basic SSPs and to guarantee comparability between different spatial scales, we choose a top-down nesting approach. In this approach, the basic SSPs serve as boundary conditions for our regionalized narratives but are enhanced with further socioeconomic context on regional and subnational (i.e., coastal) scale (Absar and Preston 2015). We strive to maintain consistency with global developments as local and regional processes are embedded in global-scale processes and do not take place independently from these (van Vuuren et al. 2010, van Ruijven et al. 2014, Kok et al. 2015, Birkmann et al. 2015).

#### Mediterranean coastal SSP elements

To enhance the basic SSPs with coast-specific context, we employ the global-scale coastal SSP narratives along with the SSP names developed by Merken et al. 2016. They established coastal SSP elements which promote or restrict human settlement in the coastal zone. These elements are shipping, fisheries, coastal tourism, lifestyle migration, and coastal zone management. To develop assumptions regarding the characteristics of each coastal SSP element, Merken et al.

2016 interpreted a number of basic SSP elements by O'Neill et al. 2017, such as urbanization, economic growth, inequality, international trade, globalization, consumption and diet, international cooperation, and technology.

We adopt the elements of Merkens et al. 2016 as well as those of O'Neill et al. 2017 and enhance them by Mediterranean-specific elements which constitute additional important driving factors of coastal socioeconomic development. We establish these region-specific elements based on the available literature. In a first step, we use the Web of Science™ database and combine the search terms “Mediterranean”, “socioeconomic development”, and “coastal” to find peer-reviewed literature for the entire region. As the combination of all three terms results in only 25 publications, we further use a combination of the two terms “Mediterranean” and “socioeconomic development” (120 publications). In a next step, we use terms related to anticipated factors of coastal migration in the region, such as “water use”, “tourism”, and “fisheries” in combination with “Mediterranean”. Additionally, we extend our search to book chapters and reports published by organizations such as Plan Bleu, the European Environment Agency (EEA), and the World Bank. We select the elements water demand (Neverre and Dumas 2015, Koutroulis et al. 2016), land subsidence (Hanson et al. 2011, Hallegatte et al. 2013), second home ownership (World Economic Forum (WEF) 2011), overfishing (European Environment Agency (EEA) 2006, Food and Agriculture Organization of the United Nations (FAO) 2014), energy demand (Benoit and Comeau 2005), migration (Kok et al. 2006), and agriculture (Kok et al. 2006, Blue Plan 2008) as these have been studied in detail and are mentioned to be of particular importance for the socioeconomic development of the Mediterranean coastal zone (see APPENDIX A, SM2.1) for an overview of all elements included). As our study focuses on the Mediterranean region, we do not consider the coastal areas of the Atlantic Ocean, Black Sea, or Red Sea.

### Geographical regions

We differentiate between geographical groups based on the current state of socioeconomic development. Therefore, we analyze freely available data of indicators which represent our SSP elements (Garschagen and Romero-Lankao 2015; SM2.2). As a further determining factor, we use the countries' membership in international organizations since all member countries are bound to policies imposed by these organizations (Benoit and Comeau 2005). Due to a lack of region-wide data coverage, it is not possible to determine the current state of socioeconomic development for every country in a consistent manner. Therefore and due to the fact that long-term scenarios are connected to high uncertainties, we decide to distinguish between two geographical regions with large differences in socioeconomic development in our narratives: the northern Mediterranean, including all countries which are members of the European Union (Spain, France, Italy, Slovenia, Croatia, Greece, Cyprus, Malta), and the southern and eastern Mediterranean, including the Maghreb countries (Libya, Tunisia, Algeria, Morocco), the countries of the Middle East (Syria, Lebanon, Israel, Palestine, Egypt), and the (potential) candidate countries of the EU (Bosnia and Herzegovina, Montenegro, Albania, Turkey). This approach has been used in previous work (Benoit and Comeau 2005, Blue Plan 2008, World

Economic Forum (WEF) 2011) and is in line with the generic nature of SSP narratives, which provide broad descriptions of future developments (O'Neill et al. 2017).

### Scenario assumptions

In a next step, we develop general assumptions for our Mediterranean coastal SSP elements, which provide the basis for the narratives. Therefore, we adopt the assumptions of Merkens et al. 2016 and extend them by the region-specific literature used for establishing the Mediterranean elements, as well as scenario literature of other regionalized scenarios (Kok et al. 2006, World Economic Forum (WEF) 2011, Kok et al. 2015) and coastal scenarios (Nicholls et al. 2008b, Foresight 2011). In case the available literature does not provide enough support for the assumptions, we additionally make use of expert judgment. An overview of the scenario assumptions along with the literature used can be found in SM2.3.

We use the current state of socioeconomic development (see above, SM2.2) as a starting point for each of the five SSP narratives, since future socioeconomic development is determined by historical development (Absar and Preston 2015, Merkens et al. 2016). Based on this current state, we adjust the general assumptions (SM2.3) to each of the five SSPs, differentiating between the two geographical regions. In our narratives, we refrain from using a specific coastal zone definition as it depends on the aim of the projection and, therefore, should be specified in the quantification of the narratives.

### **2.2.2 Gridded population projections**

For the gridded population projections, we quantify the developed narratives following the methodology employed in Merkens et al. 2016. Based on the assumption that future population patterns in coastal areas are determined by historical growth patterns, we employ the observed growth difference to account for different growth rates both within and across countries (see SM2.4 for projection equations).

To do so, we first divide each country into four zones: coastal urban (CU), coastal rural (CR), inland urban (IU), and inland rural (IR). The country boundaries are defined by the Global Administrative Areas dataset version 2.8 (Global administrative areas (GADM) 2015). To distinguish between urban and rural areas, we use the Global Rural-Urban Mapping Project's (GRUMP) urban extents grid (Center for International Earth Science Information Network - Columbia University (CIESIN) et al. 2011), which has been used in a number of previous studies (McGranahan et al. 2007, Balk et al. 2009, Jones and O'Neill 2016). We differentiate between coastal and inland locations based on a hybrid coastal zone definition, which combines an elevation-based approach using the Shuttle Radar Topography Mission (SRTM) digital elevation model (DEM) version 4.1 with a spatial resolution of 3 arcsec (approximately 90 m at the equator) (Jarvis et al. 2008, Farr et al. 2007) with a coastline buffer. Commonly used approaches based exclusively on an elevation threshold, such as the Low Elevation Coastal

Zone (LECZ) that includes all land up to 10 m in elevation with hydrological connection to the sea, would not sufficiently reflect the Mediterranean coastal zone from a socioeconomic perspective as factors of coastal migration (e.g., shipping, second home ownership) expand beyond the LECZ in this region. Therefore, we extend the definition by employing a coastline buffer that we apply to the global, self-consistent, hierarchical, high-resolution geography database (GSHHG) coastline version 2.3.6 (Wessel and Smith 1996). Buffers of different extents have been used before to define coastal areas (Small and Nicholls 2003, Nicholls et al. 2008b); a buffer of 20 km has proved most suitable for our analysis as it covers the extent of large coastal cities (Kummu et al. 2016). Using this hybrid definition, we distribute coastal population in a wider coastal zone, thus avoiding possible overestimation of the population exposed to coastal hazards.

Second, we determine growth rates for each zone and country based on past population development, employing the UN-adjusted population count grids of the Gridded Population of the World (GPWv4) dataset from 2000, 2005, and 2010. GPWv4 is currently the latest gridded population dataset that covers the whole Mediterranean. Its spatial resolution is 30 arcsec (Center for International Earth Science Information Network - CIESIN - Columbia University 2017). Based on the established growth rates, we calculate the observed urban and rural growth differences of each country. The growth difference does not reflect whether the total population grows or declines; a positive/negative growth difference indicates higher/lower population growth in coastal areas compared to inland areas whereas a growth difference of 0 shows no difference in population growth between coastal and inland locations. To differentiate between geographical regions and SSPs, we modify the observed growth differences by using modification factors that we select from the range of the observed growth differences. For this purpose, we interpret the narratives (1) to determine whether the modification factor of each SSP and geographical region is positive or negative and (2) to establish distinct modification factors per zone (urban/rural), geographical region, and SSP (see also section 2.3.1). This approach is in accordance with previous scenario literature (Nicholls 2004, Nicholls et al. 2008b, Neumann et al. 2015, KC and Lutz 2017, Jiang and O'Neill 2017) and leads to the adjusted urban and rural growth differences for each geographical region and SSP shown in Table 2.1.

Next, we employ the national-level urbanization (Jiang and O'Neill 2017) and population projections (KC and Lutz 2017) of the basic SSPs available in the SSP database (International Institute for Applied Systems Analysis (IIASA) 2016). Based on these projections, we split the total national population into urban and rural population for each SSP and projection year. To differentiate between coastal and inland population, we apply the adjusted growth differences to the urban and rural population totals. Based on the total population in each zone (CU, CR, UI, IR), we calculate the growth rate of each zone and apply it to the GPWv4 dataset in 5-year steps from 2010 to 2100 (see SM2.4 for equations). This way, we ensure both consistency with the global projections and spatial explicitness.



## 2.3 RESULTS

### 2.3.1 Mediterranean coastal SSP narratives

Each narrative presents a storyline of socioeconomic development in the Mediterranean region as well as its coastal zone for each SSP and differentiates between the two geographical regions, namely the northern Mediterranean and the southern and eastern Mediterranean. It further describes the implications of these developments for population growth in the coastal zone, in rural and urban locations. The characteristics of each coastal SSP element as described in the narratives are shown in Table 2.1 along with the modification factors used for the urban ( $GD^U$ ) and rural ( $GD^R$ ) growth differences. The following section provides excerpts of the narratives, reflecting the reasoning for future coastal population growth in each SSP. The full narrative can be found in SM2.5.

#### SSP1 – Green Coast

As this pathway focuses on sustainable development, coastal population growth decreases compared to inland locations in the whole Mediterranean. Coastal ecosystem protection and decreasing importance of fisheries lead to declining population growth in coastal rural areas. Restrictive policies inhibit migration to coastal urban areas. Nevertheless, due to the importance of shipping and inertia of urban infrastructure, coastal urban population growth is marginally lower than in inland locations. These growth trends in rural and urban areas are more pronounced in the northern Mediterranean as compared to the southern and eastern parts of the region as socioeconomic development of the countries converges gradually in the course of the century. Therefore, we reduce the observed rural growth difference by 3% in the north and by 1% in the south and east and the urban growth difference by 2 and 1%, respectively.

#### SSP2 – No Wind of Change

This pathway is characterized by continuing historical patterns. Therefore, population growth patterns in the coastal zone continue like before as well. In coastal rural areas of the Mediterranean north, population growth is mainly driven by tourism and second home ownership. In the south and east, population growth in coastal rural locations is higher due to the continuing importance of small-scale fisheries. Regarding coastal urban areas of the north, population growth is primarily determined by the importance of shipping and tourism. Compared to this, coastal urban areas of southern and eastern countries experience lower population growth, as their participation in international trade and tourism activities is limited. Consequently, we use the observed urban and rural growth differences without modifying them.

**Table 2.1** Characteristics of each Mediterranean coastal SSP element in each SSP and geographical region, with the modification factors of rural (GD<sup>R</sup>) and urban (GD<sup>U</sup>) growth differences

Mediterranean coastal SSP element	SSP1 Green Coast		SSP2 No Wind of Change		SSP3 Troubled Waters		SSP4 Fragmented Coast		SSP5 Coast Rush	
	North	South and east	North	South and east	North	South and east	North	South and east	North	South and east
Shipping	→	↗	↑	↓	↘	↓	↑	→	↑	↗
Fisheries	↓	↘	Large-scale	Small-scale	Small-scale, subsistence		↑	↑	→ Large-scale →	
Overfishing	↘	↘	↑	↗	↑	↑	↑	↑	↑	↑
Coastal tourism	→ Sustainable, low-impact, no mass tourism		↑	→	↘ No international tourism		↑	↗	↑ Mass tourism	
Lifestyle/ Second home ownership	↓	↓	↑	→	↘	↓	↑	↗	↑	↗
Coastal zone management	↑	↗	→	↓	↘ weak		↑	↓	↑	↗
Water demand	↘	↘	→	↑	↑	↑	↑	↑	↑	↑
Subsidence	↘	↘	↑	↑	↑	↑	↘	↑	→	→
Modification GD <sup>R</sup>	- 3%	- 1%	± 0%	± 0%	+ 0.5%	+ 1%	+ 1%	+ 2%	+ 2%	+ 3%
Modification GD <sup>U</sup>	- 2%	- 1%	± 0%	± 0%	- 1%	- 0.5%	+ 1%	+ 2%	+ 3%	+ 4%
↑ high, ↓ low, → moderate, ↗ increase, ↘ decrease										

### SSP3 – Troubled Waters

This pathway is characterized by regional rivalry, which decreases coastal attractiveness for human settlement. As living standards decrease, this pathway is characterized by little mobility of the population and thus little coastal migration. In coastal rural locations, population grows due to increasing importance of fisheries despite the fact that coastal waters are overfished to large extents. Coastal urban areas lose their attractiveness compared to inland cities due to declining shipping and tourism. Therefore, population growth in coastal urban locations is almost exclusively driven by natural growth and does not differ from inland areas. These population growth patterns are less pronounced in the south and east than in northern countries. In the south and east, coastal rural locations experience higher growth and coastal cities do not lose their advantage over inland cities as severely. The reason for this is the presently higher importance of fisheries and lower importance of shipping and tourism in southern and eastern countries. Especially in the south and east, the population is forced to move closer to the coast as desertification advances. To account for these growth patterns, we modify the rural growth difference by +0.5% in northern countries and +1% in southern and eastern countries and the urban growth difference by -1 and -0.5%, respectively.

### SSP4 – Fragmented Coast

This pathway is characterized by high inequalities across and within countries, with a wealthy elite which comprises a small share of the population and a poorer population group which makes up the rest of the population. Coastal population growth increases compared to inland population growth in the whole region. Among the elite, coastal population growth in rural areas is mostly driven by tourism and ownership of second homes and by small-scale subsistence fisheries among other population groups. Urban areas experience high population growth since they are regarded as economic engines. Coastal growth is higher in the south and east compared to the north because coastal population growth is mainly driven by poorer population groups. Further, in countries affected by advancing desertification, people are forced to move closer to the coast. Due to these developments, we increase the rural and urban growth differences by 1% in the north and by 2% in the south and east.

### SSP5 – Coast Rush

In this highly globalized world, the coastal zone is extremely attractive, leading to higher population growth in the coastal zone compared to inland locations in all Mediterranean countries. In coastal rural areas, tourism and second homes are the main drivers of population growth. Population in coastal urban areas increases since economic activity is concentrated in these locations. Due to high urbanization rates and urban sprawl, many rural areas are urbanized. These growth trends are more pronounced in the Mediterranean south and east than in the north because of catch-up effects. Therefore, we increase the observed rural growth difference by 2%

in northern countries and by 3% in the south and east and the urban growth difference by 3 and 4%.

### 2.3.2 Mediterranean population projections

The population grids produced (Figure 2.1) have a spatial resolution of 30 arcsec (~1 km at the equator) and are available in 5-year increments from 2015 to 2100 for each SSP. The data are publicly available at <https://doi.org/10.6084/m9.figshare.4187295.v1>. In the following section, we present the results of the coastal population patterns under each SSP. To allow for comparison with previous studies, we have calculated these numbers for the Mediterranean LECZ.

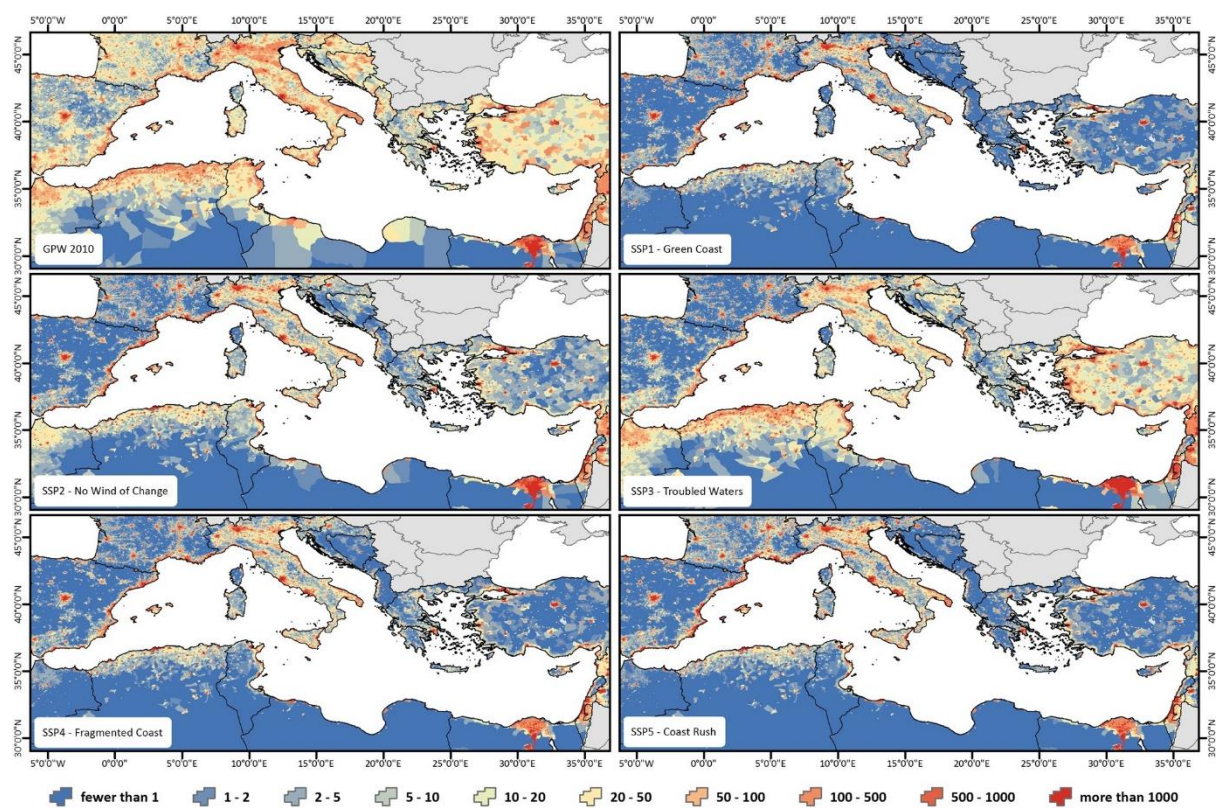


**Figure 2.1** Selected population grids. Population per grid cell for the base year 2010 and each SSP in 2100. Pixel size = 30 arcsec

The absolute LECZ population in the whole Mediterranean ranges from 34.1 (SSP1) to 96.2 million (SSP3) in 2100, which corresponds to a decline of approximately 18% in SSP1 and a growth of over 130% in SSP3 compared to 2010 (see SM2.6). The share of the coastal population increases in four SSPs from 8.9% in 2010 to up to 13.3% (SSP3) in 2100 but declines in SSP1 to 7.0%. In total, coastal population growth in the Mediterranean is higher than inland population growth in all SSPs apart from SSP1.

To illustrate regional differences, Figure 2.2 presents the LECZ population for four country groups: EU member states, EU candidate countries, the Middle East, and the Maghreb (see

section 2.2.1).<sup>4</sup> The highest population number in the Mediterranean LECZ is found in the Middle East across all SSPs (Figure 2.2a). This is due to the densely populated Nile Delta and amounts to a maximum of 78.7 million in SSP3; the lowest LECZ population lives in EU candidate countries. Compared to the base year 2010, EU member states experience an increase in LECZ population across SSP2 and SSP5 only and the coastal population ranges from 5.1 million (SSP3) to 17.5 million (SSP5). In EU candidate countries, coastal population increases in all SSPs, aside from SSP1. In 2100, the LECZ population ranges from 1.8 million in SSP1 to 5.5 million in SSP3. Countries of the Middle East experience coastal population growth in SSP2, SSP3, and SSP5. The LECZ population ranges from 20.9 million (SSP1) to 78.7 million (SSP3). Different to the other groups, coastal population increases across all SSPs in the Maghreb region and ranges from 4 million (SSP1) to 6.9 million (SSP3).

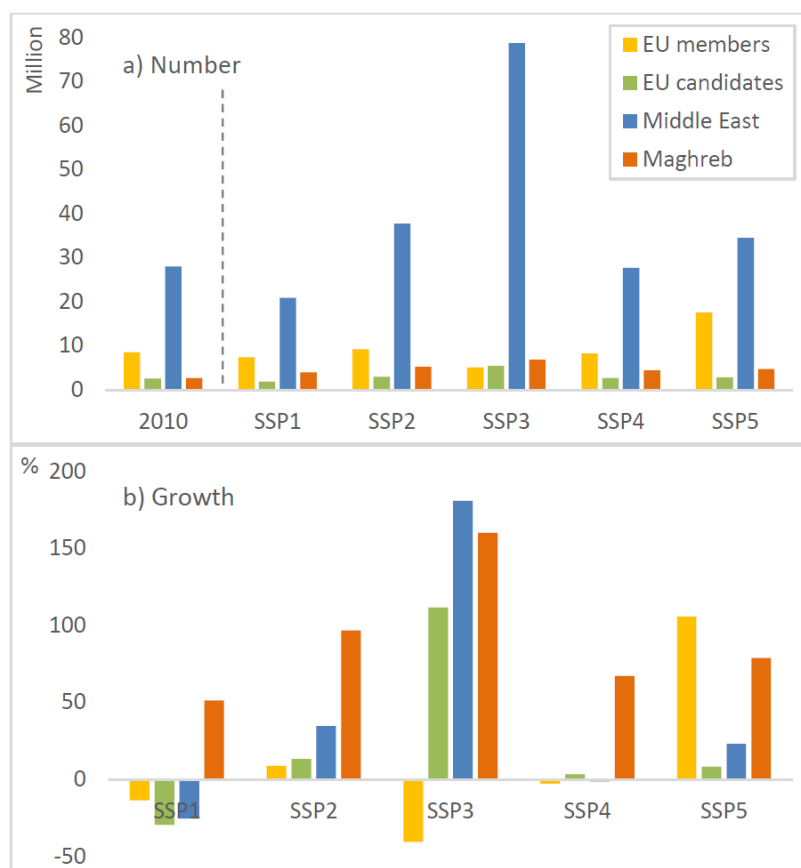


**Figure 2.2** LECZ population for each country group and each SSP in 2100 in comparison to the base year 2010. a) Number gives the total population count, b) Growth represents the growth of the LECZ population relative to the base year 2010

LE CZ population growth relative to the base year 2010 in each country group is mostly positive but decreases in SSP1 in all countries aside from the Maghreb region (Figure 2.2b). Until 2100, EU member states experience the highest increase of 106% in SSP5 and the highest decrease of over 40% in SSP3. EU candidate countries undergo the highest increase in SSP3 (112%) and the LECZ population declines by about 29% in SSP1. Similarly, in the Middle East, the highest

<sup>4</sup> See SM2.7 for the LECZ population per country.

growth occurs in SSP3, in which the LECZ population increases by over 180%, and the population decreases by approximately 25% in SSP1. In Maghreb countries, coastal population growth amounts to a minimum of 51% in SSP1 to a maximum of 160% in SSP3.

## 2.4 DISCUSSION

Our regionalized coastal SSPs can be used for IAV assessments in the Mediterranean, as they reflect regional differences in socioeconomic development in a plausible manner. Areas with high exposure to coastal hazards can be identified under different SSPs to inform adaptation planning and to raise awareness among decision makers, stakeholders, and the public regarding these locations. Individual SSPs can be compared with each other to determine the most desirable pathway and to introduce policies accordingly as to pursue this pathway (Özkaynak and Rodríguez-Labajos 2010, Birkmann et al. 2015). When doing so, challenges for mitigation and adaptation within the global SSP framework need to be incorporated.

Our narratives describe plausible pathways of socioeconomic development in the Mediterranean region and its coastal zone. Based on the developments described in each SSP narrative, SSP1 (Green Coast) could be seen as the most desirable pathway as it strives for sustainability and directs migration away from the coast. However, the projected population potentially exposed to coastal hazards can differ considerably across countries and SSPs (Figure 2.2a). In EU countries, exposure is highest in SSP5, lowest in SSP3, and only second lowest in SSP1. This is different in the other three country groups, where exposure is highest in SSP3 and lowest in SSP1. One reason for this lies in the fact that our results reflect the underlying demographic assumptions of the input data (KC and Lutz 2017, Jiang and O'Neill 2017). Therefore, exposure is highest in SSP3 in most countries, even though the coast is more attractive in SSP4 and SSP5. This is not the case in EU member states where demographic change leads to declining population in SSP3 and high international migration into the EU results in high population growth in SSP5.

Impacts of coastal hazards do not only depend on exposure but also on the adaptive capacity of the population. In the Mediterranean south and east, exposure is highest under SSP3, which is characterized by high adaptation challenges due to low living standards, weak policies and institutions, and highly dispersed settlements. Low adaptive capacity combined with high coastal population may result in high impacts in case of a coastal hazard. In the Mediterranean north, exposure is highest under SSP5, but due to high urbanization, high living standards, and effective policies and institutions, the adaptive capacity is also high. For example, technical solutions and efficient policies and institutions are expected to reduce the number of people flooded by extreme flood events. On the other hand, residual risk is high and in case adaptation measures fail during a flood event, damages in the Mediterranean north will be extremely high in SSP5 due to the concentration of population and assets in the coastal zone.

We compare our population projections with the spatial SSPs of Jones and O’Neill 2016 and the coastal SSPs of Merkens et al. 2016. All three population projections compare well in the Mediterranean but also show marked differences (Figure 2.3). In the global-scale approaches of Jones and O’Neill 2016 and Merkens et al. 2016, the Mediterranean LECZ population ranges from around 40 million in SSP4 to over 100 million in SSP3, whereas in our approach, it ranges from 34 million in SSP1 to 96 million in SSP3. The range of LECZ population is almost identical in all three approaches, but the pathway with the lowest coastal population differs (SSP4 versus SSP1). This discrepancy reflects our coastal assumptions which expect coastal population growth to be restricted in SSP1 and favored in SSP4.

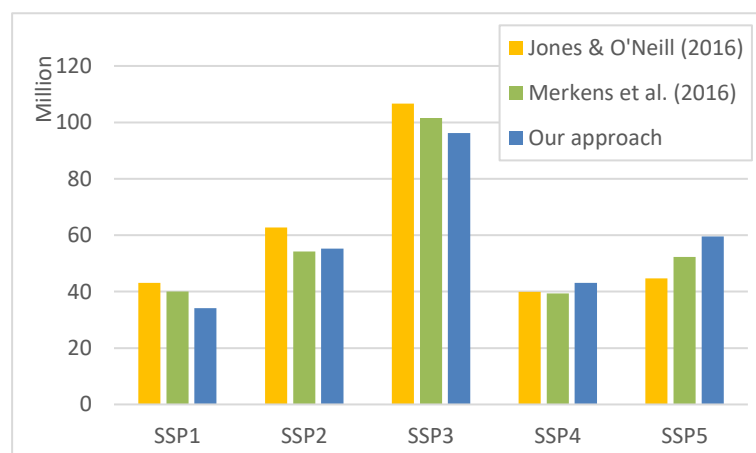


**Figure 2.3** Mediterranean LECZ population in 2100 in Jones and O’Neill 2016 and Merkens et al. 2016 compared to our regionalized SSPs

The Mediterranean LECZ population of our regionalized SSPs is lower in SSP1 and SSP3 and higher in SSP4 and SSP5 compared to both global-scale approaches. This corresponds to a relative difference ranging from  $-21\%$  (SSP1) to  $+33\%$  (SSP5) in comparison to (Jones and O’Neill 2016). These large differences reflect that (Jones and O’Neill 2016) do not specifically account for coastal development in their projections. Compared to the projections of Merkens et al. 2016, the LECZ population of our approach is between 15% lower (SSP1) and 14% higher (SSP5). This is due to the fact that although Merkens et al. 2016 implement coastal assumptions, we use higher modification factors of the observed growth differences to account for the characteristics of the region (see Table 2.1). In this way, we aim to account for a larger range of plausible coastal population development.

Our study exhibits the following limitations. In the process of developing regionalized narratives, it proved difficult to find appropriate coastal migration factors, particularly regarding rural migration. In order to develop more robust migration factors, a questionnaire survey or a participatory approach (i.e., involving stakeholders) may be useful, which would lead to higher SSP acceptance among stakeholders (Kok et al. 2006, Nicholls et al. 2008b, Absar and Preston 2015, Kok et al. 2015). Further, we only differentiate between two geographical regions. We use stylized assumptions, which may not apply to all countries of the geographical region and, therefore, should be revised for smaller-scale studies. Further, due to a lack of gridded population data with high temporal coverage, our projections rely on a short observation period



of 10 years that does not necessarily reflect long-term population development in the coastal zone. Additionally, we do not model the effects of urban sprawl on population distribution, which could lead to underestimation of urban areas in scenarios with considerable urban sprawl such as SSP5 (O'Neill et al. 2017). When using our population projections for other applications, their coastal focus should be kept in mind. We have modeled the coastal population living along the Mediterranean Sea only, excluding the coastal areas of the Atlantic Ocean, Black Sea, and Red Sea.

It is important to note that the developed SSPs do not predict what will happen by 2100 but provide plausible pathways for society to develop in course of the century. Future developments may deviate from the ones described in our SSPs and other extensions of the basic SSPs might come to different results. Despite the fact that our SSPs have specifically been developed for coastal IAV applications in a climate change context, they can also serve as boundary conditions for other utilizations due to their generic nature. The SSP framework generally assumes socioeconomic development to take place independently from climate change. This assumption is debatable (Absar and Preston 2015, Jones and O'Neill 2016) as coastal migration patterns in the Mediterranean will change once climate change impacts like sea-level rise and more frequent flooding become increasingly noticeable (European Environment Agency (EEA) 2014).

## 2.5 CONCLUSION

This study advances previous research and meets the research community's call for extensions of the basic SSPs in two ways, (1) by regionalizing them to the Mediterranean coastal zone and (2) by producing gridded population projections for the region. Our SSP narratives are consistent with the global-scale SSPs and reflect distinct socioeconomic developments in northern, southern, and eastern Mediterranean countries as well as in coastal versus inland locations, based on additional region-specific elements. We interpret these narratives to develop a set of gridded population projections for the five SSPs. Our Mediterranean coastal SSPs span the range of population growth (SSPs 2-5) and decline (SSP1) in the Mediterranean region and its coastal zone. They compare well to the global coastal SSPs of Merkens et al. 2016 but also show regional differences, therefore qualifying for continental-scale IAV assessments. The developed SSPs are particularly suitable for analysis of population exposure to sea-level rise and other coastal hazards. Thereby, locations with high exposure can be identified in order to draw the attention of decision makers towards these areas. Accordingly, adaptation strategies can be developed to reduce exposure.

Future work can adopt and further extend the Mediterranean coastal SSPs for national to local assessments. This would allow for using more location-specific variables and participatory approaches such as stakeholder workshops in order to reflect local developments. Absar and Preston 2015 suggest analyzing a number of case studies for this exercise. To be able to not only assess exposure but also vulnerability and risk, future work could additionally enhance the developed population projections by implementing socioeconomic variables like GDP and age.



In addition, it might be of interest to develop spatial population projections that account for possible rates of future sea-level rise and the influence on coastal population patterns. We encourage other researchers and decision makers to utilize the developed narratives and population projections for other applications related to IAV research.

### Acknowledgments

JLM and ATV were supported by the European research project RISES-AM (grant agreement no. 603396). We would like to thank the reviewers and editors for their valuable comments.



### **3 ACCOUNTING FOR INTERNAL MIGRATION IN SPATIAL POPULATION PROJECTIONS – A GRAVITY-BASED MODELING APPROACH USING THE SHARED SOCIOECONOMIC PATHWAYS**

---

Gridded population projections are important for climate change Impacts, Adaptation, and Vulnerability (IAV) assessments as they allow for exploring how future changes in the spatial distribution of population drive climate change impacts. We develop such spatial population projections, using a gravity-based modeling approach that, for the first time, accounts for rural-urban and inland-coastal migration as well as for spatial development patterns (i.e. urban sprawl). We calibrate the model to the socioeconomically diverse Mediterranean region, additionally considering differences in socioeconomic development in two geographical regions: the northern Mediterranean and the southern and eastern Mediterranean. We produce high-resolution population projections (approximately 1km) for 2020-2100 that are consistent with the Shared Socioeconomic Pathways (SSPs), both in terms of qualitative narrative assumptions as well as national-level projections. We find that future spatial population patterns differ considerably under all SSPs, with four to eight times higher urban population densities and three to 16 times higher coastal populations in southern and eastern Mediterranean countries compared to northern Mediterranean countries in 2100. In the South and East, the highest urban density (8,000 people/km<sup>2</sup>) and coastal population (107 million) are projected under SSP3, while in the North, the highest urban density (1,500 people/km<sup>2</sup>) is projected under SSP1 and the highest coastal population (15.2 million) under SSP5. As these projections account for internal migration processes and spatial development patterns, they can provide new insights in a wide range of IAV assessments. Furthermore, the modeling approach can be extended to other continental or global scales due to its modest data requirements based on freely available global datasets.

This chapter is currently under review as:

Reimann, L., Jones, B., Nikolettopoulos, T., Vafeidis, A.T. *under review*. Accounting for internal migration in spatial population projections – A gravity-based modeling approach using the Shared Socioeconomic Pathways. Submitted to Environmental Research Letters.

### 3.1 INTRODUCTION

The future impacts of climate change will be driven by physical changes in climatic conditions as well as by changes in socioeconomic development (Field et al. 2014). Recent studies found that socioeconomic development can be the dominant factor in driving impacts, in particular in the first half of the 21<sup>st</sup> century when climatic changes still take place at a slower pace (Rohat et al. 2019c, Marsha et al. 2018) and in regions with rapid population growth (Rohat et al. 2019a, Jones et al. 2018, Brown et al. 2018, Monaghan et al. 2018). To assess future impacts in a comprehensive manner, it is therefore important to explore the range of uncertainty regarding changes in socioeconomic conditions in locations that are exposed to climate hazards (Moss et al. 2010, Ebi et al. 2014).

The current state-of-the-art socioeconomic scenarios in climate change research, the Shared Socioeconomic Pathways (SSPs), provide a suitable basis for exploring this uncertainty (O'Neill et al. 2014, O'Neill et al. 2020). Five global-scale SSPs describe plausible alternative trends in socioeconomic development in the course of the 21st century based on societal challenges to climate change mitigation and adaptation. Each SSP has an underlying narrative that describes the socioeconomic developments of the SSP in qualitative terms (O'Neill et al. 2017; APPENDIX B, SM3.1); furthermore, the narratives have been quantified to produce national-level projections of key variables in Impacts, Adaptation, and Vulnerability (IAV) research (van Ruijven et al. 2014) such as population (KC and Lutz 2017), urbanization (Jiang and O'Neill 2017), and GDP (Leimbach et al. 2017, Dellink et al. 2017, Crespo Cuaresma 2017).

However, national-level projections can be applied in IAV research to a limited degree as these assessments require spatially downscaled projections of key variables (van Ruijven et al. 2014, van Vuuren et al. 2010), with population being one of the most-used indicators for characterizing future impacts, for instance with regard to heat stress (Jones et al. 2015, Rohat et al. 2019a), water scarcity (Chen et al. 2017, Veldkamp et al. 2016, Hanasaki et al. 2013), river flooding (Jongman et al. 2015, Winsemius et al. 2016), and coastal flooding (Hinkel et al. 2014, Neumann et al. 2015, Tiggeloven et al. 2020). A number of previous studies have spatially downscaled population projections to the grid cell level, using the national-level SSP projections as boundary conditions, for example at global scale (Jones and O'Neill 2016, Murakami and Yamagata 2019), with a focus on coastal population growth (Merkens et al. 2016); at continental scale, for Africa (Boke-Olén et al. 2017), Europe (Lüthenkötter et al. 2017, based on Batista e Silva et al. 2016), and the Mediterranean region (Reimann et al. 2018a); and at national scale, for the US (Zoraghein and O'Neill 2020a, Zoraghein and O'Neill 2020b) and China (Chen et al. 2020c).

Besides their different regional contexts, these gridded population projections differ in terms of spatial resolution, input data, and modeling approaches used. The spatial resolution of the projections ranges from 100m (Chen et al. 2020c) to 0.5° (Murakami and Yamagata 2019), depending on the complexity of the modeling approach, the intended application of the projections, and the regional focus of the study. Modeling approaches range from simple rescaling techniques (Lüthenkötter et al. 2017) to more data-intensive approaches using

distance measures from existing settlements, roads, and other infrastructure as modeling variables (Boke-Olén et al. 2017, Murakami and Yamagata 2019, Chen et al. 2020c). The approach of Merkens et al. 2016 (also used in Reimann et al. 2018a) employs a rescaling technique that differentiates population development in coastal versus inland locations. However, it does not include spatial changes in settlement patterns (i.e. urban sprawl), which are accounted for in the gravity-based approach used by Jones and O’Neill 2016 (also used in Zoraghein and O’Neill 2020a, Zoraghein and O’Neill 2020b). The approaches of Merkens et al. 2016 and Jones and O’Neill 2016 have modest data requirements, primarily relying on spatial population distributions of two time steps as model input; therefore both approaches are suitable for applications at continental to global scales where consistent input data are often lacking (Leyk et al. 2019, Vafeidis et al. 2008).

None of the above-mentioned approaches account for both urban development patterns and inland-coastal migration, although these two processes are considered key drivers of future climate change impacts, in particular in coastal locations (Merkens et al. 2018, Neumann et al. 2015, Seto et al. 2011). Historically, coastal locations have experienced high population growth, resulting in higher population densities and urbanization levels compared to inland locations (McGranahan et al. 2007, Kummur et al. 2016). Accordingly, the majority of megacities (>8 million inhabitants) are located in low-lying coastal areas (Brown et al. 2013). With urbanization projected to increase in the course of the 21st century under all SSPs (Jiang and O’Neill 2017), these settlement patterns are expected to continue in the future (Nicholls et al. 2008b, Merkens et al. 2016).

We address this gap by extending the gravity-based approach of Jones and O’Neill 2016 to account for distinct changes in settlement patterns (i.e. urban sprawl) in coastal versus inland locations. For capturing inland-coastal as well as rural-urban migration processes, we refine the spatial resolution from a resolution of 7.5 arc minutes (approximately 15km at the equator) to 30 arc seconds (approximately 1km). We use freely available global-scale input data to calibrate the model to observed changes in spatial population patterns in coastal and inland locations, using the Mediterranean region, a socioeconomically diverse region characterized by a densely populated and highly urbanized coastal zone (Lange et al. 2020, European Environment Agency (EEA) 2014), as a case study.

This regional focus allows us to calibrate the model to two geographical regions based on the largest current differences in socioeconomic development across the region, the northern<sup>5</sup> and the southern and eastern<sup>6</sup> Mediterranean (Reimann et al. 2018a). Based on the calibrated model parameters for the two geographical regions and coastal versus inland locations, we produce gridded population projections in 10-year time steps from 2020 to 2100 for each SSP that reflect the development patterns described in the SSP narratives. These projections explore the uncertainty space regarding plausible future population patterns in a comprehensive manner, and be used in a wide range of IAV assessments.

---

<sup>5</sup> Northern Mediterranean countries include Andorra, Croatia, Cyprus, France, Greece, Italy, Malta, Monaco, San Marino, Slovenia, Spain, The Vatican, and the British overseas territory Gibraltar.

<sup>6</sup> Southern and eastern Mediterranean countries include Algeria, Albania, Bosnia and Herzegovina, Egypt, Israel, Lebanon, Libya, Montenegro, Morocco, Palestine, Syria, Tunisia, and Turkey.

In section 3.2, we describe the modeling approach in more detail, including model calibration, validation, and modifications made to produce the population projections. In section 3.3, we present and describe the spatial population patterns by SSP and geographical region, focusing particularly on developments in urban population density and in coastal population across the SSPs and the 21<sup>st</sup> century. We then critically evaluate our modeling approach for producing meaningful spatial population projections in the context of IAV research by comparing our results to previous work and by reflecting upon the model limitations. Last, we conclude with ideas of how to further refine the model in future work.

## 3.2 METHODS

The following sections provide an overview of the extensions implemented in the gravity-based model to be able to produce spatial population projections that account for spatial development patterns (i.e. urban sprawl) as well as for rural-urban and inland-coastal migration. Please consult SM3.2-3.7 for further methodological detail (as referenced in the text).

### 3.2.1 Modeling approach

We used and extended the gravity-based population model described in Jones and O’Neill 2016, Jones and O’Neill 2013, and Rigaud et al. 2018. Demographic gravity models are based on Newton’s law of gravity and gravitational potential, assuming that densely populated locations are more attractive for human settlement than less densely populated locations (so-called ‘population potential’ (Grübler et al. 2007)), and that relative attractiveness decreases with increasing distance between locations (Anderson 2011). The basic notion underlying this assumption is that factors such as transport costs and travel times determine the spatial interaction of two places, which decreases with increasing distance (Rich 1980). This effect is called ‘distance-decay’ and is often represented with a negative exponential function (Skov-Petersen 2001, Iacono et al. 2008).

In addition to the distance-decay effect, we account for the contribution of local characteristics to the attractiveness of a location. Accordingly, we calculate a population potential  $v$  for each grid cell  $i$  and time step  $t$  that represents the attractiveness of any given location:

$$v_i(t) = l_i \left( \sum_{j \in N_i} P_j(t) e^{-\beta d_{ij}} + A_i P_i(t) \right) \quad (3.1)$$

where  $l_i$  is the proportion of cell  $i$  available for human settlement<sup>7</sup>,  $P$  is the population of cell  $j$  or  $i$  at time  $t$ ,  $\beta$  is a parameter reflecting the strength of the distance-decay effect,  $d_{ij}$  is the distance between cells  $i$  and  $j$ , and  $A_i$  is a factor reflecting the local attractiveness of cell  $i$ . The

---

<sup>7</sup> Please see SM3.2 for a description of how the spatial mask ( $l_i$ ) was produced.

number of neighboring cell indices  $N_i$  is determined by the gravity window within which the distance-decay effect applies.

We calculate  $v_i(t)$  separately for urban and rural populations, based on unique urban and rural  $\beta$  parameters for coastal and inland locations<sup>8</sup>, and distinct gravity windows for the two geographical regions (see next section for further detail). We then spatially distribute the national-level population of  $t+1$  to each grid cell proportional to  $v_i(t)$ .

### 3.2.2 Calibration

The model is calibrated to historical changes in population patterns; therefore, spatial population data for at least two time steps are required. We used the Global Human Settlement Layer (GHSL) (Florczyk et al. 2019) population data (GHS-POP) of the years 1990, 2000, and 2015, available at a spatial resolution of 30 arc seconds (WGS84 coordinates) (Schiavina et al. 2019). GHS-POP was developed by spatially distributing the population of the Gridded Population of the World version 4 (GPWv4) (Center for International Earth Science Information Network - CIESIN - Columbia University 2017) based on built-up area identified with the help of satellite imagery for each time step (Freire et al. 2016). As we calibrated the model to two ten-year time steps (i.e. 1990-2000; 2000-2010), we established the population distribution of 2010 by linearly interpolating the GHS-POP data of the years 2000 and 2015.

Following Jones and O'Neill 2016, we calibrated the model separately to urban versus rural changes in population patterns. Therefore, we defined the urban population per grid cell using the GHS-based settlement model (GHS-SMOD) (Florczyk et al. 2019, Pesaresi et al. 2019). To harmonize the total urban population per country based on GHS-SMOD with the UN World Urbanization Prospects' (WUP) urbanization level for each country (United Nations, Department of Economic and Social Affairs, Population Division 2019), we added (deducted) population from densely populated neighboring grid cells to (from) the urban population in a series of three steps until the urban population numbers matched those of the WUP (SM3.4).

We established the distance parameter  $\beta$  for urban and rural locations by minimizing the sum of the squared errors produced by the model at the grid cell level for each ten-year calibration period, following Jones and O'Neill 2016. As not all countries were equally suitable for this procedure due to differences in the currency and spatial detail of the census and administrative unit data underlying GHS-POP (Center for International Earth Science Information Network - CIESIN - Columbia University 2017), we selected one country per geographical region (i.e. Spain, Tunisia) as representative of the migration processes in the region. We tested different gravity windows for each region, assuming that a) daily trip distances in the Mediterranean are shorter than the 100km window used by Jones and O'Neill<sup>9</sup>, and b) daily trip distances are shorter in the southern and eastern Mediterranean compared to the northern Mediterranean, using the lower motorization rate as a proxy for trip distances (Eurostat 2019) due to a lack of

<sup>8</sup> Please see SM3.3 for a description of the coastal zone definition used in this study.

<sup>9</sup> Jones and O'Neill (2013) established the gravity window size based on daily trip distances in the US (see their supplementary data).

consistent region-wide data. We found a gravity window of 20km for the northern and 10km for the southern and eastern parts of the region to best reflect the distance-decay effect. Finally, we averaged the established urban and rural  $\beta$  parameters across the two calibration periods and modified them to be able to account for differences in population development patterns in coastal versus inland locations (SM3.5).

In a next step, we calculated the local attractiveness factor  $A_i$  in urban and rural locations for each country and grid cell by eliminating the grid-cell error  $\varepsilon_i$  produced when accounting for the distance-decay effect only. Therefore, we ran equation (3.1) for the calibration period, applying the established coastal rural (CR), inland rural (IR), coastal urban (CU), and inland urban (IU)  $\beta$  parameters in the respective settlement type (i.e. CR, IR, CU, IU). As  $A_i$  attained extremely high (low) values in some cells, we applied a two-step post-processing approach. First, to remove outliers, we used the middle 50% (so-called interquartile range, IQR) of the  $A_i$  distribution per country. Second, we scaled  $A_i$  to values ranging from -100 to 100, while retaining the original distribution of  $A_i$  per country. Using this approach, we avoided overfitting the model to the historical changes in population patterns observed during the calibration period.

**3.2.3 Validation**

We validated the model by projecting the 2010 population based on the calibration period 1990-2000. Figure 3.1 presents scatter plots of the modeled versus the observed population for the total population, for urban populations, and for rural populations (see SM3.6 for corresponding Q-Q plots). The plots illustrate better model performance for urban populations compared to rural populations, with the best performance achieved when combining urban and rural populations (panel a), as reflected in  $R^2$  and the root mean square error (RMSE). These findings agree with the findings of Jones and O’Neill 2013. A map presenting the error per grid cell relative to the observed population per cell (= relative absolute error, RAE) for the entire Mediterranean region can be found in SM3.6.

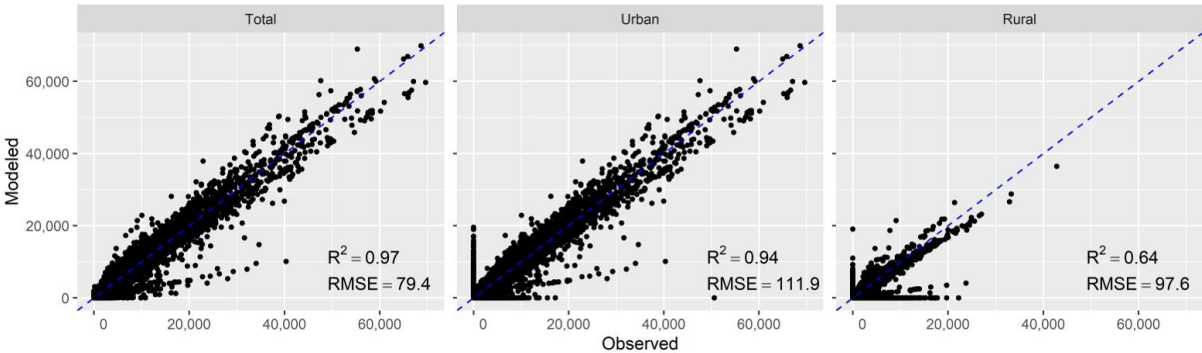


**Figure 3.1** Scatter plots of the total population, urban populations, and rural populations, along with  $R^2$  and the Root Mean Squared Error (RMSE). Blue line represents the perfect fit



We calculated further error metrics for the region to evaluate model performance in rural (CR, IR) and urban (CU, IU) locations as well as the entire Mediterranean region (Supplementary Table 3.3). In the entire Mediterranean region, the model produced a mean absolute error (MAE) of 6.6, and a weighted mean absolute percentage error (WMAPE) (weighted by the population) of 14.7%, which compared well with the original version of the model that produced a WMAPE of 11.6% at the US level (Jones and O’Neill 2013). These error metrics also illustrated better model performance in urban versus rural locations (WMAPE of 18.3% versus 34.4%) as well as in coastal versus inland locations (WMAPE of 30.9% in CR versus 35.7% in IR; 18% in CU versus 18.5% in IU).

### 3.2.4 Population projections

To produce downscaled population projections with the extended version of the model that are consistent with the SSPs, we used the national-level population (KC and Lutz 2017) and urbanization (Jiang and O’Neill 2017) projections provided in the SSP database (International Institute for Applied Systems Analysis (IIASA) 2018) as boundary conditions. To reflect the future spatial development patterns per SSP, we modified the calibrated  $\beta$  parameters for each SSP by interpreting the qualitative assumptions described in the global SSP narratives (O’Neill et al. 2017, Jiang and O’Neill 2017) and the Mediterranean coastal SSP narratives (Reimann et al. 2018a), and by conducting a sensitivity analysis (SM3.7). Additionally, we applied SSP-specific population density thresholds per grid cell based on the observed maximum population density of 2015, and accounted for future changes in habitability under the SSPs by adjusting the spatial mask  $l_i$ . Finally, we produced population projections in ten-year time steps from 2020-2100 and for each SSP by modeling urban and rural populations separately based on the respective coastal and inland  $\beta$  parameters. We further redefined some rural and urban population cells after each time step based on population density and contiguity (following Jones and O’Neill 2016) before combining them to obtain the total population.

## 3.3 RESULTS

The spatial population projection datasets produced for each SSP and ten-year time step are publicly available at <https://figshare.com/s/b4e5cadb9b1965ed010f><sup>10</sup>. Figure 3.2 presents a selected set of these data, including the baseline (2010) along with each SSP in 2100. These spatial population patterns reflect the national-level population (KC and Lutz 2017) and urbanization projections (Jiang and O’Neill 2017) (SM3.8) as well as the qualitative assumptions regarding spatial development patterns described in each SSP (O’Neill et al. 2017).

In SSP1, countries experience rapid urbanization, with urbanization levels of around 95% (2100) across the entire region. Effective management combined with population decline in the second half of the century results in high-density, compact urban settlements. In SSP2,

---

<sup>10</sup> This link will be replaced by a DOI that will be activated upon publication.

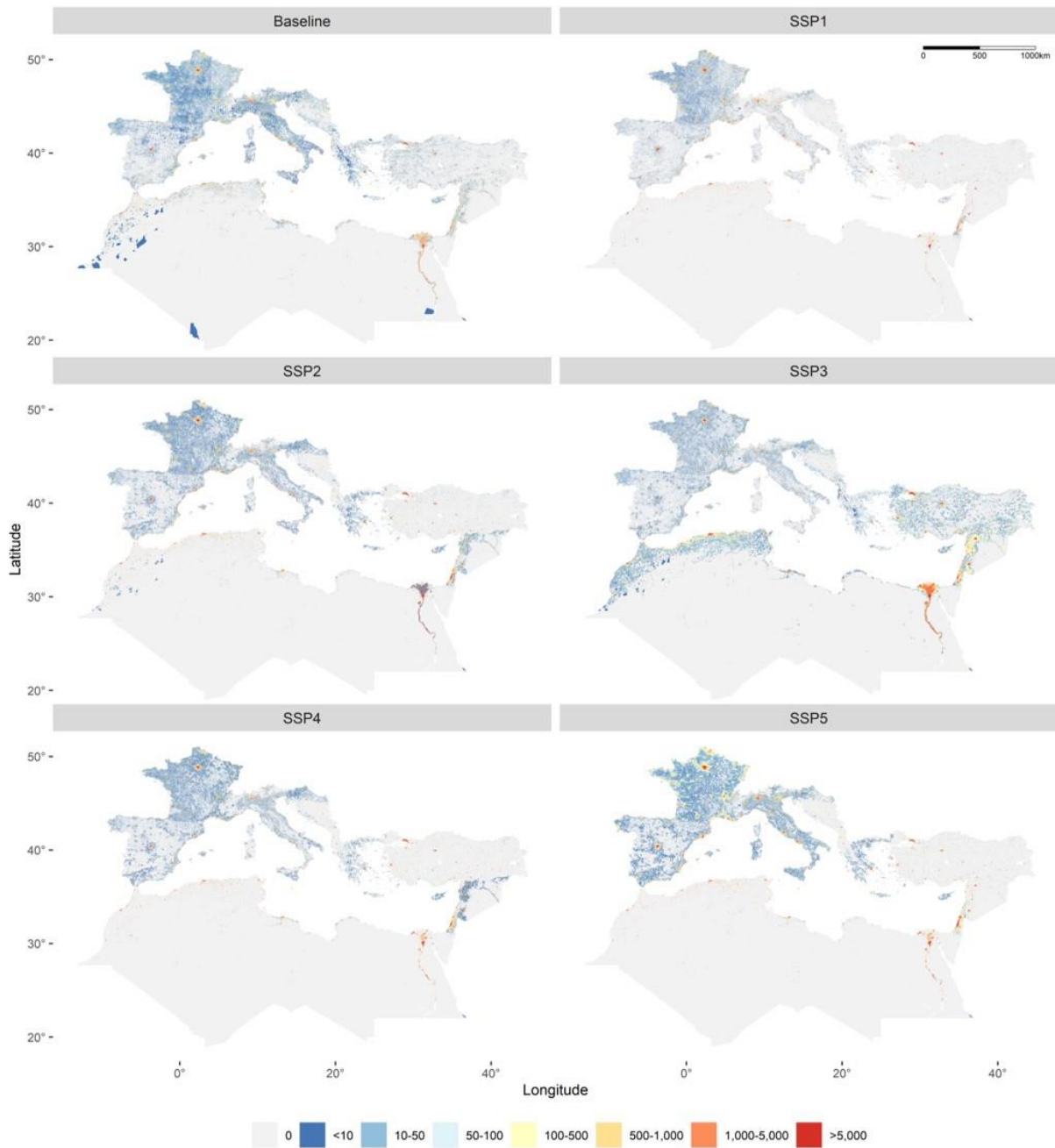


**Figure 3.2** Population per grid cell in the baseline (2010) and for each SSP in 2100. Resolution: 30 arc seconds (WGS84)

urbanization is less rapid, with higher urbanization levels in the northern parts of the region (ca. 93%) compared to the South and East (roughly 85%). Population growth is mixed across countries and spatial development is slightly more concentrated than observed in historical patterns, leading to urban sprawl in countries with high urbanization levels and a growing population (e.g. France, Israel). SSP3 is characterized by low urbanization rates, with urbanization levels of roughly 84% in the northern Mediterranean and 65% in the southern and eastern Mediterranean. Population declines in almost all northern countries and increases rapidly in southern and eastern countries, resulting in sprawling development in the South and East. In SSP4, urbanization increases rapidly, with urbanization levels of around 93% across

the region. Population decreases in most countries, notable exceptions being France and countries of the Middle East, where high urban sprawl can be observed until 2100. SSP5 is characterized by urbanization levels similar to those in SSP1, combined with rapid population growth in northern countries and the Middle East, which leads to considerable urban sprawl, particularly in northern parts of the region.

These population development patterns are further illustrated in Figure 3.3 which presents urban population densities per SSP and geographical region. In the baseline (2010), urban population density is about four times higher in southern and eastern Mediterranean countries than in countries of the Mediterranean North (Figure 3.3a); this difference is projected to increase until 2100 under all SSPs, with the largest difference in SSP3, where urban settlements are projected to be eight times more densely populated in the South and East. In northern countries, urban population density increases in SSP1 and decreases in all other SSPs in 2100, compared to the baseline. The highest urban population density (1,600 people/km<sup>2</sup>) is projected in SSP1 and the lowest density of roughly 700 people/km<sup>2</sup> in SSP5. These results reflect the continuation of high urban sprawl (except in SSP1), in combination with population decline in the second half of the century in SSPs 1-4. In the South and East, urban population density increases in SSPs 1-3 and decreases in SSPs 4 and 5 until 2100, compared to 2010. The highest urban population density of over 8,000 people/km<sup>2</sup> is projected in SSP3, the scenario with the highest expected population growth in these countries; the lowest density of ca. 4,150 people/km<sup>2</sup> is projected under SSP4.

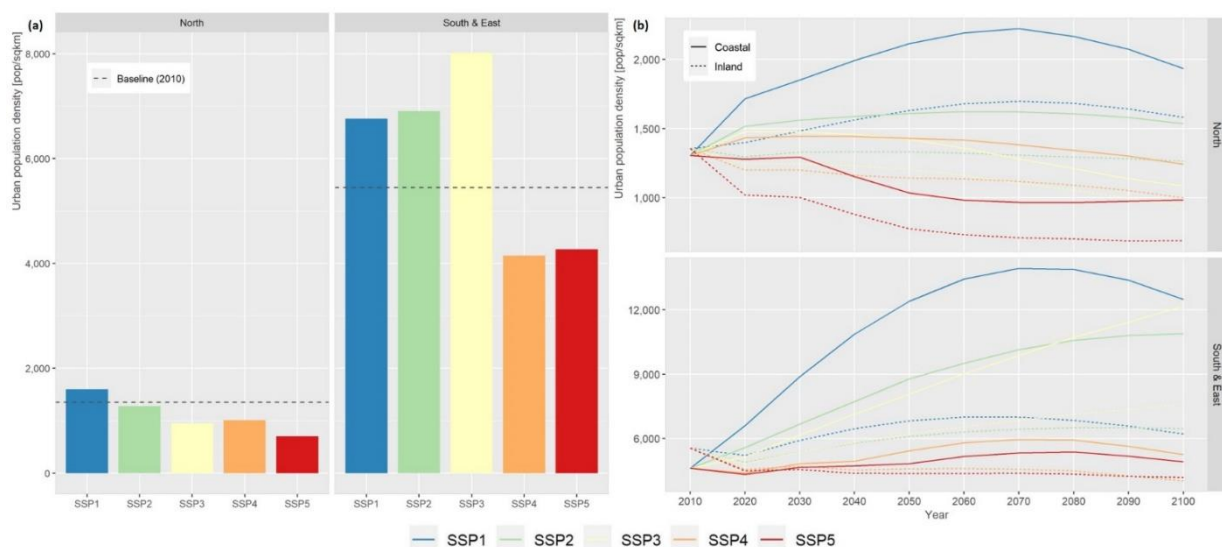


**Figure 3.3** Urban population density in each SSP and geographical region. (a) In 2100 compared to 2010, (b) development 2010-2100 in coastal versus inland locations. Coastal = Low Elevation Coastal Zone (see SM3.3; McGranahan et al 2007). Please note different scales of the y-axes

Figure 3.3b presents the development of urban population densities in the course of the century, differentiating between coastal and inland locations. In both geographical regions, density is higher in coastal locations compared to inland locations under all SSPs and time steps except the base year. In the Mediterranean North, urban population density in coastal locations first increases in SSPs 1-4, before it decreases in the second half of the century; in inland locations,

density decreases in the course of the century in all SSPs except SSP1 where it first increases and starts to decrease in 2080. In the South and East, urban population density increases in coastal and inland locations under SSPs 1-3, with a rapid increase in coastal locations, which levels off in SSP1 from 2080 onwards. Under SSPs 4 and 5, urban population density experiences some increase in coastal locations until 2070 and remains on a similar level in inland locations in the course of the century.

Comparing the population in coastal locations across SSPs and geographical regions (Figure 3.4), we observe, similar to urban population density, a population three orders of magnitude higher in coastal locations in southern and eastern countries compared to the Mediterranean North in 2010 (Figure 3.4a). This difference is projected to increase until 2100 under all SSPs except SSP5 where coastal population increases considerably in the northern Mediterranean as well, resulting in the highest coastal population (15.2 million) in 2100. Further, the number of people in coastal locations in the North increases slightly in SSP1 and SSP2 and decreases in SSPs 3 and 4 compared to the baseline, with the lowest number of roughly 6.5 million people in coastal locations under SSP3. In the South and East, we observe the opposite development: the highest coastal population of over 100 million in 2100 is projected under SSP3, whereas we find the lowest coastal population of ca. 42.7 million under SSP5. Nonetheless, the number of people in coastal locations of southern and eastern countries increases under all SSPs compared to the baseline. These results reflect the higher attractiveness of coastal locations compared to inland locations in both geographical regions, which is amplified in the southern and eastern Mediterranean by a limited land area available for human settlement in inland locations (SM3.2), and superimposed by country-level population decline in the northern Mediterranean under SSPs 3 and 4 (SM3.8).

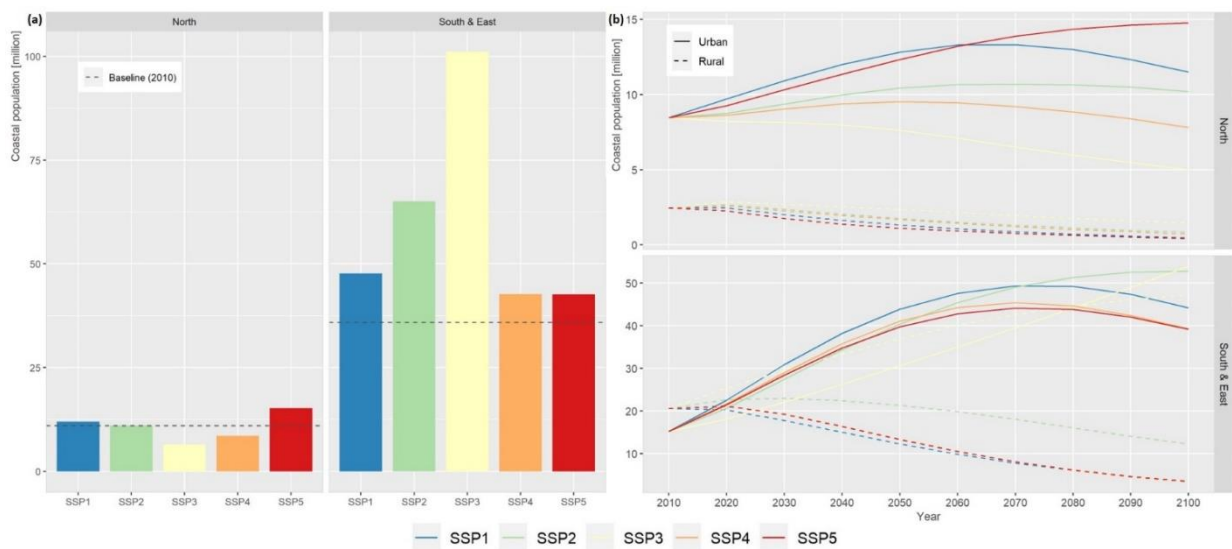


**Figure 3.4** Coastal population in each SSP and geographical region. (a) In 2100 compared to 2010, (b) development 2010-2100, differentiating urban versus rural populations. Coastal = Low Elevation Coastal Zone (see SM3.3; McGranahan et al 2007). Please note different scales of the y-axes

In Figure 3.4b, the development of the coastal population in the course of the century is shown for urban versus rural populations. In the northern Mediterranean, the coastal population lives primarily in urban settlements under all SSPs. It first increases under all SSPs except SSP3, where it decreases gradually in the course of the century. In the second half of the century, the urban population in coastal locations also declines in SSPs 1, 2, and 4. The coastal population in rural settlements decreases slowly under all SSPs. In southern and eastern countries, a similar share of the coastal population lives in urban and rural settlements in 2010, which changes considerably until 2100, when the vast majority of people in coastal locations are projected to live in urban settlements under all SSPs except SSP3. Urban population in coastal locations increases markedly under all SSPs and starts to decline in 2080 under SSPs 1, 4, and 5. The coastal population in rural settlements continuously increases under SSP3 until 2100, and gradually decreases under all other SSPs, in particular in the second half of the century.

### 3.4 DISCUSSION

Our spatially downscaled population projections account for important migration processes within countries (i.e. rural-urban and inland-coastal) as well as for plausible future spatial development patterns (i.e. urban sprawl). As such they constitute improved representations of future population distributions and are useful for a wide range of IAV assessments. The spatial resolution (30 arc seconds) is suitable for capturing these development trends and patterns while avoiding a misleading impression of certainty as future socioeconomic developments are highly uncertain (Preston et al. 2011, Sherbinin et al. 2019). Therefore, we anticipate that the developed projections are particularly meaningful for assessments at continental to regional scales, for example for analyzing exposure to extreme heat, water scarcity, and flooding (coastal, fluvial, pluvial). The insights of such assessments can support decision-making, for example in the context of adaptation planning or spatial planning, to ensure that decisions are robust under a wide range of futures (Moss et al. 2010, Walker et al. 2013, Haasnoot et al. 2020). For local-scale assessments, other methods can be used for further downscaling the developed projections (e.g. Merkens and Vafeidis 2018).

Our results suggest higher future climate change exposure in southern and eastern Mediterranean countries compared to northern Mediterranean countries due to consistently higher urban densities and coastal population under all SSPs. However, exposure would differ markedly across SSPs, depending on the socioeconomic challenges for adaptation that result from differences in the effectiveness of policies and institutions, economic growth, and technological change among others (O'Neill et al. 2017). Assuming that an increase in urban population density increases the urban heat island (UHI) effect, therefore leading to higher urban heat stress, which will exacerbate due to climate change (Chapman et al. 2017, Koomen and Diogo 2017, Vanos et al. 2020), heat exposure would be highest under SSP3 in the South and East and SSP1 in the North. As SSP1 is characterized by sustainable development with well-managed, compact urban areas and low adaptation challenges, it would result in potentially lower exposure than SSP3 (assuming all else equal), as SSP3 is characterized by high adaptation challenges due to slow economic growth, low technological development, and weak policies

and institutions. Similarly, coastal exposure would be highest in the South and East under SSP3, with a large share of the coastal population living in rural settlements, where coastal protection is expected to be rarely pursued as costs often exceed benefits (Lincke and Hinkel 2018). In the North, coastal exposure would be highest under SSP5 and SSP1, which are both characterized by low adaptation challenges. Due to high urban sprawl in SSP5, we expect coastal adaptation to be more challenging than in SSP1. Furthermore, as SSP5 experiences rapid economic growth, residual risk would be high, leading to high damages in case of adaptation failure during coastal flooding. While we are aware that the future lies somewhere between (or even beyond) the five SSPs (O'Neill et al. 2020, O'Neill et al. 2017), our results suggest that future spatial population patterns will contribute to higher exposure in the southern and eastern Mediterranean, which may exacerbate already existing disparities between the two geographical regions (MedECC 2020b).

To be able to further contextualize these results, the population projections can be enriched by additional demographic and socioeconomic variables important for IAV research, such as age, sex, race, education, poverty, and income. Such extensions are sparse in the current literature, with few examples that have downscaled IAV variables with the help of SSP-based population projections at national (i.e. the US) (Hauer 2019), European (Hurth et al. 2017, Rohat et al. 2019b), and global scales (Murakami and Yamagata 2019). Furthermore, our projections do not account for the potential impacts of climate change on migration, which is expected to increase once impacts such as flooding, heat stress, and droughts become more severe (Black et al. 2011, McLeman 2019). To account for this effect, plausible future changes in climatic conditions based on the Representative Concentration Pathways (RCPs) (van Vuuren et al. 2011a) can be integrated into the model to produce projections that account for climate change-induced migration, a first example being the work of Rigaud et al. 2018. Such integrated assessments can additionally explore potential feedbacks between climate change, adaptation strategies, and migration patterns, which are expected to influence future impacts substantially (Aerts et al. 2018).

Furthermore, we compared our results to those of previous work that accounted either for inland-coastal migration (Merkens et al. 2016, Reimann et al. 2018a) or for urban sprawl (Jones and O'Neill 2016, downscaled by Gao 2017). We find that the population numbers projected in coastal locations in 2100 for each SSP are similar across the four studies, but also show marked differences (Figure 3.5). Similar to Jones and O'Neill, we project the highest coastal population of 108 million in SSP3 and the lowest population of 51 million in SSP4. However, we project a higher coastal population than Jones and O'Neill under all SSPs except SSP3, reflecting the higher attractiveness of coastal locations implemented in our approach. The coastal approach of Merckens et al. and Reimann et al. projects the lowest coastal population of 41/35 million in SSP1, based on the assumption that sustainable and effective management of coastal areas reduces their attractiveness. In SSP5, the coastal approach results in a comparatively high coastal population of 54/61 million as it assumes coastal locations to be very attractive, while not accounting for the sprawling development that we assume under SSP5. In total, our results deviate most from the other approaches in SSP1, with a difference of up to 25 million coastal inhabitants. This difference reflects one limitation of the gravity approach, which models



aggregate population trends primarily based on the distance-decay effect (section 3.2.1) and does not account for the effects of policy on a location's attractiveness. Future work can integrate such effects into the model as an additional model layer similar to the spatial mask ( $l_i$ ).

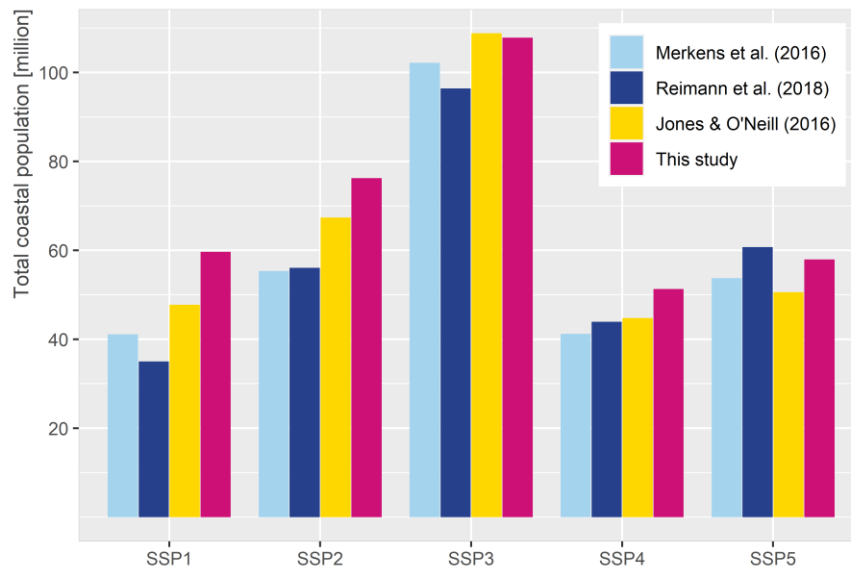


**Figure 3.5** Mediterranean coastal population in 2100 based on Merkens et al 2016, Reimann et al 2018, Jones and O'Neill 2016 (downscaled projections of Gao 2017), and the approach used in this study. Coastal = Low Elevation Coastal Zone, based on MERIT DEM (Yamazaki et al 2017)

When using our population projections, the following additional limitations need to be considered. First, we calibrated the model to a relatively short period of twenty years due to a lack of long-term gridded population data. This period was characterized by population growth in most Mediterranean countries. As we expect to see declining population numbers in the second half of the century under almost all SSPs, the observed changes in population patterns are not necessarily indicative of future patterns. Second, since we were not able to calibrate the  $\beta$  parameters for each country individually, the calibrated parameters may not reflect the spatial development patterns in all countries of the respective geographical region to the same degree. Similarly, we had to post-process the calibrated  $\beta$ s to reflect differences in development patterns in coastal versus inland locations as our calibration procedure did not produce plausible parameters for these locations. We assume the reason for this being the small strip of land defined as coastal compared to its inland counterpart, which may impede finding the optimal  $\beta$  parameter (section 3.2.2; SM3.5). Last, we would like to point out that the redefinition of grid cells into urban and rural populations after each projection time step (section 3.2.4) can follow a different algorithm than the one used in this study, one example being the ‘degree of urbanization’ (Pesaresi et al. 2016).

Despite its limitations, the extended gravity-based model produces plausible distributions of future population patterns for each SSP, which can be updated once new knowledge and data become available. The model allows for integrating additional model layers (e.g. a policy layer) as a weight on the population potential ( $v_i$ ), and can be extended to explore climate change-

induced migration, for example by correlating the local attractiveness factor  $A_i$  to changes in environmental conditions with the help of spatial regression models (Rigaud et al. 2018). Due to its modest data requirements, we expect the model to be particularly relevant for producing consistent projections in data-scarce regions like the Mediterranean region, where detailed region-wide data are often lacking (Lange et al. 2020). As we rely on freely available global input data, the model can easily be extended to other continents, regions, or the global scale, given that sufficient computing resources are available.

### 3.5 CONCLUSION

This paper presents SSP-based gridded population projections that account for rural-urban and coastal-inland migration processes as well as for spatial changes in settlement patterns (i.e. urban sprawl), which have been produced with an extended gravity-based model specifically developed for this study. We apply the model to the Mediterranean region, accounting for distinct characteristics in northern versus southern and eastern Mediterranean countries. Our projections have a spatial resolution of 30 arc seconds, a temporal resolution of ten-year time steps (2020-2100), and are consistent with the five SSPs, both in terms of qualitative narrative assumptions as well as national-level population projections. As these projections explore the range of uncertainty regarding plausible future spatial population patterns in the 21st century, they are useful for a wide range of IAV assessments. The model can be extended to account for the effects of climate change or spatial policies on a location's attractiveness for human settlement. As the model has modest data requirements and is calibrated to freely available global input data, it can be extended to other continental and/or global scales.

Future work can further refine the modeling approach by addressing its limitations such as separately calibrating the model to coastal versus inland locations; selecting a larger set of countries for the  $\beta$  calibration; and calibrating the model separately to phases of population growth and decline. A systematic assessment of the model's sensitivity to different population input data, urban versus rural population classification algorithms, and the choice of  $\beta$  parameters would further provide useful insights for model users. Moreover, the model can be extended for integrated assessments to explore feedbacks between climate change impacts, adaptation strategies, and migration processes. For such assessments, different SSPs, RCPs, and Shared Policy Assumptions (SPAs) (Kriegler et al. 2014) can be combined, as envisaged as part of the SSP-RCP-SPA scenario framework (van Vuuren et al. 2014, O'Neill et al. 2020). Additionally, future research can explore the potential of the model for producing spatial projections of other key variables in IAV research. Last, we would like to encourage use of the developed population projections in Mediterranean IAV assessments.



### Data availability statement

The gridded population projection datasets produced for each SSP and ten-year time step (2010-2100) are publicly available for download at <https://figshare.com/s/b4e5cadb9b1965ed010f><sup>11</sup>. The model scripts (R Core Team 2020) are available from the corresponding author upon reasonable request.

### Acknowledgements

We would like to thank Nora Bieker for her support in the sensitivity analysis. This work was initiated as part of a Fulbright doctoral scholarship that allowed LR to work at CIDR during a six-month research visit.

---

<sup>11</sup> This link will be replaced by a DOI that will be activated upon publication.



# 4 MEDITERRANEAN UNESCO WORLD HERITAGE AT RISK FROM COASTAL FLOODING AND EROSION DUE TO SEA-LEVEL RISE

---

UNESCO World Heritage sites (WHS) located in coastal areas are increasingly at risk from coastal hazards due to sea-level rise. In this study we assess Mediterranean cultural WHS at risk from coastal flooding and erosion under four sea-level rise scenarios until 2100. Based on the analysis of spatially explicit WHS data, we develop an index-based approach that allows for ranking WHS at risk from both coastal hazards. Here we show that of 49 cultural WHS located in low-lying coastal areas of the Mediterranean, 37 are at risk from a 100-year flood and 42 from coastal erosion, already today. Until 2100, flood risk may increase by 50% and erosion risk by 13% across the region, with considerably higher increases at individual WHS. Our results provide a first-order assessment of where adaptation is most urgently needed and can support policymakers in steering local-scale research to devise suitable adaptation strategies for each WHS.

This chapter is published as<sup>12</sup>:

Reimann, L., Vafeidis, A.T., Brown, S., Hinkel, J., Tol, R.S.J. 2018. Mediterranean UNESCO World Heritage at risk from coastal flooding and erosion due to sea-level rise. *Nature Communications* 9, 4161. DOI: 10.1038/s41467-018-06645-9.

---

<sup>12</sup> Please note: For consistency throughout the thesis, the term 'regional' has been changed to 'continental' in two instances when we refer to the scale of analysis. Further, British English has been changed to American English.

## 4.1 INTRODUCTION

Since 1972, the United Nations Educational, Scientific and Cultural Organization (UNESCO) designates the world's common heritage under the World Heritage Convention (UNESCO 1972). The World Heritage List of 2018 comprises a total of 1092 cultural and natural heritage sites, based on their Outstanding Universal Value (OUV) (UNESCO World Heritage Centre 2018). Over 77% of these sites are cultural World Heritage sites (WHS) which have high intangible value as they represent icons of human civilization (Terrill 2008, Cazenave 2014). A large share of cultural WHS are located in coastal areas as human activity has traditionally concentrated in these locations (Reeder et al. 2012, Benoit and Comeau 2005). As the risk of coastal hazards such as flooding and erosion increases with sea-level rise (SLR) (Marzeion and Levermann 2014), a considerable number of coastal WHS will gradually be exposed to these hazards in the future (Sabbioni et al. 2008, Marzeion and Levermann 2014), threatening the OUV of affected sites (UNESCO World Heritage Centre 2008, 2015b, Howard 2013, Phillips 2015) and potentially leading to losses in economic revenue as WHS are popular tourist destinations (Lollino et al. 2015, Phillips 2015). This is particularly true for the Mediterranean region as several ancient civilizations have developed in the region (Benoit and Comeau 2005, Cazenave 2014, European Environment Agency (EEA) 2014), resulting in a high concentration of cultural WHS in coastal locations. Due to the small tidal range and steep topography in coastal areas, ancient and current settlements are often located directly at the waterfront and hardly above sea-level (Benoit and Comeau 2005, UNEP/MAP 2017). Furthermore, adaptation methods and protection standards vary considerably across Mediterranean countries (Scussolini et al. 2016) due to large socioeconomic differences between northern, eastern and southern parts of the region (UNEP/MAP 2016, European Environment Agency (EEA) 2014), therefore leaving most WHS with limited protection from coastal hazards.

Although WHS are protected under the World Heritage Convention, countries themselves are responsible for their management, which includes adaptation to climate change (UNESCO World Heritage Centre 2007). However, WHS management plans rarely consider adaptation to SLR impacts (Phillips 2014, Howard 2013). Although climate change has been acknowledged as a threat to WHS in recent years (UNESCO World Heritage Centre 2008, Terrill 2008, Phillips 2014, Fatorić and Seekamp 2017), few studies have explored this aspect, leaving heritage managers and policymakers with little information on potential adaptation options. Therefore, previous work has called for more research identifying WHS at risk to inform adaptation planning and to ensure that their OUV is preserved (Perry 2011, UNESCO World Heritage Centre 2008, 2007, 2015b, Howard 2013, Howard et al. 2016). It has expressed the need for more robust data and modelling approaches on local to regional scales, as adaptation planning takes place at a national level and specific adaptation measures are implemented at a local level (UNESCO World Heritage Centre 2008, Howard 2013, Howard et al. 2016). The results of assessments based on these methods can support adaptation planning, especially in prioritizing adaptation strategies with limited financial resources (Sabbioni et al. 2008, Terrill 2008, Phillips 2014, Howard et al. 2016, Phillips 2015, Anderson et al. 2017).

Previous studies have primarily focused on local-scale assessments of various climate change impacts on UNESCO WHS (Howard 2013, Howard et al. 2016, Phillips 2014, 2015, Wang 2015, Daly 2011, Schmidt and Rudolff 2013) or on natural hazards, such as landslides and river floods, without directly considering climate change (Lanza 2003, Lollino et al. 2015, Hapciuc et al. 2016, Vojinovic et al. 2016, Cigna et al. 2018). To our knowledge, only one large-scale study has analyzed the long-term impacts of SLR on cultural UNESCO WHS (Marzeion and Levermann 2014). This study was based on aggregate WHS data provided on the UNESCO website, where every WHS is depicted by a point that represents its approximate center, even if the WHS consists of a number of so-called serial nominations (UNESCO World Heritage Centre 2015a). Consequently, the location of the point can substantially deviate from the location of the actual WHS. Further, none of the above-mentioned studies assessed the risks of coastal flooding due to extreme sea levels (ESL) or to coastal erosion due to SLR.

To address the current research gap, we assess Mediterranean UNESCO cultural WHS at risk from coastal flooding and erosion under four SLR scenarios from 2000 to 2100. We use an index-based approach that allows for ranking and comparing WHS at risk. For this purpose, we produce a WHS dataset containing spatially explicit representations of all Mediterranean WHS located in low-lying coastal areas. Results show that the vast majority of WHS at risk from either of the two hazards until 2100 are already at risk under current conditions. Risk will increase in the course of the century, its magnitude depending on the rate of SLR, with particularly high increases in coastal flood risk and at individual WHS. Our results can support adaptation planning in determining potential risk thresholds (tipping points) based on the temporal evolution of the indices. Additionally, based on the WHS most at risk policymakers can designate priority areas for further analysis in order to devise specific adaptation strategies.

## 4.2 RESULTS

### 4.2.1 UNESCO World Heritage in coastal areas

The modified and extended WHS dataset (Reimann et al. 2018b) comprises 159 data entries that represent inscribed (main) WHS (49) along with their serial nominations (110) located in the Mediterranean Low Elevation Coastal Zone (LECZ) which is defined as all land with an elevation of up to 10 m in hydrological connection to the sea (McGranahan et al. 2007). The data comprise attributes adopted from the original dataset and newly added attributes (e.g. heritage type, elevation, WHS location in urban settlements, distance from the coast). See APPENDIX C, Supplementary Table 4.1 for a complete list of attributes. Our analysis focuses on an aggregated version of the dataset that contains the 49 main WHS. Figure 4.1 shows the 49 main WHS located in the Mediterranean LECZ. Approximately one third of these WHS are located in Italy (15), followed by Croatia (7), Greece (4) and Tunisia (4). In most instances, only certain parts of the WHS (on average 35%) fall into the LECZ; five sites are fully located in the LECZ (Reimann et al. 2018b).

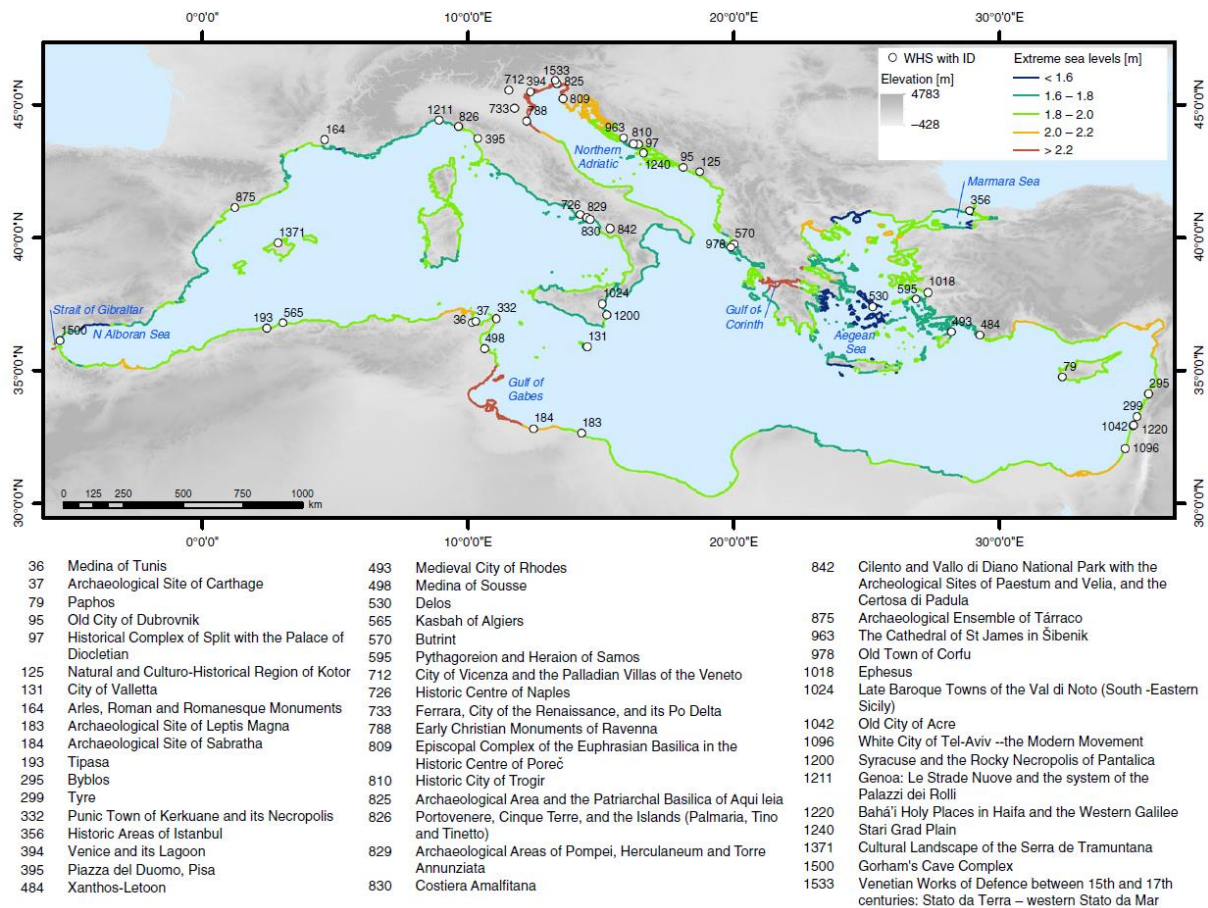


**Figure 4.1** UNESCO cultural World Heritage sites located in the Mediterranean Low Elevation Coastal Zone (LECZ). All sites are shown with their official UNESCO ID and name. The map also shows extreme sea levels per coastal segment based on the Mediterranean Coastal Database (Wolff et al. 2018a) under the high-end sea-level rise scenario in 2100

## 4.2.2 Flood risk

Under current conditions (base year 2000), 37 WHS are at risk from ESL, defined as the 100-year storm surge (including tides) plus the amount of SLR for the respective scenario and year (see section 4.4.3), which corresponds to 75% of all sites located in the LECZ. This number increases to 40 WHS at risk under the high-end (HE) scenario. The flood area ranges from 0.03% of the total WHS at Archaeological Site of Leptis Magna (183) and Cultural Landscape of the Serra de Tramuntana (1371) to 97% at Venice and its Lagoon (394), with a mean of 11.3%. The average flood area increases to over 14% in 2100 under the HE scenario, corresponding to an increase of 24% compared to 2000. Under Representative Concentration Pathway (RCP) 2.6, RCP4.5 and RCP8.5, the average flood area increases to around 12% in 2100 (Figure 4.2a). In 2000, the highest flood depth of 1.2m can be found at Archaeological Area and the Patriarchal Basilica of Aquileia (825) while the mean of maximum flood depths for all sites amounts to 0.4m. The maximum flood depth increases by approximately 70% to a mean of 0.6m under RCP2.6, 92% (over 0.7m) under RCP4.5, 121% (approximately 0.8m) under RCP8.5 and 290% (roughly 1.5m) under the HE scenario (Figure 4.2b), where the highest flood depth of 2.5m can be found at Venice and its Lagoon (394). The flood risk index that results from combining flood area and flood depth (see section 4.4.3) has a mean of 3.7 in 2000,

which increases by 25% to 4.6 under RCP2.6 and by almost 50% to 5.5 under the HE scenario (Figure 4.2c).

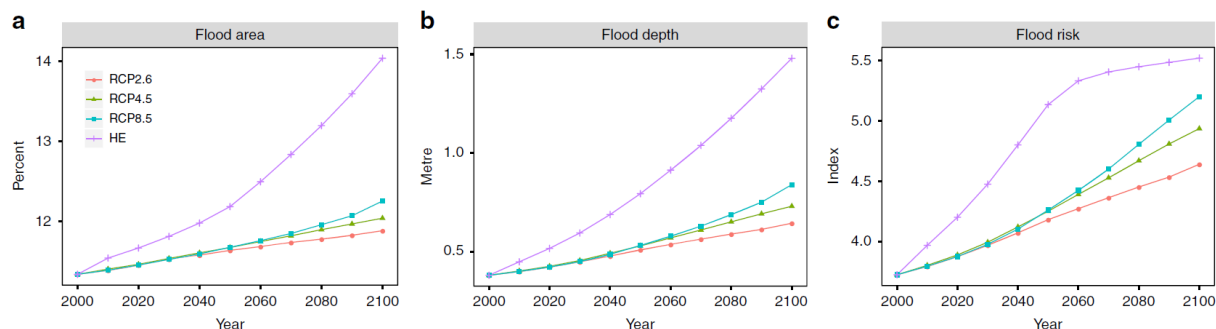


**Figure 4.2** Temporal evolution of the flood risk indicators at each World Heritage site, averaged across the Mediterranean region. Results are shown from 2000 to 2100 for RCP2.6, RCP4.5, RCP8.5 and the high-end (HE) scenario. a) Mean area flooded (in %), b) mean flood depth (in m), c) mean flood risk index

In the base year, the risk index ranges from 0 for those sites that are not at risk to a maximum of 10 at Venice and its Lagoon (394), Ferrara, City of the Renaissance, and its Po Delta (733) and Archaeological Area and the Patriarchal Basilica of Aquileia (825). These WHS are located along the northern Adriatic Sea where ESL are highest as high storm surges coincide with high regional SLR (Figure 4.1; Supplementary Figure 4.1). Under the HE scenario, a total of six WHS have the highest risk index of 10, four of which are located in Italy and two in Croatia (Figure 4.3). In 16 Mediterranean countries (including Gibraltar), at least one WHS is at risk under at least one of the four scenarios. The highest number of WHS at risk can be found in Italy (13), which corresponds to 87% of the Italian WHS located in the LECZ, followed by Croatia (6; 86%) and Greece (3; 75%). See also Supplementary Figure 4.2 for the flood risk indicators at each WHS and Supplementary Data 1 for the raw data of the indicators.

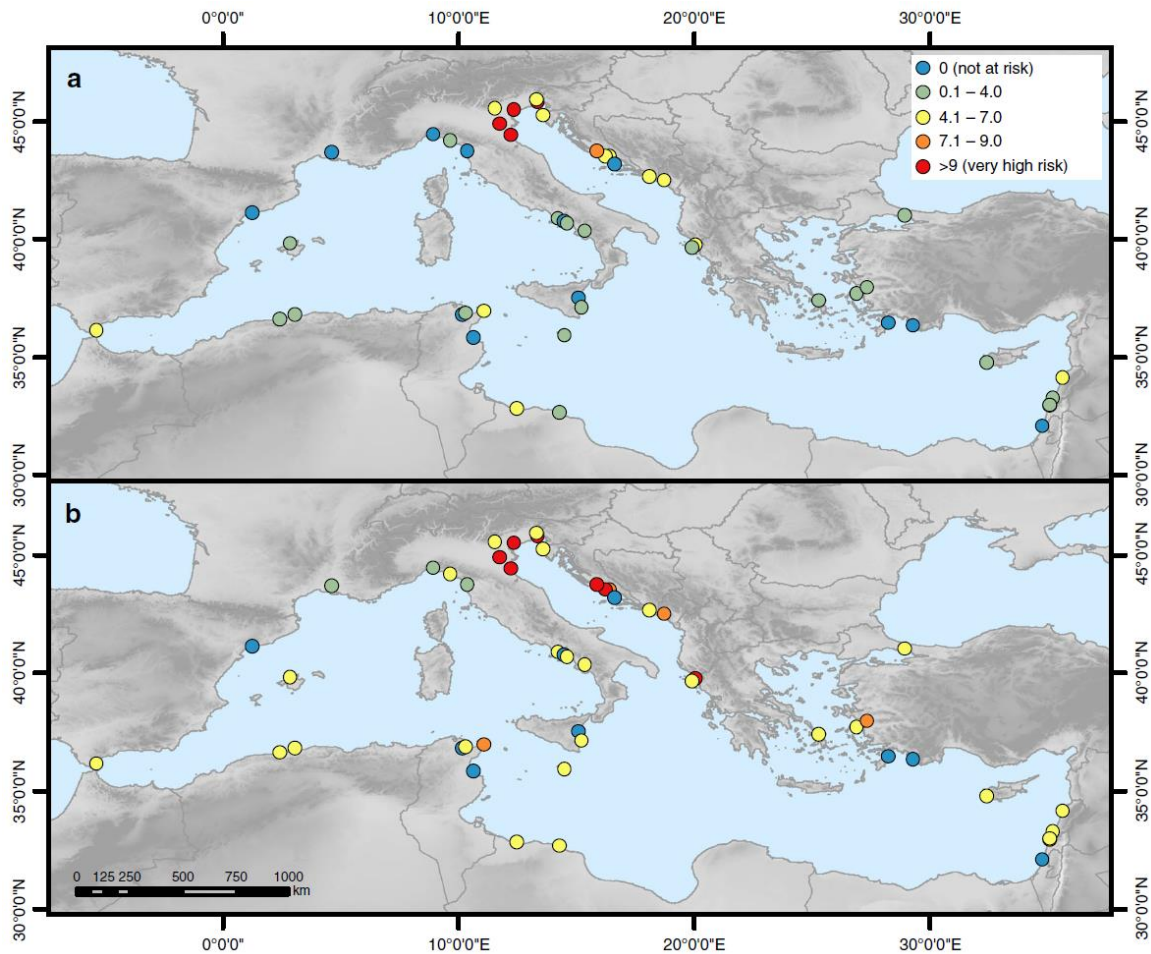


**Figure 4.3** Flood risk index at each World Heritage site under current and future conditions. a) In 2000 and b) in 2100 under the high-end sea-level rise scenario

### 4.2.3 Erosion risk

Under current conditions, 42 WHS are at risk from coastal erosion, which corresponds to 86% of all sites located in the LECZ. This number increases to 46 WHS under the HE scenario. Erosion risk is predominantly determined by the distance of a WHS from the coastline. Already in 2000, 31 WHS are at least partly located within 10m of the coastline, which increases to 39 sites under the HE scenario (Supplementary Figure 4.3), based on the assumption that all areas below the amount of SLR are permanently inundated (see section 4.4.4). The average distance from the coast decreases from roughly 1.1km in 2000 by 30% to 762 m under RCP2.6 and by more than 90% to slightly above 100m under the HE scenario (Figure 4.4a). As we assume the erosion risk indicators coastal material, mean wave height and sediment supply to remain constant in the course of the century, the erosion risk index increases only slightly from 2000 to 2100. The average erosion risk index increases from 6.2 in 2000 to 6.3 in 2100 under RCP2.6 and RCP4.5. Under RCP8.5 it increases to 6.4 and under the HE scenario it increases to 7, which corresponds to an increase of 13% compared to 2000 (Figure 4.4b).



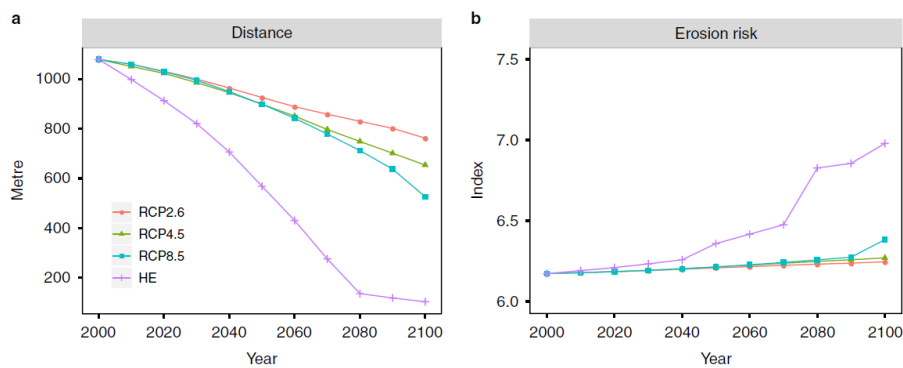


**Figure 4.4** Temporal evolution of two erosion risk indicators at each World Heritage site, averaged across the Mediterranean region. Results are shown from 2000 to 2100 for RCP2.6, RCP4.5, RCP8.5 and the high-end (HE) scenario. a) Mean distance from the coastline (in m), b) mean erosion risk index

In the base year, the erosion risk index ranges from 0 for those sites not at risk to 9.8 (very high) at Tyre (299) (Figure 4.5), which is located directly at the coastline (very high risk) and is characterized by sandy material (very high risk), a mean wave height of 0.7m (high risk) and sediment supply of just below  $1\text{mg l}^{-1}$  (high risk). The second highest risk index can be found at Pythagoreion and Heraion of Samos (595). Under the HE scenario, erosion risk remains highest at Tyre, followed by Archaeological Ensemble of Tàrraco (875), Pythagoreion and Heraion of Samos (595) and Ephesus (1018), all of which have a very high index of 9 and higher. Similar to flood risk, in 16 Mediterranean countries (including Gibraltar) at least one WHS is at risk from coastal erosion under at least one of the four scenarios. The highest number of WHS at risk can be found in Italy (14), which corresponds to 93% of the Italian WHS located in the LECZ, followed by Croatia (7; 100%) and Greece (4; 100%). Erosion risk varies moderately across the Mediterranean region and no regional pattern can be discerned as erosion risk indicators are mostly site-specific. (Please see Supplementary Figure 4.3 and Supplementary Figure 4.4 for the erosion risk indicators at each WHS and Supplementary Data 2 for the raw data of the indicators).

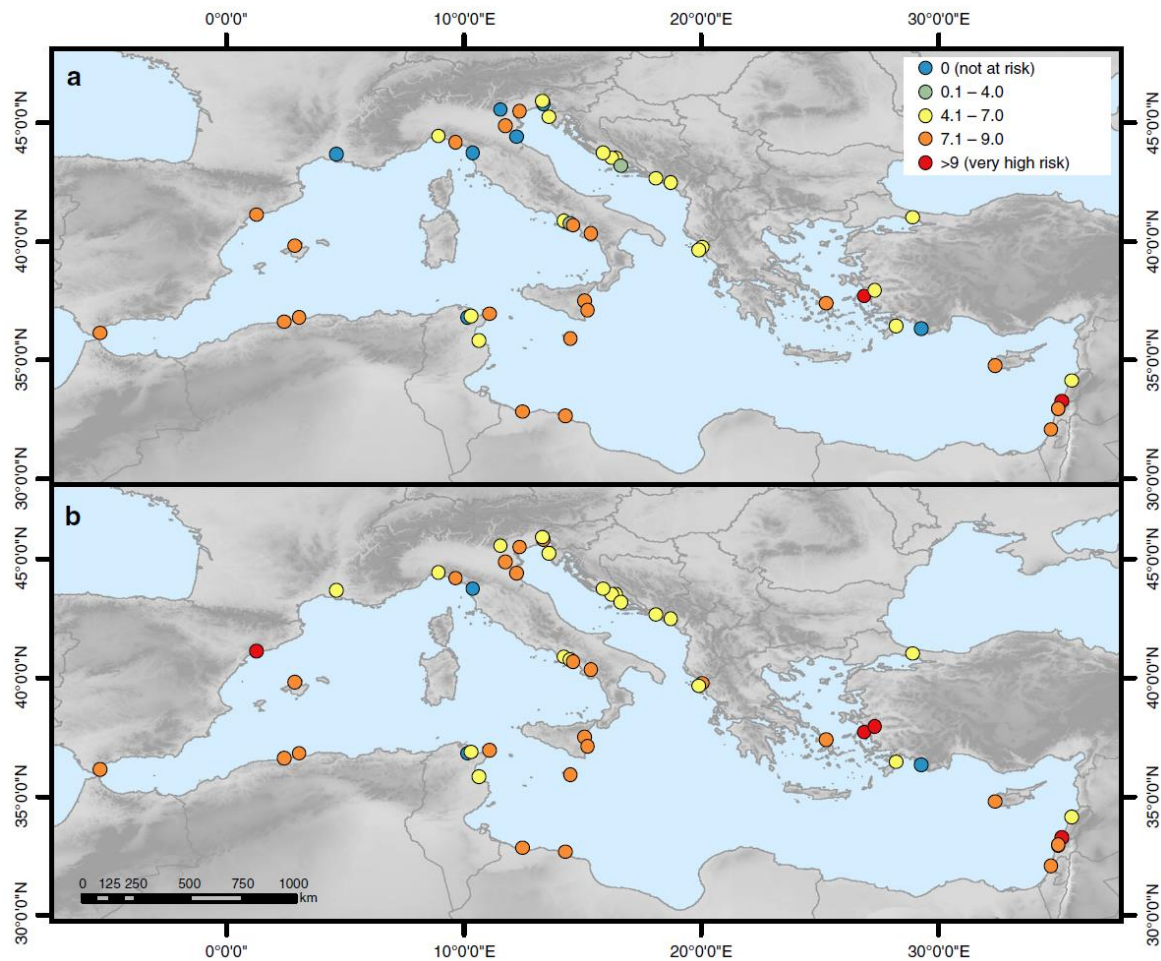


**Figure 4.5** Erosion risk index at each World Heritage site under current and future conditions. a) In 2000 and b) in 2100 under the high-end sea-level rise scenario

### 4.3 DISCUSSION

In this study, we assess UNESCO WHS at risk from coastal flooding and erosion under four SLR scenarios until 2100, based on revised and extended spatially explicit WHS data. The use of an index-based approach enables a quick evaluation of both risks that can easily be applied to other locations (Reeder-Myers 2015, Ramieri et al. 2011, Seenath et al. 2016). With the help of the risk indices we are able to rank and compare WHS, while at the same time we avoid attaching a monetary value to them (Moel et al. 2009). The results of this study can therefore support adaptation planning at different spatial scales: at the national scale, especially in countries with a large number of WHS at risk such as Croatia, Greece, Italy and Tunisia; at the EU scale, as, for example, regulated under the EU Floods Directive (European Union 2007); and at the basin scale, as prescribed under the Barcelona Convention which is the basis for the Mediterranean Action Plan and the Protocol on Integrated Coastal Zone Management (ICZM) in the Mediterranean (UNEP/MAP 2008). Our results can be particularly useful in designating priority areas with urgent need for adaptation and can serve as a basis for further, more in-depth assessments (McLaughlin and Cooper 2010). Furthermore, the temporal evolution of the risk indices and their individual components can provide valuable information on the point in time

when a WHS may be at risk or when a certain risk threshold may be exceeded (Anderson et al. 2017). This threshold can be referred to as an adaptation tipping point as its exceedance requires a (new) policy action (Hermans et al. 2017, Kwakkel et al. 2016). An example of such potential tipping points for both risk indices is shown in Figure 4.6. These insights can be used to ensure that the OUV of WHS at risk from either of the two hazards is preserved in the long term.

In total, 47 WHS may be at risk from at least one of the two hazards by the end of the century, with Piazza del Duomo, Pisa (395) potentially at risk from flooding only and seven sites (UNESCO IDs 493, 498, 829, 975, 1024, 1096, 1240) from erosion only. Based on these results, only two sites, Medina of Tunis (36) and Xanthos-Letoon (484), are not at risk from any of the two hazards by 2100. Further, we find that 93% of the sites at risk from a 100-year flood and 91% of the sites at risk from coastal erosion under any of the four scenarios are already at risk under current conditions, which stresses the urgency of adaptation in these locations (Figure 4.6).

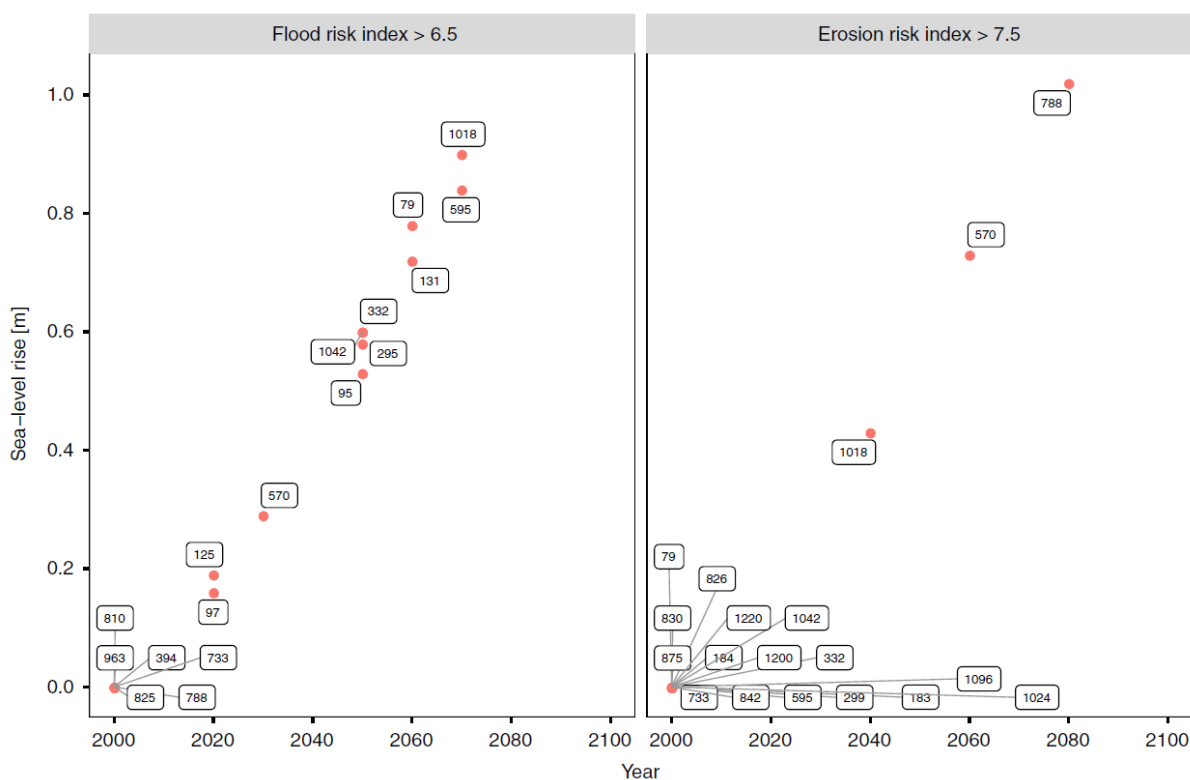


**Figure 4.6** Examples of potential adaptation tipping points for the flood risk index and the erosion risk index. Both graphs show points in time when a World Heritage site may exceed a certain risk threshold with the respective amount of sea-level rise under the high-end scenario. Point labels show the official UNESCO ID of the sites affected. a) Flood risk index threshold of 6.5, b) erosion risk index threshold of 7.5

Risk will further increase by 2100, in particular in the second half of the century, when projections of SLR diverge considerably based on the respective scenario. Therefore, the magnitude of risk increase largely depends on global mitigation efforts in the next years, which should pursue the aim not to exceed RCP2.6 (van Vuuren et al. 2011b) as planned under the Paris Agreement (UNFCCC 2016). If the goal of the Paris Agreement is not met, the amount of SLR may exceed the height of a 100-year storm surge by a factor of 1.4 under RCP8.5 and a factor of 3 under the HE scenario in 2100. Therefore, SLR may become a larger threat to

WHS than a present-day 100-year storm surge. A recent study of future ESL at the European scale has come to similar results, suggesting that present-day 100-year events in the Mediterranean may occur much more frequently, up to several times per year, by 2100 (Vousdoukas et al. 2017). Our results illustrate the value of rigorous global-scale mitigation efforts which could be crucial in preventing WHS from losing their OUV, especially as protection measures only work effectively up to a certain water level. Recent research has shown that RCP2.6 may be exceeded by 2100 (Rockström et al. 2016, Rogelj et al. 2016, Schleussner et al. 2016), therefore adaptation planning should prepare for higher SLR scenarios.

As adaptation measures need to be integrated into the WHS without compromising its OUV, adaptation planning at WHS is particularly challenging (Margottini 2015, Howard 2013). Since a site's OUV is bound to its location, retreat seems to be the least favorable adaptation option (Phillips 2014, Howard 2013, Wang 2015). While relocation of individual monuments such as the Early Christian Monuments of Ravenna (788) or The Cathedral of St James in Šibenik (963) may be technically possible, it seems to be impossible to relocate WHS that extend over large areas such as urban centers, archaeological sites and cultural landscapes. Examples of non-UNESCO cultural heritage monuments that have been moved inland are Clavell Tower (Bowcott 2008) and Belle Tout lighthouse in the UK (Belle Tout lighthouse 2018) and Cape Hatteras Lighthouse in the USA (U.S. National Park Service 2015). However, we could not find any examples in the existing literature where a UNESCO WHS was relocated. Relocation should be assessed carefully on a case-by-case basis and may be a suitable adaptation strategy for those WHS where risk is very high.

Common accommodation strategies such as hazard insurance, emergency planning or land-use planning (Klein and Nicholls 1998) cannot be applied to WHS, but strategies to raise awareness can be pursued. Terrill 2008 suggests to use the iconic nature of WHS to emphasize the severity of their loss in order to raise awareness of policymakers and heritage managers and to promote climate change mitigation. Recent efforts at the national to local level that monitor cultural heritage and provide guidance for managing heritage in the light of climate change show that awareness is gradually increasing. Examples are the Irish Heritage Council, Historic England, the U.S. National Park Service's Cultural Resources Climate Change Strategy and the Scottish Coastal Heritage at Risk project which has developed a smartphone app for surveying cultural heritage at risk from coastal erosion. This project raises awareness of local communities and authorities who can help designate priority areas and can therefore support heritage management (Hambly 2017). Further, Khakzad et al. 2015 suggest to include coastal heritage into ICZM, which may help in increasing the efficiency of adaptation planning. Another accommodation strategy would be to remove the inventory of WHS, such as paintings or statues, during flood events.

Coastal protection seems to be a suitable adaptation strategy as it may be possible to integrate it into any type of cultural WHS (i.e. urban heritage, archaeological site, cultural landscape or monument) without compromising its OUV. One example is the MOSE (Modulo Sperimentale Elettromeccanico/Experimental Electromechanical Module) project currently under construction in Venice ([www.mosevenezia.eu](http://www.mosevenezia.eu)). The entire lagoon will be protected by submerged mobile barriers at the lagoon inlets that will be raised during high waters of at least

1.1m. These barriers do not interfere with the appearance of Venice and the fragile ecosystem of the lagoon as long as they are not raised frequently (Margottini 2015, UNESCO World Heritage Centre 2007). This example illustrates that, in order to preserve the aesthetic value of a WHS, very expensive protection measures may have to be pursued. An alternative to hard protection measures may be the use of coastal ecosystems as soft, nature-based protection by attenuating water levels and stimulating sedimentation in certain locations (Temmerman et al. 2013, van Wesenbeeck et al. 2017).

A combination of awareness-raising strategies and protection measures seem to be the most suitable adaptation strategies, but relocation also needs to be considered, in particular where risk is very high. However, local-scale assessments are needed in order to devise adaptation measures that are tailored to the characteristics of individual WHS and the type of hazard they are at risk from (Phillips 2014, Howard 2013). With regard to flood risk, such local-scale assessments should additionally consider a potential low bias in return flood heights due to uncertainties regarding the rate of sea-level rise to avoid an underestimation of risk in the adaptation process (Buchanan et al. 2016).

As a first-order risk assessment, using a simple methodology based on publicly available region-wide data, this study can easily be reproduced and applied to other regions where a high number of WHS is potentially at risk from coastal hazards due to SLR (e.g. South-East Asia). However, such assessments should bear in mind the limitations of this study. We have refrained from analyzing the vulnerability of WHS to the two hazards as local-scale data concerning the internal characteristics of a WHS such as heritage material or heritage inventory are not readily available and including those in the analysis goes beyond the scope of this first-order assessment. Furthermore, we regard the use of depth-damage functions that are commonly applied in large-scale flood risk assessments to represent vulnerability (Ward et al. 2015, Hinkel et al. 2014, Muis et al. 2015, Jongman et al. 2012, Aerts et al. 2014, Ward et al. 2017) as problematic in the context of UNESCO World Heritage. Due to the high intangible value of WHS (Howard 2013, Terrill 2008), it is very difficult and ethically questionable to quantify the damages at a WHS, which would imply that one WHS is more valuable than another (Phillips 2015). However, if appropriate local-scale data are available, it may be possible to assess the tangible costs of coastal flooding and erosion by accounting for e.g. loss of revenue or cost of repairs (Taylor et al. 2007).

The elevation-based (bathtub) approach used for modelling the floodplain tends to overestimate the flood extent, in particular in low-lying, mildly sloping terrain such as the Nile, Rhone and Po deltas (Vousdoukas et al. 2016, Vousdoukas et al. 2018a), as hydrodynamic and hydraulic processes are not considered (Ramirez et al. 2016, Poulter and Halpin 2008, Seenath et al. 2016). However, in steep terrain the flood extent is only slightly overestimated or even underestimated (Vousdoukas et al. 2016, Ramirez et al. 2016, Vousdoukas et al. 2018a). As large parts of the Mediterranean are characterized by steep topography (Benoit and Comeau 2005), we expect this approach to provide a reasonable approximation of maximum potential flood extent at the majority of WHS. Furthermore, this modelling approach is extensively used in large-scale flood modelling (Jongman et al. 2012, Hinkel et al. 2014, Wolff et al. 2016,

Hoozemans et al. 1993, Muis et al. 2015, Muis et al. 2016, Muis et al. 2017) and can be regarded as a standard in such assessments (Moel et al. 2015, Ramieri et al. 2011).

As we do not consider defense structures in place due to lack of data on coastal protection measures (Scussolini et al. 2016), we may additionally overestimate risk in locations where protection measures exist. This appears to be the case at the Early Christian Monuments of Ravenna (788) and Archaeological Area and the Patriarchal Basilica of Aquileia (825), both located along the northern Adriatic Sea, where flood risk is modelled to be very high and erosion risk is modelled to increase rapidly at the end of the century, even though these WHS are currently located 6.7 and 3.5km inland (Supplementary Data 2). A further example is Venice and its Lagoon (394) which is, according to our results, one of the WHS most at risk from coastal flooding (Figure 4.3) and erosion (Figure 4.5) until 2100. However, once construction of the MOSE project is completed (expected in 2018 as of the last official status (Città di Venezia 2017)), risk will be reduced considerably as the flood barriers will protect the city and the lagoon from ESL of up to 3m ([www.mosevenezia.eu](http://www.mosevenezia.eu)). According to our results, this protection level will be sufficient until 2100, with ESL projected to be 2.5m under the HE scenario. As Venice has struggled with flood waters for centuries (Margottini 2015), it forms a special case; we did not find any other Mediterranean example where protection measures have been installed to protect an entire WHS.

We must also note that we may underestimate the floodplain in certain locations as it was not possible to account for human-induced subsidence even though it can be high in cities (Hanson et al. 2011, Hallegatte et al. 2013) such as Venice (Bock et al. 2012) and Istanbul (Nicholls 1995) and in river deltas such as those of the Nile, Po and Rhone (Syvitski et al. 2009, Taramelli et al. 2015) due to ground water extraction. Currently, there is a lack of consistent data and of reliable scenarios projecting future development of human-induced subsidence (Hinkel et al. 2014). Furthermore, the Shuttle Radar Topography Mission (SRTM) digital elevation model (DEM) used is a surface model and as such it may overestimate elevation in forested and built-up areas (Lichter et al. 2011, Sampson et al. 2015). We observe this effect in Venice and its Lagoon (394) where only small sections of the city's built-up areas are located at elevation increments of 1-3m AMSL although the City of Venice reports the island to be almost fully inundated (91%) during a flood of 2m (Città di Venezia 2016). A second example is Ferrara, City of the Renaissance, and its Po Delta (733) where forest directly located at the coast (Wolff et al. 2016) has elevation values of more than 10m. Across the whole Mediterranean, built-up areas make up over 75% of the WHS located in the LECZ (see Reimann et al. 2018b), potentially leading to an underestimation of elevation, and therefore the risks of flooding and erosion in these locations. Despite its limitations, the SRTM DEM is currently the most consistent and commonly used global elevation model (Kulp and Strauss 2016) and we did not have access to any other higher-resolution region-wide DEM as LiDAR (Light Detection And Ranging) data are only available for certain parts of the Mediterranean and the newly created CoastalDEM (Kulp and Strauss 2018) is not freely available. Please consult Kulp and Strauss 2016 for an in-depth discussion of the SRTM limitations.

The limitations of this study can be addressed in local-scale assessments that should be conducted to develop specific adaptation strategies and to select suitable adaptation measures

for individual WHS. We encourage other researchers to use the revised and extended WHS data as a starting point for such assessments that allow for applying hydrodynamic modelling approaches, including higher-resolution local-scale data, and accounting for vulnerability.

Our results can raise awareness of policymakers and heritage managers by pointing to the urgent need for adaptation as a large number of WHS are already at risk from coastal flooding and erosion under current conditions. Both risks will exacerbate in the course of the twenty-first century and possibly beyond, their magnitude depending on the global-scale mitigation effort in the coming years. However, adaptation can only be implemented to a limited degree, especially with regard to WHS, as their OUV may be compromised by adaptation measures. If no steps are taken, WHS may lose their OUV in the next centuries and may consequently be removed from the UNESCO World Heritage list. Therefore mitigation efforts are as much needed as adaptation to protect our common heritage from being lost. As UNESCO WHS are monitored at least to a certain degree under the World Heritage Convention, they will more likely receive the necessary attention and funding for adaptation measures against the risks of SLR. This is particularly true for WHS in densely populated locations such as the cities of Venice, Dubrovnik, Tyre or Tel-Aviv due to the high potential impacts of coastal hazards (Anderson et al. 2017, Hinkel et al. 2014). Cultural heritage not inscribed in the World Heritage list will receive much less attention and many of these will slowly disappear with SLR even though these sites are important parts of human history as well (Anderson et al. 2017).

## **4.4 METHODS**

### **4.4.1 General framework**

We employ the conceptual risk framework of the Intergovernmental Panel on Climate Change (IPCC) widely used in the current literature (Jongman et al. 2012, Jongman et al. 2015, Muis et al. 2015, Zhou et al. 2017, Klijn et al. 2015), in which risk results from the interaction of hazard, exposure and vulnerability (Field 2012, Oppenheimer et al. 2014). To assess coastal flood risk we define hazard as the intensity (i.e. surge height) and frequency (i.e. return period) of a storm surge and exposure as the area of a WHS flooded, along with the flood depth. To assess the risk of coastal erosion we define the amount of SLR as the hazard and determine exposure of a WHS to coastal erosion by the distance of a WHS from the coast, combined with the characteristics of the coastal zone that determine its sensitivity to coastal erosion. We do not assess a site's vulnerability to either coastal flooding or erosion as analysis of the internal characteristics of a WHS, such as heritage material and inventory, are needed. Such data are not readily available, and therefore this work is beyond the scope of this continental-scale assessment.

In order to quantify flood risk and erosion risk we use an index-based approach, which is a well-established method in the literature (Reeder-Myers 2015, Gornitz et al. 1994, Torresan et al. 2012, Satta et al. 2015, Daire et al. 2012, Mavromatidi et al. 2018, Peduzzi et al. 2009, Balica et al. 2012, Daly 2014) and particularly suitable for first-order assessments on continental scale to support adaptation planning (Torresan et al. 2012, McLaughlin and Cooper 2010, Daly 2014).



With the help of the risk indices we are able to assess potential impacts on WHS with rising sea levels and compare WHS with each other without attaching monetary value to them (Moel et al. 2009). For transparency reasons and to ease application of our methodology to other regions, we select risk indicators that are based on publicly available data. An overview of the data used can be found in Supplementary Table 4.2.

#### **4.4.2 UNESCO World Heritage data processing**

We use the UNESCO World Heritage List data of 2018 provided on the UNESCO website (UNESCO World Heritage Centre 2018), in which each WHS is represented as a point, with longitude and latitude coordinates. We extract all cultural WHS located along the Mediterranean Sea. To account for WHS consisting of more than one site, so-called serial nominations (UNESCO World Heritage Centre 2015a), we manually check each WHS and add further point data entries for serial sites based on maps and descriptions provided on the UNESCO website (UNESCO World Heritage Centre 2018). To reflect each WHS location as accurately as possible, we follow the methodology used in Chang et al. 2009 and Dassanayake et al. 2012. Therefore, we correct the location of misplaced WHS by using Google Earth™ satellite imagery. Where in doubt, we additionally compare photos and site descriptions provided on the UNESCO website with photos of the Panoramio web service embedded in Google Earth™ (as of January 2018 replaced by photos from Google Maps). Next, we examine WHS maps downloaded from the UNESCO website and digitize the outline of each site with the help of Google Earth™, resulting in one polygon for each serial WHS. We validate our WHS polygons by comparing them to those produced as part of the European PROTHEGO project, available in a map viewer (PROTHEGO project 2018).

Subsequently, we extract the WHS located in the LECZ based on the lowest elevation value of each WHS polygon in the SRTM DEM version 4.1 (Jarvis et al. 2008, Farr et al. 2007). The LECZ represents all land with an elevation of up to 10m in hydrological connection to the sea (McGranahan et al. 2007). This way we ensure that all sites potentially exposed to coastal flooding and erosion are included in the analysis.

#### **4.4.3 Flood risk**

To assess WHS at risk from ESL, we calculate the floodplain of a storm surge with a 100-year return period under four SLR scenarios from 2000 to 2100. We use a 100-year storm surge as it is a standard measure for coastal protection and has been widely used in previous assessments (Muis et al. 2015, Muis et al. 2016, Muis et al. 2017, Jongman et al. 2012, Kron 2005, Neumann et al. 2015, Nicholls et al. 2008a, Hallegatte et al. 2013, Hanson et al. 2011, Hinkel et al. 2014). To account for spatial differences in the floodplain across the Mediterranean basin, we use storm surge data from the Mediterranean Coastal Database (MCD) (Wolff et al. 2018b, 2018a), where surge heights are available for each of the approximately 12,000 coastal segments. We select surge heights that are derived from the Global Tide and Surge Reanalysis (GTSR) dataset which accounts for ESL due to storm surges and tides. A detailed description of the methods








used for developing the dataset can be found in (Muis et al. 2016). In the MCD, a downscaled version of the GTSR data is available. To ensure that all data used for the analysis are referenced to the same vertical datum, we convert the vertical datum of the surge data, referenced to the mean sea-level, to the EGM96 geoid, the vertical datum of the SRTM data (Ramirez et al. 2016, Muis et al. 2017, Kulp and Strauss 2016, Kulp and Strauss 2018). To do so, we use the mean dynamic ocean topography (Rio et al. 2014), which is the difference between mean sea-level and the geoid.

To account for plausible increases in ESL due to SLR, we combine the adjusted surge heights with four SLR scenarios based on the Representative Concentration Pathways (RCPs) (van Vuuren et al. 2011a). We use the regionalized SLR projections by (Kopp et al. 2017) that account for three ice sheet components, glacier and ice cap surface mass balance, thermal expansion and other oceanographic processes, land water storage and non-climatic factors such as Glacial Isostatic Adjustment (Kopp et al. 2014, Kopp et al. 2017). These projections are available as grid points with a spatial resolution of  $2^\circ$  by  $2^\circ$ . We select the median projections (50<sup>th</sup> percentile) of RCP2.6, RCP4.5 and RCP8.5 for 2010-2100 to cover the likely range of uncertainty regarding SLR, as well as the 95<sup>th</sup> percentile of RCP8.5 (5% probability) to account for a HE scenario. We spatially join the grid points of the SLR projections to the coastal segments of the MCD closest to each point and calculate the ESL of a 100-year storm surge for each coastal segment, scenario and 10-year time step. We do not account for potential changes in storminess as confidence in these projections is low (Church et al. 2013).

We model the 100-year coastal floodplain for each SLR scenario with the help of a planar elevation-based (bathtub) approach using the SRTM DEM, which is extensively used in large-scale flood modelling (Jongman et al. 2012, Hinkel et al. 2014, Wolff et al. 2016, Muis et al. 2015, Muis et al. 2016, Muis et al. 2017). The SRTM data used have a spatial resolution of 3 arc seconds (approximately 90m at the equator) and a vertical resolution of 1m (Farr et al. 2007). Based on these data, we determine the area of each WHS located at elevation increments from 0m up to 4m in hydrological connection to the sea in a first step. Next, we attribute the calculated ESL to the nearest WHS. If more than one ESL can be attributed to one WHS, we calculate a weighted mean based on the number of raster cells with a specific ESL height assigned to each WHS. To determine the area of each WHS flooded (in %), we linearly interpolate between respective elevation increments based on the ESL assigned, following the method of Hinkel et al. 2014. We further calculate the maximum flood depth per WHS (in m) based on the difference between the ESL and the elevation value in the SRTM DEM. For WHS located below 0m according to the SRTM data, we assume the minimum elevation value of each WHS to be 0m. We apply this assumption to correct for artefacts present in the SRTM data, such as individual pixels with very low elevation values (e.g. -20 m at Venice and its Lagoon (394)) (Hirt 2018). Using these values would result in unrealistically high maximum flood depths. Further, we do not account for existing flood protection measures in our analysis due to a lack of consistent region-wide data. Data of existing flood defenses may be available for specific locations across the region, but integrating those into our analysis would compromise the consistency of our results.

For the flood risk index, we scale flood area and flood depth linearly to values ranging from 0 (not at risk) to a maximum value of 5 (very high risk), assuming that a WHS is at very high risk when at least 50% of the site are flooded with a flood depth of at least 1m (Hinkel et al. 2014, Messner et al. 2007) (Table 4.1). We must note that we could not find any studies assessing flood risk based on the area of an object flooded; therefore we assume that the OUV of a WHS is seriously threatened if at least half of the site is flooded. In a last step, we calculate the sum of the scaled flood risk indicators, which results in an index ranging from 0 to 10.

**Table 4.1** Scale values used for the components of the flood risk index and the erosion risk index

INDEX	0	1	2	3	4	5
INDICATOR	NOT AT RISK	VERY LOW	LOW	MODERATE	HIGH	VERY HIGH
<b>FLOOD RISK</b>						
Flood area [%]	0	> 0				≥ 50
Flood depth [m]	0	> 0				≥ 1
<b>EROSION RISK</b>						
Distance [m]	> 500	500				< 10
Coastal material		rocky	-	muddy; rocky with pocket beaches	-	sandy
Mean wave height [m]		0.1				> 0.8
Sediment supply [mg l <sup>-1</sup> ]		11.5				< 0.5

#### 4.4.4 Erosion risk

To analyze WHS at risk from coastal erosion due to SLR, we calculate an erosion risk index for each WHS from 2000 to 2100 under the four SLR scenarios (RCP2.6, RCP4.5, RCP8.5, HE). We adopt the indicators used in previous index-based approaches on coastal erosion (Mavromatidi et al. 2018, Gornitz et al. 1994, Boruff et al. 2005, Torresan et al. 2012, McLaughlin and Cooper 2010, Satta et al. 2015, Pendleton et al. 2004) and cultural heritage at risk from coastal erosion (Reeder et al. 2012, Reeder-Myers 2015, Daire et al. 2012) and select those that play a key role in the Mediterranean (UNEP/MAP 2012) and for which data are publicly available. Accordingly we assume that erosion risk is determined by a WHS's distance from the coast, the coastal material, mean wave height and sediment supply.

We use the coastline of the MCD (Wolff et al. 2018a) to calculate the shortest distance of each WHS from the coast. In several instances the coastline of the MCD considerably deviates from the actual coastline as detected with the help of Google Earth™, for example, around the cities

of Trogir and Šibenik in Croatia or the city of Catania in Italy. In these instances we use the distance from the coastline of the global self-consistent, hierarchical, shoreline database version 2.3.7 (Wessel and Smith 1996, see Reimann et al. 2018b). We calculate the change in coastline due to SLR with the help of the SRTM data under the assumption that all areas below the amount of SLR in hydrological connection to the sea are inundated (Antonioli et al. 2017). Again we interpolate linearly between elevation increments (Hinkel et al. 2014) and calculate the decrease in a WHS's distance from the coastline for each scenario and 10-year time step. Further, we use the MCD to assign the coastal material and mean wave height to each WHS based on the coastal segments attributed to the site. If more than one coastal material type or wave height is attributed to a WHS, we adopt the dominant one. To account for sediment supply, we use a newly created dataset of mean monthly Total Suspended Matter (TSM) concentration. TSM is a measure of water turbidity in coastal locations that can be used as an indicator for sediment supply (Schuerch et al. 2018). The original data were produced in the context of the GlobColour project and were calculated based on satellite imagery (Doerffer and Schiller 2010). We spatially join the grid point data of the TSM to the coastal segments of the MCD closest to each grid point. If more than one grid point can be attributed to a segment, we calculate the mean of the points that extend along that segment. Subsequently, we attribute TSM values to each WHS, following the same procedure. We must point out that TSM represents sediment supply only to a limited degree as it does not include river bedload supplied at river mouths, which plays an important role in counteracting coastal erosion in the Mediterranean (Ninfo et al. 2018, Besset et al. 2017). A dataset of bedload sediment transport is currently not available for the entire Mediterranean region. For the erosion risk index, we scale the four indicators linearly to values ranging from 0 (not at risk) to a maximum value of 5 (very high risk) based on scale values used in the literature that we adapt to the environmental conditions in the Mediterranean basin (Table 4.1).

Accordingly, we assume a WHS to be at risk from coastal erosion if it is located at least within 500m from the coast with the highest risk at or below 10m distance (Daire et al. 2012), accounting for a two-fold increase in observed erosion rates in the Mediterranean due to SLR (Reeder et al. 2012, Özhan 2002). For coastal material we use the scale values of Reeder et al. 2012 and Mavromatidi et al. 2018 and for mean wave height we adapt the values of Mavromatidi et al. 2018. For sediment supply we assume risk to be very high when the TSM concentration is below  $0.5\text{mg l}^{-1}$ . We calculate one erosion risk index (ERI) for each WHS based on equation (4.1) where  $D$  stands for distance under the respective scenario and time step,  $M$  for coastal material,  $mWH$  for mean wave height and TSM for Total Suspended Matter. We follow the weighting used in Reeder-Myers 2015, which is largely based on previous assessments (Reeder et al. 2012, Gornitz et al. 1994, Pendleton et al. 2004) and we adjust it to the indicators included in this analysis, ensuring that the relative importance of each indicator remains unchanged. As sediment supply primarily plays a role in calm waters (i.e. beaches, wetlands, inlets) where it can get deposited (UNEP/MAP 2012), we exclude TSM from the risk index at WHS in rocky locations. In a last step we scale the ERI to a possible maximum value of 10.

$$\begin{aligned} ERI_{rocky} &= (3D + 2M + mWH) * \frac{1}{3} \\ ERI_{other} &= (3D + 2M + mWH + TSM) * \frac{1}{4} \end{aligned} \quad \text{if } D > 500, ERI = 0 \quad (4.1)$$

#### 4.4.5 Code availability

Spatial data processing was conducted in the Geographic Information System (GIS) software ArcGIS. The results of the spatial analysis were further processed in the software environment R to calculate the flood risk and erosion risk indices. The computer code of these calculations is available upon request.

### 4.5 DATA AVAILABILITY

The WHS datasets produced for this study are available in text format (CSV) and polygon vector format at <https://doi.org/10.6084/m9.figshare.5759538> (Reimann et al. 2018b).

#### Acknowledgments

We thank Jorid Höffken for her help in assembling the UNESCO World Heritage data used in this study. S.B. was funded by a joint United Kingdom Natural Environment Research Council and United Kingdom Government Department of Business Energy & Industrial Strategy grant “ADJUST1.5,” numbered NE/P01495X/1. We acknowledge financial support by the federal state of Schleswig-Holstein, Germany, within the funding program Open Access Publikationsfonds.

# 5 CONCLUSIONS AND OUTLOOK

---

## 5.1 MAIN ACHIEVEMENTS AND FINDINGS

The work carried out in Chapter 2 to 4 has advanced the spatial representation of variables that represent exposure to SLR-related hazards, i.e. population and cultural assets, to facilitate their integrated analysis in coastal risk assessments at continental (i.e. Mediterranean) scale. A particular focus has lain on accounting for future changes in coastal risks, by exploring uncertainty in exposure under alternative socioeconomic scenarios (i.e. SSPs) and increasing SLR-related hazards under a range of SLR scenarios (i.e. RCPs). This section synthesizes the main achievements of this thesis by discussing how the three key research needs established in section 1.3.1 have been addressed across the three preceding chapters.

### 5.1.1 Downscaling global-scale data and modeling approaches to the continental scale

As shown in section 1.2, coastal risk assessments at continental scale have been scarce in the literature, with the majority of assessments focusing on the global scale. Even when coastal risks are assessed at continental scale (i.e. European scale), these assessments are almost exclusively based on global data, modeling approaches, and scenario assumptions (e.g. Hinkel et al. 2010, Vousdoukas et al. 2018b, Vousdoukas et al. 2020a, Athanasiou et al. 2020). Each of the three preceding chapters has addressed the need for downscaling global data and modeling approaches to the continental scale to be able to reflect regional differences, using the Mediterranean region as a case study.

Chapter 2 downscales the global modeling approach of Merkens et al. 2016 based on coastal SSP narratives extended to the Mediterranean region. The continental-scale focus allows for establishing Mediterranean-specific SSP elements, such as water demand and second home ownership, as well as for differentiating socioeconomic developments across two geographical regions (i.e. the northern Mediterranean versus the southern and eastern Mediterranean). Based on these refined scenario assumptions, distinct model parameters (i.e. modification factors for the established urban and rural growth differences, GD) for each geographical region and SSP are developed (section 2.2.2). As a result, the number of people projected to live in the Mediterranean LECZ in 2100 based on the refined model version can deviate by as much as 15% (SSP1) from the results produced with the original version of the model. Similarly, Chapter 3 downscales the global gravity-based modeling approach of Jones and O'Neill 2016, calibrating the model to the two geographical regions established in Chapter 2, and integrating inland-coastal migration into the model (section 3.2.2). As in Chapter 2, the calibration process results in distinct model parameters (i.e.  $\beta$  parameters for coastal rural (CR), inland rural (IR), coastal urban (CU), inland urban (IU) areas) for each geographical region and SSP. The downscaled model projects an up to 25% higher population in the LECZ (SSP1), which, in particular, reflects the integration of inland-coastal migration processes into the model. Due to

their refined scenario assumptions and modeling approaches, the downscaled models in Chapters 2 and 3 produce projections that deviate considerably from their respective global counterpart. As these projections plausibly reflect socioeconomic developments at continental scale, they can be used in a wide range of (coastal) IAV assessments. The differences between the two modeling approaches are discussed in further detail in section 5.1.2.

In Chapter 4, the global UNESCO WHS data are downscaled to the Mediterranean region by correcting the WHS point data and producing spatial representations (i.e. polygons) of each cultural WHS located in the LECZ (see also 5.1.3). The continental-scale focus allows for assembling this high-resolution spatial database in a timely manner. Further, it allows for assessing Mediterranean WHS at risk from SLR-related hazards with the help of the MCD (Wolff et al. 2018a), where regional differences in the physical parameters needed for such an assessment (e.g. ESL, coastal material) are represented in roughly 12,000 coastal segments (section 4.4). The results of this assessment exhibit clear regional patterns regarding the severity of flood risk and erosion risk due to SLR at each WHS, which further emphasizes the need for incorporating regional characteristics in coastal risk assessments.

### **5.1.2 Developing spatial population projections that account for internal migration processes**

The second key research need addressed in this thesis is the use of socioeconomic scenarios for exploring plausible future socioeconomic developments in coastal locations. Specifically, this thesis extends previous research that has assumed homogenous population growth per country by applying national-level growth rates to the current population distribution, therefore neglecting spatial differences in population growth due to internal migration (e.g. Jongman et al. 2012, Nicholls et al. 2018, Lincke and Hinkel 2018, Vafeidis et al. 2019).

Chapter 2 accounts for inland-coastal and rural-urban migration based on observed differences in population growth (i.e. GD) between coastal and inland locations in each country, calculated separately for rural and urban settlements. To account for the uncertainty in future migration patterns, the GD are modified for each SSP and geographical region by interpreting the Mediterranean coastal SSP narratives and are applied to each of the four zones (i.e. CR, IR, CU, IU) established per country. The resulting spatial population projections reflect plausible changes in population distributions for each country, SSP, and time step. As the GD are applied to fixed delineations of the four zones, urban sprawl is not captured in this approach, which may result in an overestimation of population exposure when assessing coastal risks due to a potential overconcentration of the population in coastal locations (Merkens et al. 2018). The gravity-based modeling approach used in Chapter 3 allows for exploring the uncertainty related to future spatial changes in settlement patterns (i.e. urban sprawl), rural-urban migration, and inland-coastal migration across the SSPs. To capture the spatial patterns of these processes, in particular in coastal locations, the model uses a 15 times finer spatial resolution (i.e. 30 arc seconds) than the original version of the model. Similar to the approach in Chapter 2, the calibrated model parameters for the four zones (CR, IR, CU, IU) are modified for each SSP and

geographical region to account for the uncertainty in future migration patterns. The gravity-based model dynamically distributes the population in each time step based on a population potential per grid cell calculated with a distance-decay function that additionally includes the contribution of local effects to the potential of a cell (section 3.2.1), thereby producing diverse settlement patterns. Compared to the static model used in Chapter 2, the gravity-based model projects 12-70% higher population numbers in the LECZ (in 2100) under all SSPs except SSP5, which is characterized by considerable urban sprawl in the twenty-first century, thereby resulting in a 5% lower LECZ population. In SSP1, the large difference in projected LECZ population (i.e. 70%) results from the assumption in the static approach that effective coastal zone management leads to population decline in coastal locations, which is not accounted for in the gravity-based model.

It is worth noting that, although the spatial population projections produced in Chapter 3 account for more processes driving spatial population patterns, the projections produced in Chapter 2 span a broader range of uncertainty concerning the number of people living in the LECZ (range of 56.5 versus 61.4 million) as potential population decline in coastal locations is included as well. Conversely, Chapter 3 projects the highest total number of people in the LECZ in 2100 (SSP3). From a risk management perspective, an approach resulting in high LECZ populations may be more meaningful than one exploring a broader uncertainty range, as decision-makers would be able to plan for a ‘worst-case’ scenario. Consequently, the strengths and weaknesses of the produced projections should be considered when selecting a set of spatial population projections based on the application at hand.

### **5.1.3 Advancing the spatial representation of exposure variables not commonly used in coastal risk assessments**

The third key research need addressed in this thesis is to advance the spatial representation of exposure variables other than population or population-based variables such as GDP per capita, which the majority of coastal risk assessments at continental to global scales have focused on in previous research. Consequently, examples of studies that account for other exposure variables such as infrastructure (Koks et al. 2019, Yesudian and Dawson 2021) and cultural assets (Marzeion and Levermann 2014) are scarce in the current literature.

Chapter 4 develops a spatial database of cultural assets, i.e. UNESCO WHS, located in the Mediterranean LECZ. The database is assembled by correcting the point coordinate data provided in the UNESCO World Heritage List (as of 2018) and by drawing polygons of each WHS with the help of satellite imagery and photos of the WHS. In addition to the attributes provided in the World Heritage List, the developed database contains attributes of interest to coastal risk assessments such as heritage type, distance from the coast, and percent of the WHS located in the LECZ. A first-order assessment of WHS at risk from flooding and erosion under four RCP-based SLR scenarios finds the vast majority of the 49 WHS included in the database to be already at risk under current climatic conditions, with over 75% and 85% at risk from flooding and erosion, respectively. It also shows that awareness regarding SLR-related risks at

WHS is low and that adaptation planning is urgently needed. As adaptation measures must not compromise the site's OUV, innovative solutions are needed that are tailored to the characteristics of each WHS. These results stress the importance of including additional exposure variables in continental-scale coastal risk assessments, as coastal risks may otherwise be underestimated in locations where multiple elements (e.g. population, cultural assets, and infrastructure) are exposed to SLR-related hazards.

## **5.2 RECOMMENDATIONS FOR FURTHER RESEARCH**

This thesis has addressed the three key research needs in continental-scale coastal risk assessments summarized in the preceding section. Several additional research needs have been identified during this work, which, if addressed, can further advance coastal risk assessments at continental scales. Therefore, I conclude this thesis with six recommendations for further research that focus on work that builds directly on this thesis (points 1-4), before turning to a set of broader recommendations to advance (coastal) risk assessments in general (points 5-6).

### **1. Employ and enhance data to include characteristics of vulnerability in Mediterranean coastal risk assessments**

As all spatial data produced as part of this thesis are publicly available from an online repository, they can be used for assessing exposure and vulnerability to coastal hazards at continental to national scales. To do so, the developed exposure data can be enhanced with further variables to characterize vulnerability. In the case of population, indicators such as age, sex, ethnicity, education, and income are commonly discussed in the literature (e.g. Cutter et al. 2003, Madajewicz 2020). While several studies have developed SSP-based projections of such indicators at administrative unit level, the projections are available either for single countries (Hauer 2019, Chen et al. 2020b, Jiang et al. 2020) or for Europe (Terama et al. 2019), where the baseline data needed for such projections are readily available. Apart from gridded projections of GDP (Hurth et al. 2017, van Huijstee et al. 2018, Murakami and Yamagata 2019, Wang and Sun 2021), spatially explicit projections that include variables for characterizing vulnerability are not available at continental scales. The global-scale gridded data of current sex and age structures available from the WorldPop project (Tatem 2017, Pezzulo et al. 2017) are an example of a potentially suitable starting point for enhancing the population projections developed in this thesis with vulnerability variables. In the case of UNESCO WHS, variables such as material, tourist revenue, or cost of repairs (Taylor et al. 2007) can be added to the database, although assessing vulnerability of WHS is challenging due to their high intangible value (Chapter 4).

Coastal risk assessments that additionally account for the vulnerability of exposed elements can help establish hotspots of future coastal risks more comprehensively. Further, by combining exposure variables (i.e. population and cultural assets), hotspots of 'compound exposure/vulnerability' can be established, i.e. where a high number of exposed population coincides with a UNESCO WHS. This may especially be the case in old towns inscribed in the



World Heritage List such as Venice, Dubrovnik, and Tel Aviv. Such assessments should also explore possible ways to assess future risks due to compound flooding (e.g. ESL + heavy precipitation) as it further amplifies impacts in exposed locations (Zscheischler et al. 2020), but has not been analyzed in continental-scale assessments yet (Ward et al. 2020).

## **2. Extend data and modeling approaches for coastal risk assessments at other scales of analysis**

The methods used in this thesis can be extended to other continent-scale study areas. Applying the population modeling approach of Chapter 2 at other continental scales is rather straightforward due to its modest computing requirements, as long as extended SSP narratives are available to account for regional characteristics. In contrast, the gravity-based approach (Chapter 3) is computationally expensive, which can impede its applicability in large countries such as Brazil and China due to its refined spatial resolution compared to the original version of the model (Jones and O'Neill 2016). Furthermore, the development of a continental-scale cultural heritage database can be very time consuming, as each site needs to be digitized individually. The lack of a consistent and coherent spatial database of cultural assets has been a main constraining factor in previous risk assessments, in particular when it comes to including cultural heritage other than UNESCO WHS in such a database (Anderson et al. 2017; section 4.3).

For regional to national assessments, the data and modeling approaches can be further refined, thereby allowing for including additional variables to characterize vulnerability (see point 1). While the UNESCO WHS database assembled in Chapter 4 can be readily applied in such assessments, the modeling approaches for characterizing coastal flooding and erosion need to be refined. At these scales of analysis, application of the two-dimensional hydrodynamic model LISFLOOD-FP may be feasible, and may further allow for including protection measures in place, for instance, by assembling a spatial database of protection measures based on satellite imagery. Applying the population projection approaches at regional to national scales allows for further refining their spatial resolution, by using spatial population data such as WorldPop (Tatem 2017) or GHS-POP (Schiavina et al. 2019) as model input, which are available at spatial resolutions of 3 arc seconds and 9 arc seconds, respectively. Furthermore, uncertainty in future socioeconomic development can be explored in more detail based on an extended set of SSP narratives for the region or country analyzed. Participatory approaches to co-produce regional to national narratives such as the Living Lab approach are worth exploring at these scales of analysis to ensure that the narratives are considered relevant and plausible by the involved stakeholders (Reimann et al. 2021).

For local-scale assessments, other modeling approaches need to be explored that account for migration decisions at the individual level such as Agent-Based Modeling (ABM). A possible way forward is using the results of the approaches used in this thesis as boundary conditions for an ABM approach and accounting for more refined migration assumptions based on agent decisions (see point 3 for further details) (Wrathall et al. 2019).

### **3. Account for feedbacks between SLR-related hazards, exposure, and vulnerability**

Current continental-scale coastal risk assessments overlay spatial information of the hazard, exposure, and vulnerability without considering potential feedbacks between the three risk drivers. However, SLR-related hazards will affect exposure and vulnerability, by leading to migration of exposed populations (Black et al. 2011, McMichael et al. 2020) as well as to adaptation responses that reduce vulnerability of the exposed elements (Oppenheimer et al. 2019, Hauer et al. 2020). As these feedbacks can influence future risks considerably, it is important to account for these dynamics to explore how adaptation strategies (including migration) can affect future risks (Aerts et al. 2018). The SSP-RCP scenario framework offers a flexible tool to do so, as it is designed to explore plausible SSP, RCP, and SPA combinations (O'Neill et al. 2020). Developing SPAs for adaptation allows for exploring potential effects of adaptation policies such as managed retreat, implementation of hard protection measures, or the designation of setback zones on future SLR-related damages as well as on residual risk. For instance, when hard protection measures are pursued, residual risk is likely to be high due to increasing population and assets in protected locations ('levee effect') (Di Baldassarre et al. 2015, Haer et al. 2020).

To account for these feedbacks, the gravity-based model developed in Chapter 3 offers a flexible approach to explore the potential effects of broad-scale adaptation policies on SLR-induced migration. It also allows for integrating the feedbacks of other climate change impacts such as heat stress, crop yields, and desertification on internal migration (e.g. Rigaud et al. 2018). As gravity models reflect aggregate human behavior only (section 3.2.1), other modeling approaches such as ABM are needed to capture individual adaptation decisions. By using decision rules of different agents such as governments, insurers, and individual households, ABM allows for exploring adaptation decisions at an individual level (Aerts 2020). Further, ABM can be used to account for the influence of changes in risk perception on adaptation decisions after a hazard has hit (Aerts et al. 2018). While ABM has been primarily applied at local to national scales (e.g. Lázár et al. 2020) due to the high computational demands and data requirements (Aerts 2020), a recent study has applied ABM at continental scale to assess the future risks of river flooding in Europe (Haer et al. 2020). In this context, the coupling of different modeling approaches may be an interesting way forward, for instance, using the DIVA modeling framework (Hinkel et al. 2014) for establishing where dikes are built and where beach nourishment is pursued based on the concentration of population and assets (including UNESCO WHS) in exposed locations. At Mediterranean scale, the high-resolution MCD (Wolff et al. 2018a) can provide the underlying coastal database for such a DIVA application.

### **4. Combine modeling approaches for more robust projections**

This thesis has shown that coastal risk assessments use different modeling approaches for characterizing SLR-related coastal hazards and exposure. The strengths and weaknesses of different modeling approaches to characterize the coastal floodplain are relatively well documented in the literature and have been established by comparing the modeled floodplain

to the observed floodplain of a past event (e.g. Vousdoukas et al. 2016, Seenath et al. 2016, Ramirez et al. 2016). Studies that compare modeling approaches for characterizing exposure are hampered by a lack of ‘ground truth’ validation data. While the delineation of static exposure elements such as cultural assets and infrastructure is rather straightforward, spatial population or urban land use data are based on census data with varying spatial and temporal resolution per country, which are often further refined with the help of redistribution algorithms based on satellite imagery (Leyk et al. 2019). Therefore, exposure data are characterized by high uncertainties already under current conditions that will further increase in the future due to the uncertainties related to future socioeconomic development and internal migration. Two studies have compared different modeling approaches for producing future projections of population and urban land use at continental to global scales and have concluded that the selected modeling approach can influence projected exposure substantially (Merkens et al. 2018, Rohat et al. 2019b).

Similar to the current practice in climate modeling where multi-model ensembles are used to balance the strengths and weaknesses of different climate models (Flato et al. 2013), future work can use multi-model ensembles of different socioeconomic modeling approaches to produce results that are robust across a range of models (as proposed in van Ruijven et al. 2014). Concerning population projections, such ensembles can be produced from the static approach used in Chapter 2, the gravity-based approach of Chapter 3, and ABM, among others. Similarly, a multi-model ensemble approach could be used for the different urban land use projections available in the literature, such as Chen et al. 2020a, Gao and O'Neill 2020, and Wolff et al. 2020. In recent years, several so-called ‘Model Intercomparison Projects’ (MIP) such as the Inter-Sectoral Impact Model Intercomparison Project (ISIMIP)<sup>13</sup> or the Coastal impact Model Intercomparison Project (CoastMIP)<sup>14</sup> have been established with the aim to compare modeling approaches. A similar MIP could be initiated for socioeconomic modeling approaches (e.g. SocioMIP).

## 5. Take stock of available exposure and vulnerability data

Different disciplines are involved in the development of exposure and vulnerability data based on their specific interests and needs; for example, historians or archaeologists have a particular interest in cultural heritage, demographers in population, and engineers in infrastructure and/or protection measures in place. As all of these data are important for assessing future climate risks, a joint collaborative effort across disciplines would be desirable to harmonize the development of these data and to share them on a shared data platform. An example of such a data platform is the Socioeconomic Data and Applications Center (SEDAC)<sup>15</sup> hosted by the Center for International Earth Science Information Network (CIESIN) at Columbia University, New York, which provides a wide range of datasets related to human-environment interactions such as data on agriculture, health, population, and poverty. Further, the recently established

---

<sup>13</sup> <https://www.isimip.org/>

<sup>14</sup> <http://coastmip.org/>

<sup>15</sup> <https://sedac.ciesin.columbia.edu/>

POPGRID Data Collaborative<sup>16</sup> (also hosted by CIESIN) offers tools for comparing different gridded population and urban extent datasets to guide application of these data in policy and research (Leyk et al. 2019, POPGRID Data Collaborative 2020).

There is need for extending these data platforms with additional exposure and vulnerability variables and for establishing new data platforms that focus on specific variables such as cultural assets, infrastructure, or adaptation measures. In this context, a data platform of spatially explicit SSP-based projections is of particular interest as data and modeling approaches related to the SSPs have increased considerably in recent years. At Mediterranean scale, for instance, five sets of gridded population projections are currently available (i.e. Merkens et al. 2016, Jones and O'Neill 2016, Murakami and Yamagata 2019 in addition to those developed in this thesis), which have been produced based on different data and modeling approaches. Systematic and comparative documentation of the projections' strengths and weaknesses is currently unavailable, which would help select a set of projections depending on the user needs and would ease combining modeling approaches for more robust projections (point 4).

The need for making data and modeling approaches publicly available to the research community has been increasingly acknowledged in recent years (Gewin 2016, Wilkinson et al. 2016), and will likely result in an increase in data platforms similar to SEDAC or POPGRID. Through improved documentation of data and transparency of modeling approaches, new research avenues can be established more swiftly, which will also open up opportunities for future collaborations. One such collaboration opportunity could be to explore the potential of coupling modeling approaches to produce SSP-based projections of future urban land use with the help of spatial population projections, or vice versa.

## **6. Harness other sources of exposure and vulnerability data**

Recent research has increasingly explored new methods for generating spatial exposure and vulnerability data, in particular in data-scarce environments, where census data are unavailable or out of date. Mobile phone data can provide important information on human mobility, by capturing diurnal to seasonal work-related migration (Dujardin et al. 2020), short-term migration (hours to weeks) during hazard events (Lu et al. 2016), and long-term migration patterns (Deville et al. 2014, Lai et al. 2019). These insights allow for validating available spatial population datasets, refining these data both temporally and spatially, as well as validating and calibrating migration models for producing population projections. Furthermore, recent work has increasingly focused on harnessing social media data, in particular Twitter data, for real-time information on the location of hazard events such as coastal flooding and river flooding (Arthur et al. 2018, Bruijn et al. 2018, Barker and Macleod 2019, Bruijn et al. 2020) as well as infrastructure disruptions resulting from such hazards (Roy et al. 2020). Based on these data, warnings can be issued and evacuation of population and assets can be initiated, therefore reducing exposure and vulnerability in at-risk locations.

---

<sup>16</sup> <https://www.popgrid.org/>

Additional innovative ways for harnessing exposure and vulnerability data are the use of OpenStreetMap (OSM) data for information on infrastructure (Koks et al. 2019) and real estate data from Zillow for building structures and property prices in the US (Bernstein et al. 2019). Further, citizen science projects offer great potential for generating new data related to building structures, adaptation measures, infrastructure, and cultural assets among others. Two examples that can support coastal risk assessments are the Coastwards project, which pursues the aim to produce a global database of coastal materials<sup>17</sup>, and the Scottish Coastal Heritage at Risk project that has developed a mobile app to monitor coastal erosion at cultural heritage sites in Scotland (Hambly 2017).

Future research can further explore methods to harness these data sources systematically to produce, refine, and validate spatial exposure and vulnerability datasets. Additionally, such data can advance our understanding of migration processes at different spatial and temporal scales, based on which we can refine migration models to reflect future migration patterns more plausibly in data-scarce regions, but also at continental to global scales.

---

<sup>17</sup> <http://coastwards.org/>



# APPENDICES

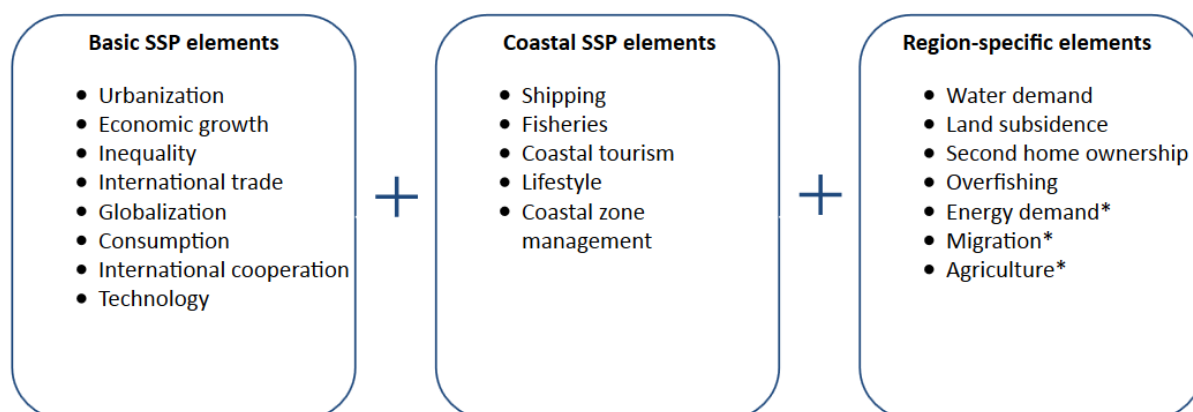
---





# APPENDIX A

## SM2.1 Mediterranean coastal SSP elements



\* = region-specific elements also included in the basic elements (O'Neill et al. 2017)

## SM2.2 Data used to determine the current state of socioeconomic development in each Mediterranean country

Mediterranean SSP element	Indicator	Reference
Urbanization	Urbanization level (2014) Urbanization rate (2000-2014)	The World Bank 2016
Economic growth	GNI per capita (in US\$, 2014) Annual GDP growth (2000-2014)	
Inequality	GINI index	
International trade, globalization	Export-import ratio (% of GDP, 2014)	
Agriculture	Agriculture (% of GDP, 2014)	
Shipping	Maritime freight (in t, relative to population, 2013)	Eurostat 2015a, 2015b, The World Bank 2016
Fisheries	Fish captures (in t, 2013)	Food and Agriculture Organization of the United Nations (FAO) 2016
Tourism	International tourism (no of arrivals, relative to country size, 2013)	The World Bank 2016
Water demand	Annual freshwater withdrawal (in %, 2013)	
Energy demand	Net energy imports (in %, 2012)	

## SM2.3 General scenario assumptions

SSP elements	Assumptions	References
International cooperation; Technological development	<ul style="list-style-type: none"> <li>○ If international cooperation is effective and technological development and transfer rapid, socioeconomic development is converging in the whole region.</li> </ul>	
Inequality; Migration	<ul style="list-style-type: none"> <li>○ If inequality is high, willingness to migrate is high, with the primary goal to improve living standards.</li> <li>○ If the population's mobility is high and visa regulation are low, migration is high.</li> </ul>	Hugo 2011, Foresight 2011
Coastal tourism	<ul style="list-style-type: none"> <li>○ If living standards improve, tourism demand increases, especially in coastal areas.</li> </ul>	Sanna and Le Tellier 2013, Manca and Santarossa 2016
International trade; Globalization; Shipping	<ul style="list-style-type: none"> <li>○ If international trade and globalization are high, the importance of the region's shipping industry is high.</li> </ul>	Sanna and Le Tellier 2013, World Economic Forum (WEF) 2011, Hanson et al. 2011
Fisheries; Agriculture	<ul style="list-style-type: none"> <li>○ If inequality is high, small-scale fisheries are particularly important to secure the population's protein intake.</li> <li>○ If agricultural productivity increases, efficiency in fishing practices increases.</li> </ul>	Sauzade and Rousset 2013
Overfishing	<ul style="list-style-type: none"> <li>○ If seafood consumption is high and efficiency in fishing practices low, overfishing is high.</li> <li>○ If policies are effective and oriented towards sustainability, overfishing is managed successfully.</li> </ul>	Food and Agriculture Organization of the United Nations (FAO) 2014
Water demand	<ul style="list-style-type: none"> <li>○ If living standards are high, water demand is high, which includes high water demand due to tourism.</li> <li>○ If technological development in agriculture is low, a large amount of available freshwater is used for irrigation, which leads to water stress, particularly in semi-arid areas.</li> </ul>	World Economic Forum (WEF) 2011, Benoit and Comeau 2005, Adams et al. 2014, Sanna and Le Tellier 2013, Kok et al. 2006
Energy demand	<ul style="list-style-type: none"> <li>○ If use of renewables and energy efficiency are high, (fossil) energy demand decreases.</li> <li>○ If energy demand of fossil fuels is high, demand for international energy infrastructures in the coastal zone is high.</li> </ul>	Benoit and Comeau 2005, Bauer et al. 2017
Land subsidence	<ul style="list-style-type: none"> <li>○ If water demand is high and productivity in agriculture low, land subsidence is high as groundwater is increasingly exploited.</li> <li>○ If policies are effective and oriented towards sustainability, water resources are managed successfully.</li> </ul>	Adams et al. 2014, Nicholls et al. 2008b, Syvitski et al. 2009
Coastal zone management	<ul style="list-style-type: none"> <li>○ If international cooperation is high and if institutions work effectively, coastal zone management is effective.</li> <li>○ If coastal policies focus on sustainability, ecosystems are protected and land use change is restricted.</li> <li>○ If policies are oriented towards economic growth, socioeconomic development in the coastal zone is high as industry and services are concentrated in Mediterranean coastal locations.</li> </ul>	Adams et al. 2014, European Environment Agency (EEA) 2014, World Economic Forum (WEF) 2011, Nicholls et al. 2008b

Lifestyle/Second home ownership	<ul style="list-style-type: none"> <li>○ If international migration and living standards are high and if policies do not restrict settlement in coastal locations, second home ownership in the coastal zone is high.</li> <li>○ If second home ownership is high, additional jobs are created, which attract more people to move to the coast.</li> </ul>	Benson and O'Reilly 2009, Huete and Mantecón 2012
---------------------------------	--	---

### SM2.4 Mathematical equations used for the population projections

$$P^T = P^{CU} + P^{CR} + P^{IU} + P^{IR} \quad (1)$$

where  $P^T$  is the total population of one country and  $P^{CU}$ ,  $P^{CR}$ ,  $P^{IU}$ ,  $P^{IR}$  the population in each of the four zones ( $z$ ).

$$GD_{obs}^U = 1/2 * (gr_{\Delta t1}^{CU} - gr_{\Delta t1}^{IU} + gr_{\Delta t2}^{CU} - gr_{\Delta t2}^{IU}) \quad (2)$$

$$GD_{obs}^R = 1/2 * (gr_{\Delta t1}^{CR} - gr_{\Delta t1}^{IR} + gr_{\Delta t2}^{CR} - gr_{\Delta t2}^{IR}) \quad (3)$$

where  $GD_{obs}^U$  ( $GD_{obs}^R$ ) is the observed growth difference between the coastal urban (rural) and inland urban (rural) zone,  $gr$  is the growth rate,  $\Delta t1$  ( $\Delta t2$ ) refers to the years 2000 to 2005 (2005 to 2010), and  $CU$ ,  $IU$ ,  $CR$ , and  $IR$  to the four country zones ( $z$ ).

$$P_t^U = P_t * u_t \quad (4)$$

$$P_t^R = P_t * (1 - u_t) \quad (5)$$

where  $P_t^U$  ( $P_t^R$ ) is the projected urban (rural) population at time  $t$ ,  $P_t$  the population based on KC and Lutz 2017, and  $u_t$  the urbanization level based on Jiang and O'Neill 2017.

$$P_t^{CU} = \frac{P_{t-1}^{CU}(P_t^U - P_{t-1}^{IU} * GD_{SSP}^U)}{P_{t-1}^U} \quad (6)$$

$$P_t^{CR} = \frac{P_{t-1}^{CR}(P_t^R - P_{t-1}^{IR} * GD_{SSP}^R)}{P_{t-1}^R} \quad (7)$$

where  $P_t^{CU}$  ( $P_t^{CR}$ ) is the coastal urban (rural) population at time  $t$  and  $GD_{SSP}^U$  ( $GD_{SSP}^R$ ) the modified urban (rural) growth differences for each SSP. The inland urban (rural) population results from the difference of total urban (rural) population and coastal urban (rural) population.

$$r_t^z = \frac{P_t^z - P_{2010}^z}{P_{2010}^z} \quad (8)$$

where  $r_t^z$  is the population growth rate of a given zone  $z$  between time  $t$  and the base year 2010. Finally, we multiply  $r_t^z$  by the GPWv4 of 2010 in 5-year time steps until 2100.

## **SM2.5 Full Mediterranean coastal SSP narratives**

### *SSP1 – Green Coast*

This pathway focuses on sustainable development. Due to effective international cooperation and rapid technological development and transfer, best practices are circulated in the whole region, which results in converging socioeconomic development. Economic growth is moderate in northern Mediterranean countries and high in the south and east, which reduces inequality across countries. As a result, international migration decreases although migration between all Mediterranean countries is possible. Urbanization is high and well managed in all countries; policies promote compact cities without urban sprawl. The focus on more regionalized production results in moderate international trade, in which markets of the whole region are interconnected. As southern and eastern Mediterranean countries get increasingly integrated into international trade, the shipping industry gains importance in these countries. It remains on a similar level in the Mediterranean north, with increasing efficiency in all countries.

Similarly, agricultural productivity increases. This leads to improved efficiency in fishing practices and fleet, particularly in southern and eastern Mediterranean countries. Due to less material-intensive consumption and low-meat diets, the importance of fishing decreases. Also, effective regulation in the form of fishing quotas allows for overfished stocks to recover. Further, water demand decreases in all countries due to more sustainable water use as well as more efficient water treatment. Similarly, demand for international energy infrastructures decreases, as renewable energies are pursued and energy efficiency increases considerably. Tourism demand increases in the southern and eastern Mediterranean because of higher living standards and remains on a similar level in the northern part of the region. All countries pursue sustainable tourism. Hence tourism activities concentrate on regional travel, leading to decreasing total international tourism demand.

Coastal zone management is highly effective in the whole region. Policies acknowledge the protective function of coastal ecosystems and focus on their conservation and restoration. Therefore, policies prevent migration to coastal areas. As a consequence, population growth in delta regions declines, which reduces the rate of land subsidence. Second home ownership in the coastal zone is restricted in the whole region.

Considering these developments, coastal population growth decreases compared to inland locations in the whole Mediterranean. Coastal ecosystem protection and decreasing importance of fisheries lead to declining population growth in coastal rural areas. Restrictive policies inhibit migration to coastal urban areas. Nevertheless, due to the importance of shipping and inertia of urban infrastructure, coastal urban population growth is marginally lower than in the inland. These growth trends in rural and urban areas are more pronounced in the northern Mediterranean as compared to the southern and eastern parts of the region as socioeconomic development of the countries converges gradually in the course of the century. Therefore, we reduce the observed rural growth difference by 3% in the north and by 1% in the south and east and the urban growth difference by 2% and 1%, respectively.

*SSP2 – No Wind of Change*

This pathway is characterized by continuing historical patterns. Efforts for more efficient international cooperation across the region are made, but success is limited. Technological development is uneven, with generally high development in the northern Mediterranean and slow transfer to southern and eastern countries. Economic growth and reduction in inequality are uneven, with higher economic growth in the south and east, but lower reductions in inequality than in northern countries. Limited mobility as well as restrictive visa regulations lead to moderate international migration. Urbanization is high in northern Mediterranean countries and moderate elsewhere, with considerable urban sprawl. International trade takes place in semi-globalized markets which are dominated by northern Mediterranean countries and interconnection with southern and eastern markets is limited. Consequently, the shipping industry is of high importance in the Mediterranean north and of lower importance in the south and east.

Agricultural productivity increases gradually, which results in increasing efficiency of fishing practices and fleet, especially in southern and eastern countries. Since consumption is material-intensive and meat-rich, fisheries remain important. As a result, overfishing is a problem in the whole region. Water demand is high in all Mediterranean countries and mainly driven by tourism in northern countries and agriculture in southern and eastern Mediterranean countries. In the north, water resources are more effectively managed over time. In semiarid areas, in particular in the Middle East and the Maghreb, water stress leads to progressing desertification. Energy demand is high in northern Mediterranean countries and moderate in the south and east. As energy efficiency is moderate and renewables are used unevenly, demand for international energy infrastructures is high in the north and moderate in the south and east. Tourism is characterized by mass tourism in northern countries. The cruise sector plays an important role as well. In other Mediterranean countries, tourism is directed towards international tourists and experiences a gradual increase.

In the whole region, coastal zone management focuses on local issues and is moderately successful. Coastal ecosystems are lost to built-up areas, particularly in the northern Mediterranean, but increasingly so in the south and east. This development, combined with increasing exploitation of groundwater, results in progressing subsidence of river deltas in the whole region. Second home ownership in the coastal zone continues to increase in northern Mediterranean countries and experiences moderate demand in the south and east.

In this pathway, population growth patterns in the coastal zone continue like before. In coastal rural areas of the Mediterranean north, population growth is mainly driven by tourism and second home ownership. In the south and east, population growth in coastal rural locations is higher due to the continuing importance of small-scale fisheries. Regarding coastal urban areas of the north, population growth is primarily determined by the importance of shipping and tourism. Compared to this, coastal urban areas of southern and eastern countries experience lower population growth, as their participation in international trade and tourism activities is limited. Consequently, we use the observed urban and rural growth differences without modifying them.

*SSP3 – Troubled Waters*

This pathway is characterized by regional rivalry. Policies aim for national interests and security. Thus international cooperation is weak and international organizations (e.g. EU, Arab League) fall apart. Therefore, technological development and transfer are slow, which particularly affects eastern and southern Mediterranean countries. Economic growth is low in the whole region and inequalities between countries increase. Consequently, demand for international migration is high, in particular from southern and eastern countries to the north, but extremely limited due to strict visa regulations. The entire region is characterized by low and poorly managed urbanization, resulting in sprawling urban areas which are unattractive for further settlement. The de-globalizing economy concentrates on national markets. Therefore, international trade is strongly constrained, leading to considerable reduction in shipping in all countries. The remaining shipping routes are primarily located in the northern Mediterranean and are hardly interconnected with the south and east.

Low technological development in agriculture leads to inefficient fishing practices. Particularly southern and eastern Mediterranean countries are characterized by a high share of small-scale artisanal fisheries. Fishing concentrates on domestic demand which is characterized by material-intensive consumption in the whole region, leading to severe overfishing. Further, groundwater is exploited extensively for agricultural use. This results in serious environmental degradation which advances desertification in semiarid locations. Energy demand is moderate due to low economic growth and low energy efficiency. As domestic energy sources are pursued, international energy infrastructures are decommissioned. Tourism demand decreases in all countries because of lower living standards and concentrates on domestic destinations.

Coastal management is weak and uncoordinated. If policies are in place, they concentrate on local issues. As a consequence, coastal ecosystems experience serious degradation. River deltas are put under high stress and land subsidence accelerates in the entire region. Due to low international migration and a low income level, second home ownership in the coastal zone decreases.

In this pathway, coastal attractiveness for human settlement decreases. As living standards decrease, this pathway is characterized by little mobility of the population and thus little coastal migration. In coastal rural locations, population grows due to increasing importance of fisheries despite the fact that coastal waters are overfished to large extents. Coastal urban areas lose their attractiveness compared to inland cities due to declining shipping and tourism. Therefore, population growth in coastal urban locations is almost exclusively driven by natural growth and does not differ from inland areas. These population growth patterns are less pronounced in the south and east than in northern countries. In the south and east, coastal rural locations experience higher growth and coastal cities do not lose their advantage over inland cities as severely. The reason for this is the presently higher importance of fisheries and lower importance of shipping and tourism in southern and eastern countries. Especially in the south and east, the population is forced to move closer to the coast as desertification advances. To account for these growth patterns, we modify the rural growth difference by +0.5% in northern

countries and +1% in southern and eastern countries and the urban growth difference by -1% and -0.5%, respectively.

#### *SSP4 – Fragmented Coast*

This pathway is characterized by high inequalities across and within countries. The Mediterranean region is divided into two groups: a wealthy elite which comprises a small share of the population and a poorer population group which makes up the rest of the population. The majority of the elite lives in the northern Mediterranean and is connected globally. Although technological development and transfer are high among the elite, transfer to poorer population groups is limited. Therefore, economic growth is uneven, with high growth primarily in northern countries and low growth in the south and east. Inequality is high, both within and across countries. Especially in northern Mediterranean countries, low population growth leads to aging of the population. In combination with high economic growth, this results in high demand for human resources. However, owing to low mobility of poorer populations in the Mediterranean south and east, international migration is moderate. Despite high attractiveness of urban areas in the Mediterranean north, urbanization is moderate due to aging of the population. Effective management leads to low urban sprawl. Urbanization is high in the south and east since cities are regarded as economic engines. Due to a lack of management, these areas experience considerable urban sprawl, with poorer population groups living in peri-urban slums in vulnerable locations, which are characterized by high unemployment. International trade is high among the elite, but is not connected with other population groups. Consequently, in northern Mediterranean countries shipping is high and interconnected with efficient fleets. In the south and east, shipping is moderate and mainly characterized by poor equipment and little interconnection. Generally, poorer population groups are dependent on manufactured goods from the elite and supply the elite with raw products.

Agricultural productivity increases for large-scale farming and is low in small-scale agriculture. Therefore, fisheries in the north are mainly characterized by highly efficient large-scale fisheries, whereas the Mediterranean south and east are dominated by small-scale fisheries with low efficiency. The importance of fisheries increases in the whole region due to high consumption of fish by both, the elite and poorer population groups. Among poorer population groups, fish is a main source of protein intake and fisheries mostly operate for subsistence purposes. In the course of the century, overfishing becomes a serious problem. Further, high water demand leads to extreme water stress and progressing desertification in semiarid locations. Around the elite, especially in northern countries, water is used excessively for luxurious lifestyles, but is well-managed; among the rest of the population, water-intensive agriculture is the main driver of water demand. Energy demand decreases among the elite due to an increase in efficiency and use of renewable energies. These new technologies are not accessible to the remaining population, resulting in moderate demand for international energy infrastructures, especially in the south and east. Tourism demand is high among the elite; it pursues high-class tourism at international destinations. Therefore, most tourists come from the Mediterranean north, whereas the majority of the population cannot afford travel.

Management of the coastal zone is efficient at the local level. It is directed towards the elite's benefit with little interest in sustainable solutions. Coastal ecosystems are destroyed for land reclamation to realize prestigious building projects in these highly attractive environments. Poor coastal management results in serious degradation. Due to the importance of agriculture, population growth is high in delta regions, especially in the south and east; this leads to accelerating land subsidence. The elite aims for engineered solutions to slow down subsidence rates. Second home ownership in the coastal zone is popular among the elite.

In this pathway, coastal population growth increases compared to inland population growth in the whole region. Among the elite, coastal population growth in rural areas is mostly driven by tourism and ownership of second homes and by small-scale subsistence fisheries among other population groups. Urban areas experience high population growth since they are regarded as economic engines. Coastal growth is higher in the south and east compared to the north because coastal population growth is mainly driven by poorer population groups. Further, in countries affected by advancing desertification, people are forced to move closer to the coast. Due to these developments, we increase the rural and urban growth differences by 1% in the north and by 2% in the south and east.

#### *SSP5 – Coast Rush*

This pathway focuses on economic growth. Effective international cooperation leads to rapid technological development and transfer across the whole region. Economic growth is high in all Mediterranean countries and inequality is strongly reduced, particularly in the south and east. International migration is high due to an open migration policy and high mobility. It mostly takes place from the south and east to the north because of a lack of human resources resulting from demographic change and aging. Urbanization is high in all countries with some urban sprawl, which becomes more effectively managed over time. In this highly globalized world, international trade is high and all Mediterranean countries are increasingly interconnected. Consequently, the shipping industry experiences a marked increase in volume and efficiency. Especially the south and east profit from this development.

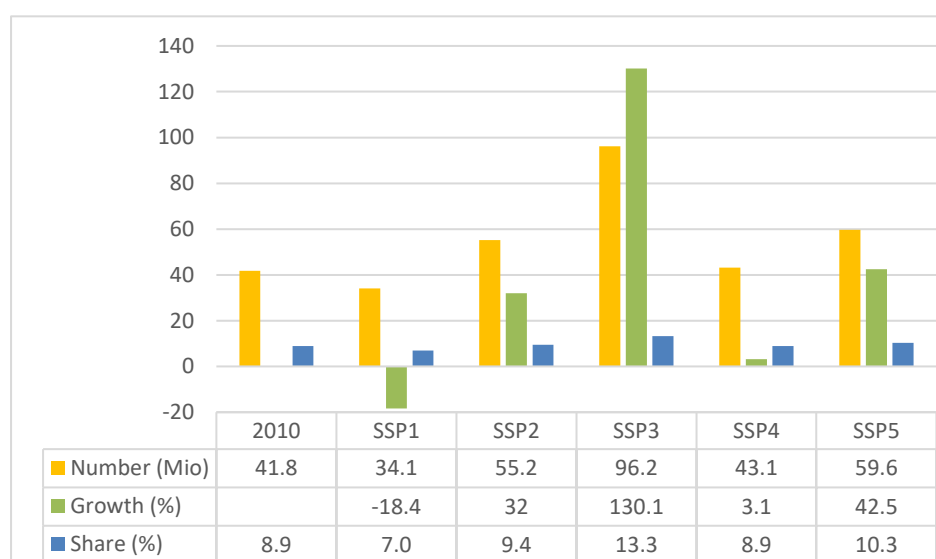
Increasing productivity in agriculture leads to higher efficiency in fisheries and small-scale fisheries are almost completely replaced by large-scale enterprises. Material-intensive consumption and meat-rich diets lead to relatively high importance of fisheries. Therefore, overfishing becomes a serious threat in the whole region, which is counteracted by increased use of aquaculture. Further, high water demand leads to groundwater depletion, particularly in semiarid locations. Engineering solutions, such as desalination plants and water pipelines, provide affected regions with freshwater. Similarly, demand for international energy infrastructures is high to meet the high demand of fossil fuels in all Mediterranean countries. Due to high living standards and mobility, all Mediterranean countries participate in tourism activities, resulting in a substantial increase in tourism demand in the south and east. Tourism mostly takes place in the form of mass tourism across national borders, including the cruise sector.



Coastal zone management is highly effective in the north and increasingly so in the south and east. However, it focuses on economic growth rather than environmental issues. Loss of coastal ecosystems and continuing land subsidence are managed by engineering solutions at a local scale to ensure well-being of the population. Since international mobility is high, the number of second homes in the coastal zone increases particularly in the Mediterranean south and east, as the coastal zone of the north is densely built up.

In this highly globalized world, the coastal zone is extremely attractive, leading to higher population growth in the coastal zone compared to inland locations in all Mediterranean countries. In coastal rural areas, tourism and second homes are the main drivers of population growth. Population in coastal urban areas increases since economic activity is concentrated in these. Due to high urbanization rates and urban sprawl, many rural areas get urbanized. These growth trends are more pronounced in the Mediterranean south and east than in the north because of catch-up effects. Therefore, we increase the observed rural growth difference by 2% in northern countries and by 3% in the south and east and the urban growth difference by 3% and 4%.

## SM2.6 Total LECZ population in the Mediterranean in 2010 and 2100



Number (Mio) gives the total population count, Growth (%) represents the change of the LECZ population relative to the base year 2010, and Share (%) is the share of people living in the LECZ compared to the total population.

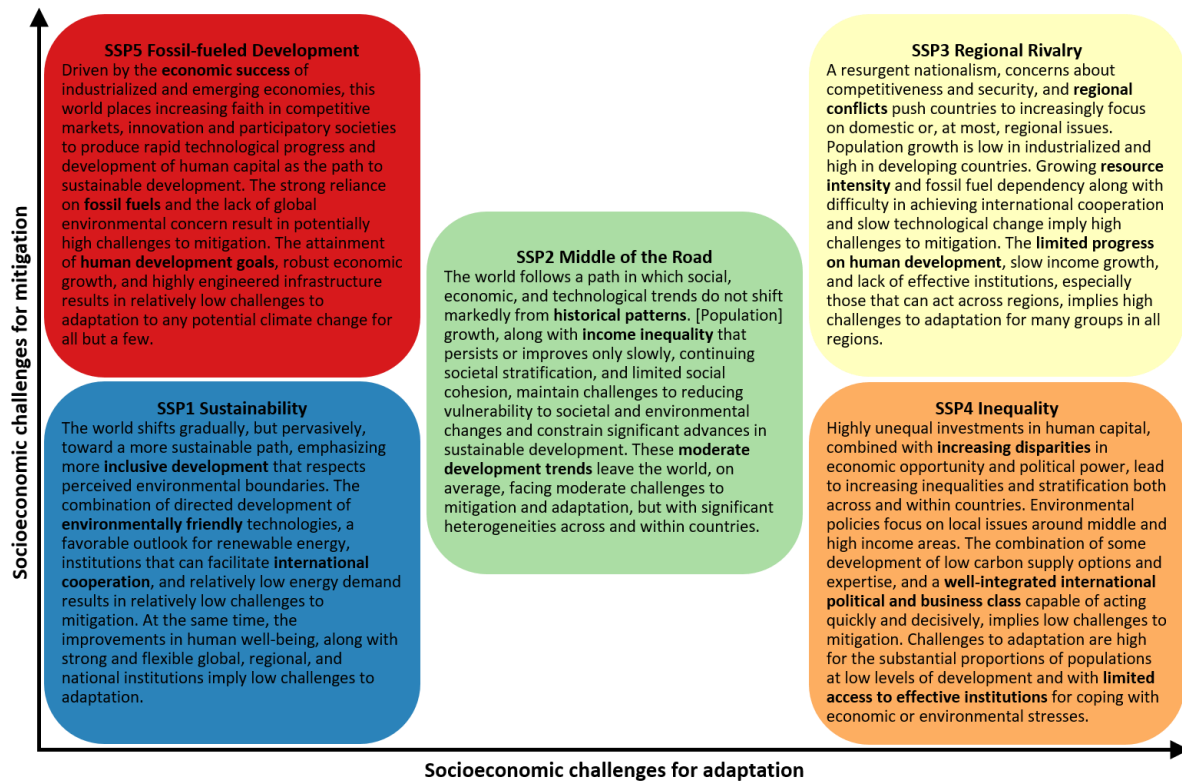
## SM2.7 LECZ population per country for each SSP in 2050 and 2100 compared to the base year 2010

Country	ISO	GPWv4 <sup>18</sup> 2010	SSP1		SSP2		SSP3		SSP4		SSP5	
			2050	2100	2050	2100	2050	2100	2050	2100	2050	2100
Albania	ALB	444,563	377,316	141,629	455,875	293,312	563,793	533,301	430,734	198,819	456,389	243,262
Algeria	DZA	766,270	1,531,805	1,209,261	1,643,533	1,681,836	1,674,679	2,161,783	1,710,406	1,508,606	1,769,957	1,652,208
Bosnia and Herzegovina	BIH	6,805	1,195	139	2,027	803	3,070	2,350	1,587	289	1,734	371
Croatia	HRV	110,735	104,589	61,590	116,011	98,059	107,395	108,155	114,484	81,116	138,703	114,122
Cyprus	CYP	73,104	103,982	74,345	108,912	107,952	95,947	106,666	104,693	87,571	126,685	110,276
Egypt	EGY	27,023,874	31,659,993	19,582,337	41,574,667	36,133,737	58,322,636	76,944,136	35,649,489	25,791,780	37,598,322	32,188,092
France	FRA	694,496	971,476	1,047,405	1,084,240	1,420,165	872,299	744,753	1,085,378	1,268,721	1,510,806	3,162,200
Greece	GRC	954,875	885,139	702,661	885,643	740,672	770,371	443,713	854,779	606,888	1,038,545	1,141,313
Israel	ISR	367,166	629,070	849,707	647,749	955,577	527,231	546,976	611,164	770,746	832,065	1,724,143
Italy	ITA	4,819,787	4,209,723	2,687,993	4,524,282	3,483,454	3,770,642	1,981,219	4,516,665	3,144,140	5,864,348	6,545,776
Lebanon	LBN	357,157	250,043	171,187	268,158	220,804	290,508	321,707	253,031	163,048	258,184	178,485
Libya	LBY	252,773	785,213	659,722	829,867	874,646	907,176	1,311,088	810,826	701,702	803,087	683,558
Malta	MLT	23,062	20,696	13,166	21,540	17,916	21,177	22,009	20,078	13,111	21,740	14,360
Montenegro	MNE	27,882	39,052	22,786	41,649	32,815	41,447	42,761	42,878	30,397	48,897	37,452
Morocco	MAR	256,009	368,068	254,016	389,408	344,728	416,149	525,565	466,320	442,807	474,595	464,321
Palestine	PSE	115,843	192,461	164,367	218,523	253,201	298,485	595,084	280,434	471,527	190,008	131,586
Slovenia	SVN	22,117	32,089	38,797	31,730	44,632	20,955	17,426	32,113	40,747	51,042	121,401
Spain	ESP	1,830,301	2,836,191	2,758,142	2,908,755	3,368,237	2,164,089	1,666,767	2,916,075	3,046,001	4,002,058	6,326,101
Syria	SYR	173,960	214,479	130,392	247,142	200,860	275,420	313,370	344,939	500,330	291,794	279,320
Tunisia	TUN	1,382,041	2,472,017	1,895,227	2,512,180	2,329,742	2,493,724	2,914,805	2,480,666	1,789,299	2,534,351	1,951,964
Turkey	TUR	2,129,580	2,684,526	1,678,642	3,068,951	2,629,922	3,530,439	4,942,771	3,156,732	2,469,884	3,179,355	2,546,452
<b>Total</b>		<b>41,832,399</b>	<b>50,369,123</b>	<b>34,143,511</b>	<b>61,580,842</b>	<b>55,233,070</b>	<b>77,167,632</b>	<b>96,246,405</b>	<b>55,883,471</b>	<b>43,127,529</b>	<b>61,192,665</b>	<b>59,616,763</b>

<sup>18</sup> GPWv4 = Gridded Population of the World, Version 4

## APPENDIX B

### SM3.1 SSP narrative excerpts



**Supplementary Figure 3.1** The five SSPs based on their challenges for adaptation and mitigation, with excerpts of each narrative (O'Neill et al. 2017, own emphasis added)

### SM3.2 Spatial mask processing

The spatial mask  $l_i$  determines the habitability of each grid cell based on five geographic variables: water bodies, protected land, elevation, slope, and bare land. We assembled the spatial mask based on high-resolution datasets that were publicly available for the entire Mediterranean region (Supplementary Table 3.1). Grid cell values range from 0 (uninhabitable) to 1 (fully inhabitable) based on the proportion of each cell that is inhabitable. By analyzing the current population distribution (2015) for the respective input variable, we assigned a likelihood to each cell (ranging from 0 to 1) to be inhabited.

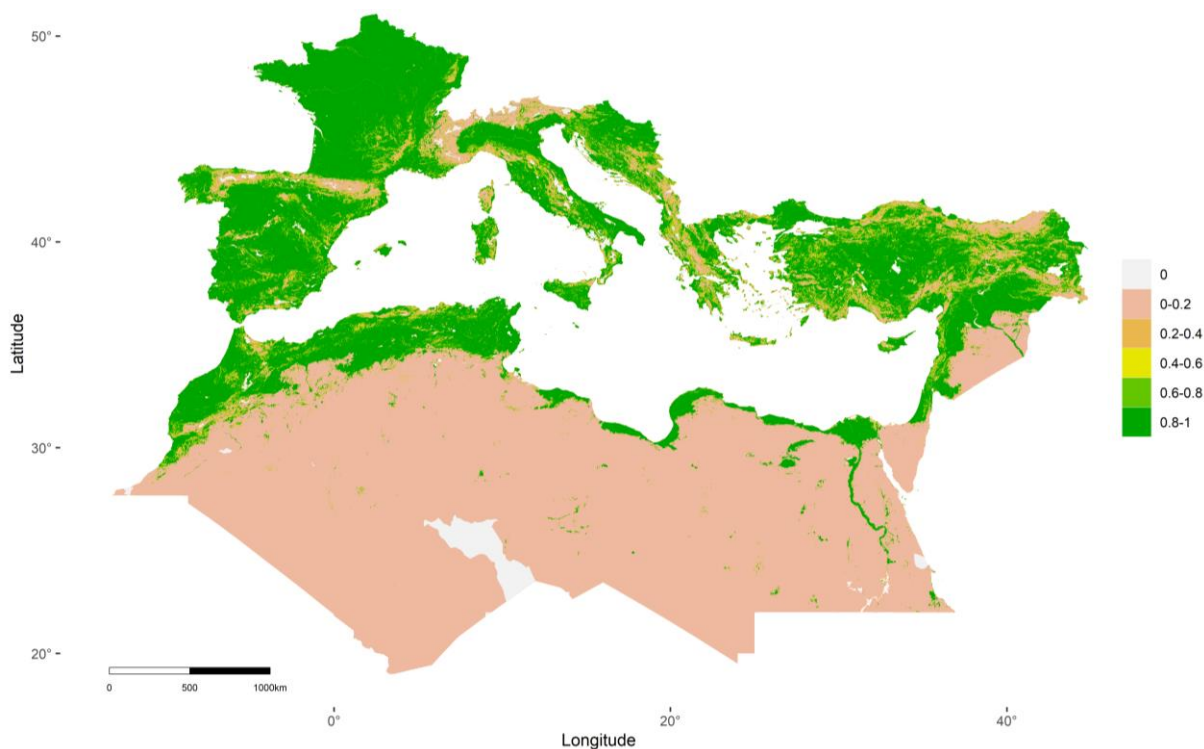
To establish water bodies, we used the full maximum water extent of Pekel et al. 2016 (as of 2015) and set the spatial mask to zero in those locations. For protected land, we selected the International Union for the Conservation of Nature (IUCN) protection categories Ia (nature reserve), Ib (wilderness area) and II (national park) from the World Database on Protected Areas (WDPA) database and masked these out for human settlement, assuming that mandate for protection will remain constant until 2100. Further, we established the currently highest-

elevation settlement based on the Multi-Error-Removed Improved-Terrain Digital Elevation Model (MERIT DEM) by analyzing the population distribution of 2015. As a result, we excluded all elevation above 3832m. We used MERIT DEM as, in the US, it has a root mean square error (RMSE) of 3.14m, which is considerably lower than that of other widely used DEMs such as the SRTM DEM or ASTER DEM (Gesch 2018).

**Supplementary Table 3.1** Data used for spatial mask processing

<b>Variable</b>	<b>Data name</b>	<b>Original horizontal resolution</b>	<b>Reference</b>
Water bodies	Global Surface Water	1 arc second	Pekel et al. 2016
Protected land	World Database on Protected Areas (WDPA)	Polygon shapefiles	UNEP-WCMC and IUCN 2019
Elevation + Slope	MERIT DEM	3 arc seconds	Yamazaki et al. 2017
Bare land	ESA CCI land cover	10 arc seconds	ESA 2017

We also calculated slope [in degrees (°)] from MERIT DEM and analyzed how the current population is distributed in different slope classes. We found 98% of the 2015 population to live in terrain with a maximum slope of 15°; the remaining 2% of the population lived in terrain with slopes between 15° and 45°. Accordingly, we masked out all terrain with slopes over 45°, assigned terrain with slopes of 15° to 45° a probability value of 0.02, and set the mask values for slopes up to 15° to 1. As large parts of the southern and eastern Mediterranean region are semi-desert or desert areas, we additionally accounted for the land cover class ‘bare land’. To do so, we established patches of connected cells of bare land and selected the largest patches in the southern and eastern parts of the region. We then analyzed the proportion of population living in these patches in the year 2015, and applied this value (i.e. 0.025) to the spatial mask. In a final step, we combined all mask layers by multiplying them, and aggregated the spatial mask to a resolution of 30 arc seconds, retaining the proportional degree of habitability of the higher resolution (Supplementary Figure 3.2).



**Supplementary Figure 3.2** Spatial mask: Habitability per grid cell. Resolution: 30 arc seconds (WGS84)

### SM3.3 Coastal Zone Definition

To differentiate coastal versus inland locations, we produced a coastal mask that combined a coastal buffer with an elevation-based definition of the coastal zone, following Reimann et al. 2018a. We used a 20km coastal buffer as it covers large urban areas in coastal locations (Kummu et al. 2016). In the Mediterranean in 2015, over 50% of the population living within 100km from the coastline lived within the 20km distance buffer, which corresponded to almost one third of the total Mediterranean population (based on GHS-POP). Second, we combined the distance buffer with the Low Elevation Coastal Zone (LECZ), which includes all land with an elevation of up to 10m in hydrological connection to the sea (McGranahan et al. 2007). We established the LECZ with the help of MERIT DEM (SM3.2).

### SM3.4 Urban population definition

The GHS-based settlement model GHS-SMOD differentiates seven settlement classes, four of which can be attributed to urban land (i.e. urban centers, dense urban clusters, semi-dense urban clusters, and suburban/peri-urban areas) (Florczyk et al. 2019). We defined the urban population of 2015 for each country, using the GHS-SMOD data of 2015 (Pesaresi et al. 2019). To do so, we used a three-step process: first, we used full SMOD classes, starting with urban centers and adding further settlement classes (as the definition of ‘urban’ differs markedly

across countries (Seto et al. 2011), we had to use different SMOD classes for each country). Second, we added individual settlements of the next SMOD class; third, we added population cells next to the settlements defined in steps 1 and 2, starting with the highest population density, until the population defined as urban equaled the total urban population number provided by the WUP (United Nations, Department of Economic and Social Affairs, Population Division 2019).

To define the urban population of the years 2000 and 1990, we followed a slightly different process: for the year 2000, we used the cells defined as urban in 2015 as a mask for urban population and deducted (added) population from (to) this mask until the total population matched the urban population as defined by the WUP. We then repeated this process for 1990, where we used the urban population grid of 2000 as a mask.

### **SM3.5 Development of coastal versus inland $\beta$ parameters**

As our  $\beta$  calibration procedure did not produce plausible results for coastal versus inland locations (i.e. it resulted in negative  $\beta$  parameters), we had to modify the calibrated urban and rural  $\beta$  parameters to account for the differences in spatial development patterns in these locations. This issue possibly arose due to the relatively small strip of land defined as coastal, which covers only 2.8% of the Mediterranean land area. To establish the differences in coastal versus inland locations, we analyzed the spatial patterns of urban and rural population changes in those locations for the calibration period (i.e. 1990-2010).

Our analysis showed that urban sprawl (i.e. number of additional urban grid cells) was higher in the northern Mediterranean than the southern and east Mediterranean (as reflected in the urban  $\beta$  parameters calibrated for the two regions: 0.459 versus 0.617). Further, we found sprawl to be higher in coastal locations compared to inland locations in both regions, with higher sprawl in coastal locations of the South and East relative to the inland. In terms of population growth in coastal rural (CR), inland rural (IR), coastal urban (CU), and inland urban (IU) locations, we established the same patterns, with higher population growth rates in coastal locations compared to the respective inland locations. We calculated the growth difference (GD) between coastal and inland locations following Merkens et al. 2016 and found GDs of 0.10/0.20 in urban/rural locations in the northern Mediterranean and GDs of 0.28/0.09 in urban/rural locations in the southern and eastern Mediterranean. We used these GDs as modification factors to adjust the calibrated  $\beta$  parameters, resulting in the four parameters (i.e. CR, IR, CU, IU) per geographical region presented in Supplementary Table 3.2.

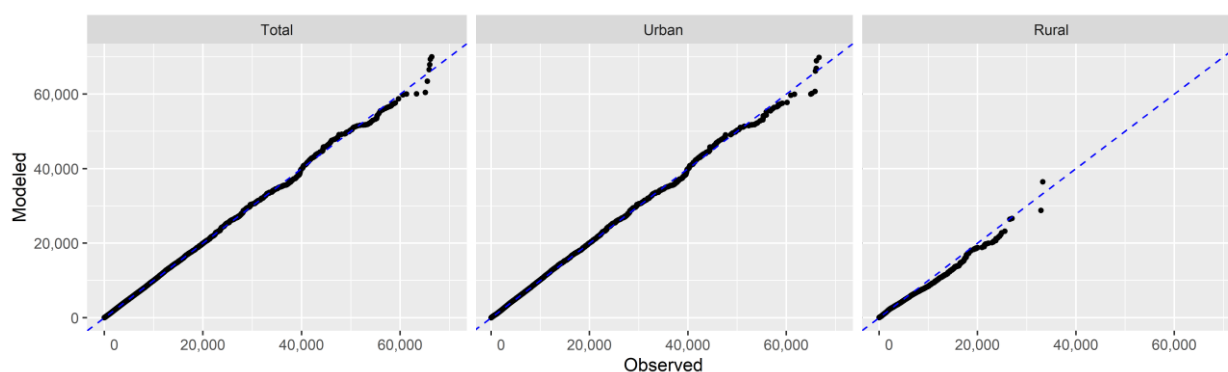
**Supplementary Table 3.2** Established  $\beta$  parameters for coastal rural (CR), inland rural (IR), coastal urban (CU), and inland urban (IU) locations in both geographical regions

Settlement type	North		South & East	
	Factor	$\beta$	Factor	$\beta$
<b>Rural</b>		<b>2</b>		<b>0.089</b>
CR	- 10%	1.8	- 5%	0.084
IR	+ 10%	2.2	+ 5%	0.093
<b>Urban</b>		<b>0.459</b>		<b>0.617</b>
CU	- 5%	0.436	- 15%	0.524
IU	+ 5%	0.482	+ 15%	0.710

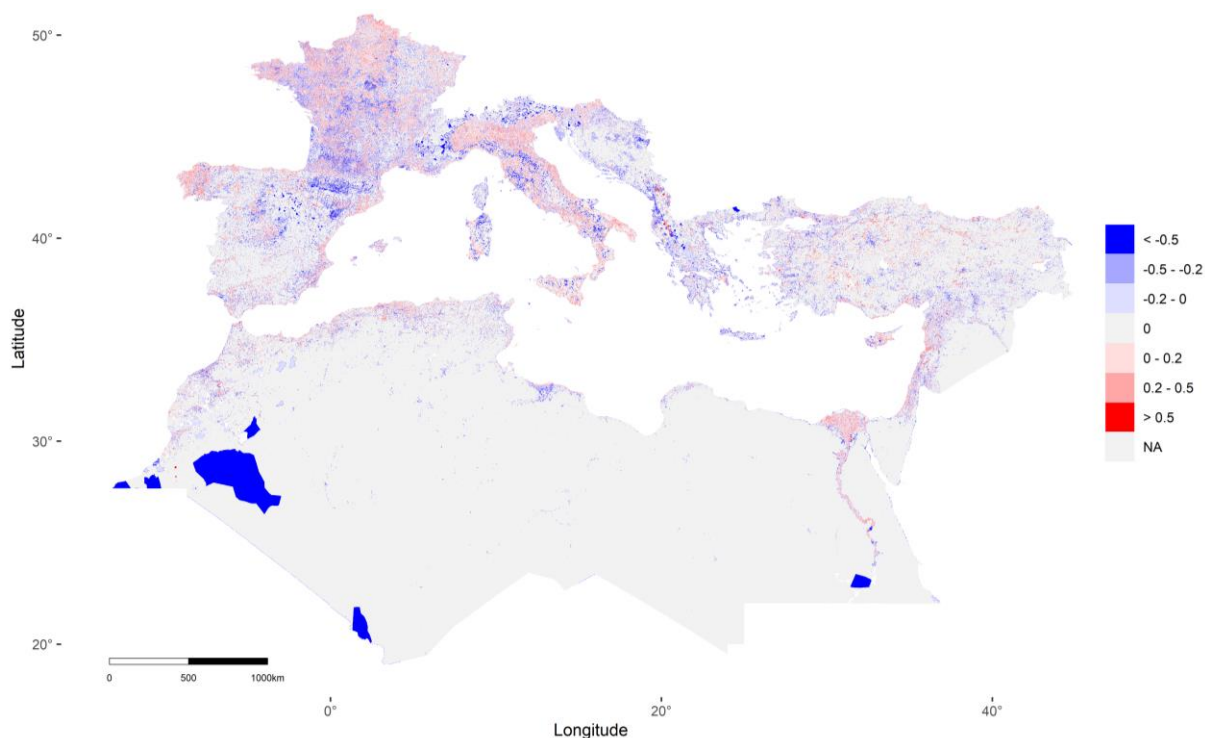
### SM3.6 Model validation

Supplementary Figure 3.3 presents Q-Q plots of the modeled versus the observed population for the total population, urban populations, and rural populations, reflecting the best model fit for the total population (i.e. when combining urban and rural populations). Supplementary Figure 3.4 presents the relative absolute error (RAE) per grid cell, calculated by dividing the error per cell by the observed population in that cell. Similar to Jones and O’Neill 2013, high positive or negative RAEs can primarily be associated with rural locations where the relative error is high, although the total error is small (mostly <100 persons).

The error metrics calculated for the entire Mediterranean region can be found in Supplementary Table 3.3. We would like to point out that we avoided overfitting the model to current population patterns and trends as the aim of this work was to produce population projections that explore the range of uncertainty regarding plausible future population patterns. As future patterns of spatial population change can be considerably different from observed trends, we left flexibility in the model to allow for patterns to emerge that have not been observed in the past.



**Supplementary Figure 3.3** Q-Q plots of the total population, urban populations, and rural populations. Blue line represents the perfect fit



**Supplementary Figure 3.4** Relative absolute error (RAE) per grid cell for the observed versus modeled total population in 2010. Blue colors = model underestimates population, red colors = model overestimates population

**Supplementary Table 3.3** Model performance metrics for the entire Mediterranean region (MAE = mean absolute error, WMAPE = weighted mean absolute percentage error, RMSE = root mean square error)

<b>Settlement type</b>	<b>MAE</b>	<b>WMAPE [%]</b>	<b>RMSE</b>	<b>R<sup>2</sup></b>
<b>Rural</b>	7.6	34.4	97.6	0.64
CR	32.2	30.9	169.3	0.75
IR	5.9	35.7	90.3	0.59
<b>Urban</b>	7.0	18.3	111.9	0.94
CU	34.1	18.0	217.4	0.96
IU	5.2	18.5	100.6	0.92
<b>Total</b>	6.6	14.7	79.4	0.97

### SM3.7 Model modifications for each SSP

We modified the calibrated  $\beta$  parameters to ensure consistency of the future spatial development patterns with the socioeconomic (O'Neill et al. 2017) and urban (Jiang and O'Neill 2017) developments described in the SSP narratives. To establish multiplication factors for each  $\beta$  parameter, SSP and geographical region, we used a three-step approach, similar to Reimann et al. 2018a. First, we ranked the SSPs with regard to their differences in urban development patterns, also establishing whether the spatial development patterns become more

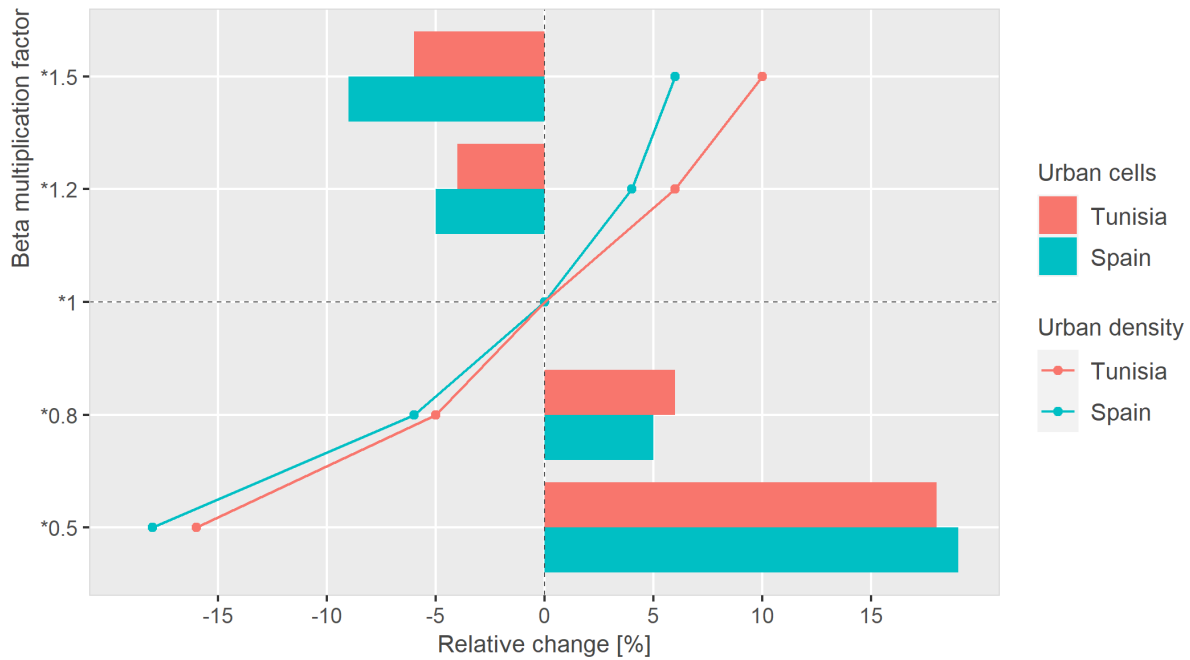


concentrated or more sprawling compared to the observed patterns; second, we established differences between the two geographical regions based on the Mediterranean coastal SSP narratives (Reimann et al. 2018a); third, we extensively tested different multiplication factors to establish those that produced plausible spatial population patterns for each SSP and geographical region. This process resulted in the multiplication factors presented in Supplementary Table 3.4, representing compact development under SSP1, slight decrease in sprawl under SSP2 (compared to historical patterns), and an increase in sprawl under SSPs 3-5, with generally slightly higher sprawl in southern and eastern countries due to less effective management (Reimann et al. 2018a).

**Supplementary Table 3.4** Multiplication factors for the calibrated  $\beta$  parameters per SSP and geographical region derived from the qualitative assumptions in the SSP narratives (O'Neill et al. 2017, Jiang and O'Neill 2017)

	Qualitative assumptions	Multiplication factor	
		North	South & East
<b>SSP1</b>	- Well-managed, compact urban development - Reduce incentives that promote urban sprawl and population de-concentration	4	3
<b>SSP2</b>	- Continuation of historical patterns - Slow adoption of sustainable technologies	1.5	1.2
<b>SSP3</b>	- Poorly managed, unattractive cities - Lack of regulation	0.98	0.98
<b>SSP4</b>	- Mixed development across and within cities - Middle Income Countries: Cities as engines of growth - High Income Countries: high concentration of elites	0.95	0.9
<b>SSP5</b>	- Large metropolitan areas with urban sprawl	0.9	0.85

The reason for using high multiplication factors for more compact development patterns compared to those for increasing sprawl lies in the fact that the model is sensitive to changes in the  $\beta$  parameter, in particular the closer  $\beta$ s are to 0. We tested the model's sensitivity to changes in  $\beta$  by producing population projections for Tunisia and Spain based on a range of multiplication factors. We found that a 50% decrease in calibrated  $\beta$  values led to an increase in urban grid cells of 18-19%, while a 50% increase led to a decrease of 6-9% (Supplementary Figure 3.5). Similarly, a 50% decrease in  $\beta$  resulted in 16-18% less densely populated urban locations, while a 50% increase resulted in an increase in urban population densities of 6-10%. To account for this asymmetry/skewness, we chose multiplication factors close to 1 for SSPs 3-5 (increase in sprawl), and relatively high multiplication factors for SSP1 and SSP2 (more compact development).

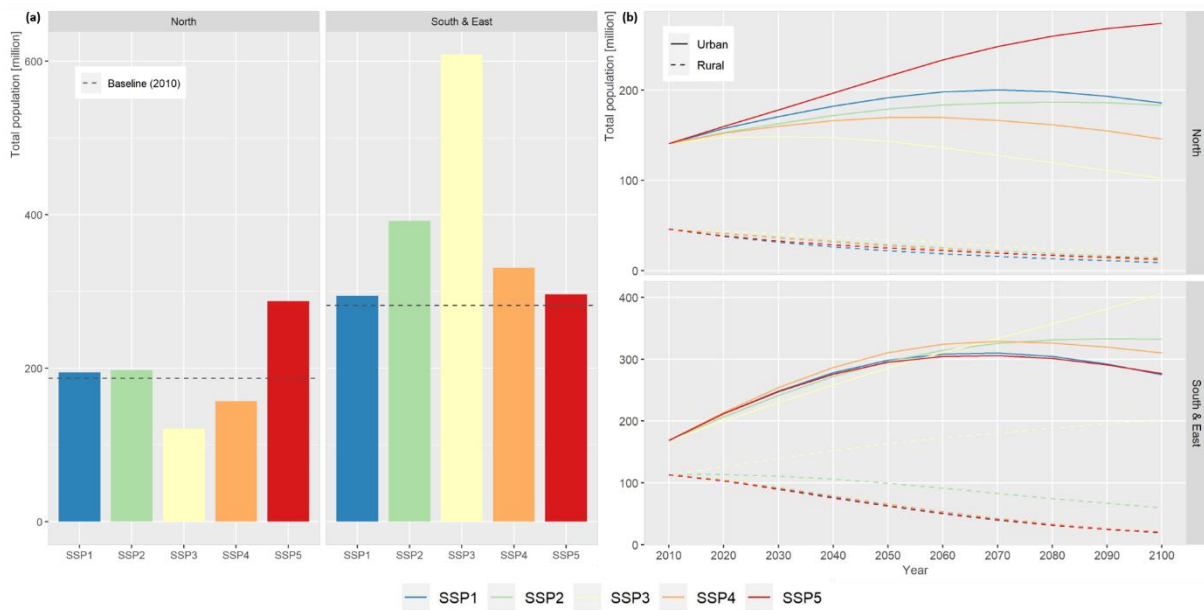


**Supplementary Figure 3.5** Relative changes in urban grid cells and urban population density when using different beta multiplication factors. Results for Tunisia and Spain under SSP2 in 2100

We additionally applied a population density threshold per grid cell to avoid unrealistically high population densities, using the currently (2015) highest density grid cell in urban and rural locations in each geographical region as a baseline. Similar to the multiplication factors derived for the  $\beta$  parameters, we increased the observed values under SSP1 (+10%) and SSP2 (+5%) and decreased them under SSP4 (-5%) and SSP5 (-10%).

Furthermore, we produced two additional spatial masks (in addition to the baseline spatial mask described in SM3.2) to reflect future changes in habitability consistent with the SSP narratives. As SSP1 is a scenario of sustainable development, we assumed the IUCN protection categories III (national monument) and IV (habitat/species management area) to be additionally unavailable for human settlement; we decreased the maximum elevation available for settlement by 10%; and we reduced the probability values for slope and bare land by half. As SSPs 4 and 5 are characterized by high technological change and effective management but limited awareness of sustainable solutions, we assumed only IUCN category III to become additionally unavailable for human settlement; we increased the elevation threshold by 10%, and we doubled the probability values for slope and bare land. For SSPs 2 and 3, we assumed no future changes in habitability, and therefore used the baseline spatial mask.

### SM3.8 National-level population and urbanization projections under the SSPs



**Supplementary Figure 3.6** Population and urbanization projections for each SSP and geographical region. (a) in 2100 compared to 2010, (b) differentiating urban versus rural populations. Please note different scales of the y-axes. Data source: International Institute for Applied Systems Analysis 2018

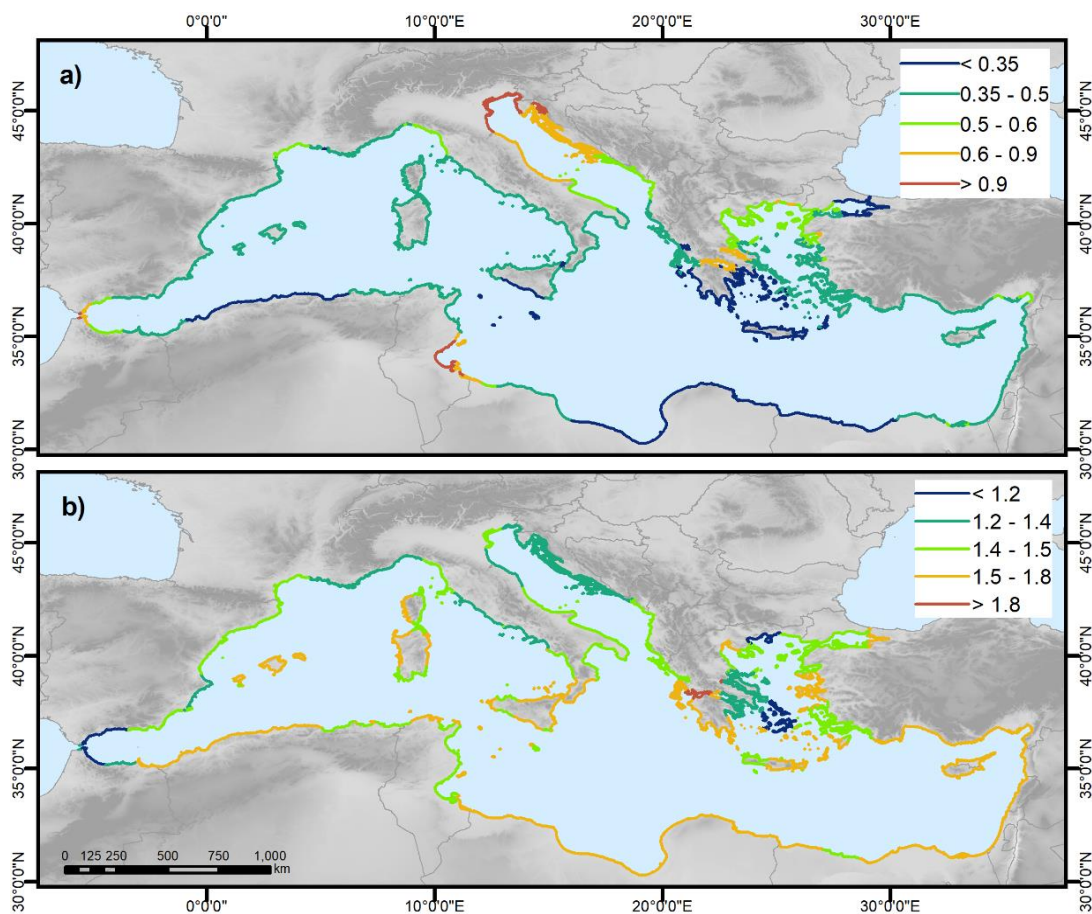


## APPENDIX C

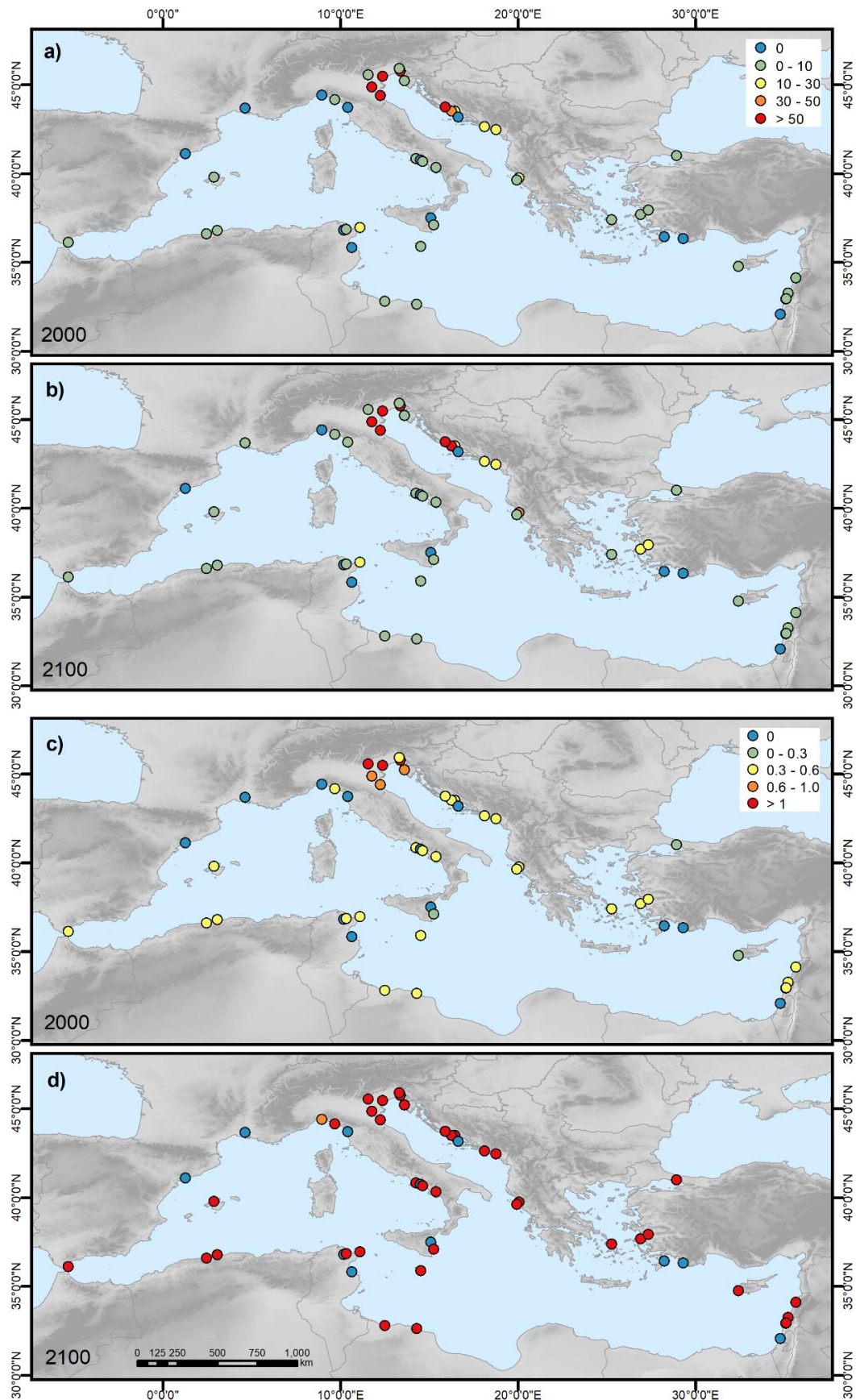
Please note:

In addition to the Supplementary Figures and Tables listed here, Supplementary data were published along with Chapter 4. The data can be found in the ‘Electronic supplementary material’ section in the online version of the published article at <https://doi.org/10.1038/s41467-018-06645-9>. These materials include the following files:

Name	Description
Description of Additional Supplementary Files	Description of the variables included in Supplementary Data 1 and 2
Supplementary Data 1	Results of the flood risk calculations
Supplementary Data 2	Results of the erosion risk calculations

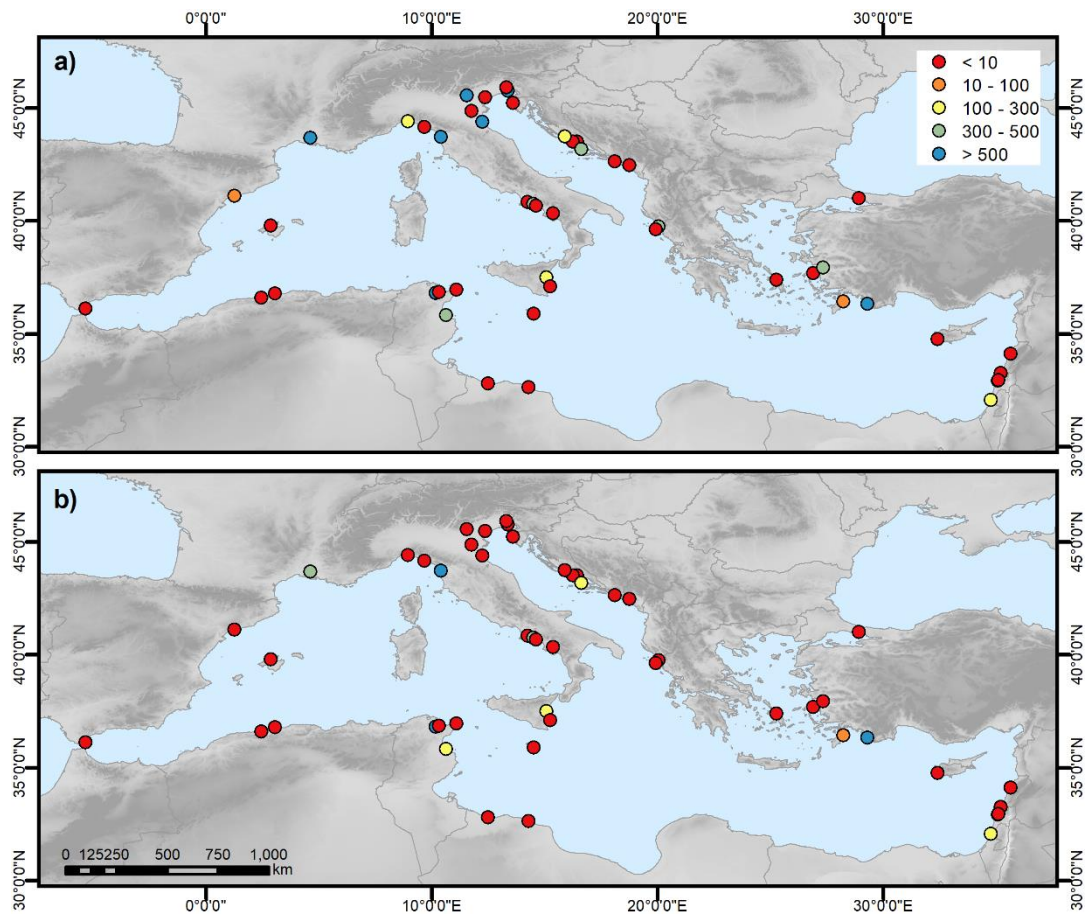


**Supplementary Figure 4.1** Spatial patterns of the extreme sea level components storm surge and sea-level rise. **a)** 100-year storm surge (in m) taken from the Mediterranean Coastal Database (Wolff et al. 2018), **b)** regional sea-level rise (in m) in 2100 under the high-end scenario based on Kopp et al. 2017

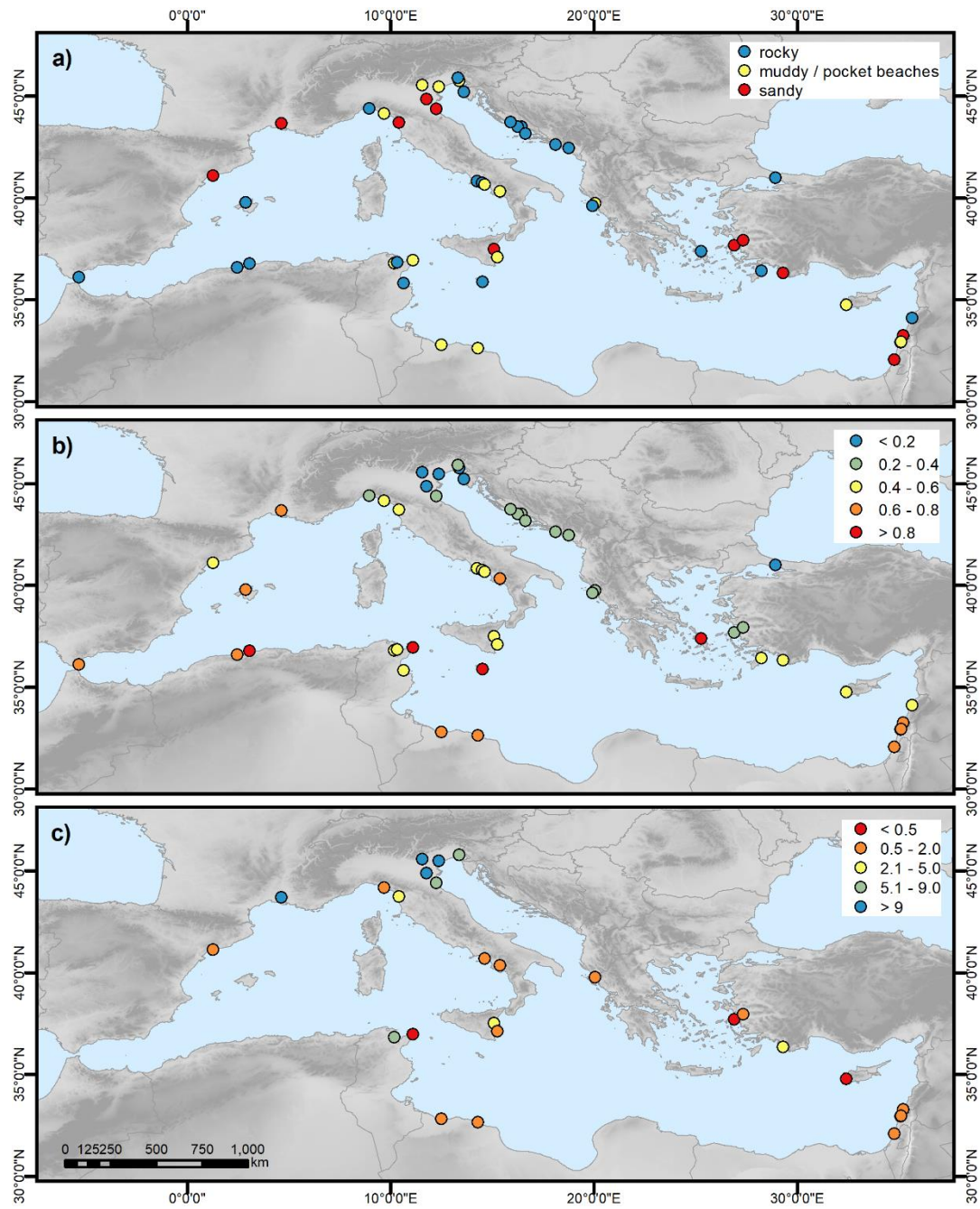


**Supplementary Figure 4.2** Characteristics of the flood risk indicators flood area and flood depth at each World Heritage site under current and future conditions. **a)** and **b)** area flooded (in %) in the base year 2000 (a) and in 2100 under the high-end sea-level rise scenario (b), **c)** and **d)** maximum flood depth (in m) in 2000 (c) and in 2100 under the high-end sea-level rise scenario (d)





**Supplementary Figure 4.3** Characteristics of the erosion risk indicator distance from the coastline (in m) at each World Heritage sites under current and future conditions. **a)** in 2000, **b)** in 2100 under the high-end sea-level rise scenario



**Supplementary Figure 4.4** Characteristics of the static erosion risk indicators at each World Heritage site. **a)** coastal material, **b)** mean wave height (in m), **c)** sediment supply (in mg l<sup>-1</sup>) given for coastal materials other than rocky



**Supplementary Table 4.1** Attributes of the corrected Mediterranean UNESCO World Heritage site data

Attribute name	Description	original dataset <sup>a</sup>	added <sup>b</sup>
unique_id	unique ID of each serial site		x
id_no	ID of main site	x	
site_id	ID of serial nomination		x
name_seria	Name of serial nomination		x
name_en	Name of main site in English	x	
name_fr	Name of main site in French	x	
date_inscr	Date when it was inscribed in the list	x	
sec_date	Date when changes have been made (e.g. adjusting boundary)	x	
danger_lis	Date when it was put on the danger list (if applicable)	x	
longitude	X coordinate of center point in decimal degrees	x	x*
latitude	Y coordinate of center point in decimal degrees	x	x*
area_ha	Area of site in hectares (excl. buffer zone) (-9999 = not given)	x	x*
area_ha1	Area of site in hectares (excl. buffer zone) as calculated based on the WHS polygons produced		x
C1 – C6	Criteria of Outstanding Universal Value (OUV) (1/0)	x	
criteria_t	OUV criteria in text	x	
category	Cultural (or natural)	x	
category_s	C for cultural	x	
states_en	Name of the country (countries) in English	x	
states_fr	Name of the country (countries) in French	x	
region_en	Name of the region in English	x	
region_fr	Name of the region in French	x	
iso_code	2-digit country code	x	
undp_code	3-digit country code of the UNDP (United Nations Development Programme)	x	
transbound	Cross-border site (1/0)	x	
no_serial	Number of serial sites		x
her_type1	Heritage type based on International Council on		x
her_type2	Monuments and Sites (ICOMOS) 2011 and Daly 2014		
her_type3	1 = cultural landscape		

APPENDIX C

	2 = built heritage/architecture/historic urban center 3 = archaeological remains 4 = single monument		
buffer_ha	Buffer area in hectares (-9999 = not given)		x
srtm_min	Lowest site elevation in the SRTM90 DEM (Farr et al. 2007, Jarvis et al. 2008)		x
srtm_max	Highest site elevation in the SRTM90 DEM		x
srtm_mean	Mean site elevation in the SRTM90 DEM		x
p_lecz	Percent of site located in the LECZ		x
ur_grump	Location of WHS in urban areas based on the GRUMP urban extents grid (Center for International Earth Science Information Network - Columbia University (CIESIN) et al. 2011) (1/0)		x
ur_mod_buf	Location of WHS in urban areas based on the MODIS urban extents grid (Schneider et al. 2009) with a 500 m buffer (1/0)		x
ur_joined	Combination of ur_grump and ur_mod_buf based on Google Earth™ satellite imagery		x
dist_MCD	Distance from the coast [m] based on the Mediterranean coastal database (MCD) (Wolff et al. 2018a)		x
dist_gshhs	Distance from the coast [m] based on the global self-consistent, hierarchical, shoreline database (GSHHS) version 2.3.7 (Wessel and Smith 1996)		x
dist_join	Combination of dist_MCD and dist_gshhs based on Google Earth™ satellite imagery		x
<p> = included in the serial site dataset only</p> <p> = included in the main site dataset only</p> <p><sup>a</sup> taken over from the original World Heritage List data of 2018 (UNESCO World Heritage Centre 2018)</p> <p><sup>b</sup> added to the original World Heritage List data with the help of the data sources stated in the description</p> <p>* modified from original World Heritage List data</p>			

Supplementary Table 4.2 Data used

<b>Variable</b>	<b>Indicator(s)</b>	<b>Reference</b>
Coastal World Heritage	World Heritage sites 2018	UNESCO World Heritage Centre 2018
Elevation	Shuttle Radar Topography Mission (SRTM) DEM	Farr et al. 2007, Jarvis et al. 2008
<b><i>Flood risk</i></b>		
Sea-level rise scenarios	RCP2.6, RCP4.5, RCP8.5 (50 <sup>th</sup> percentile) High-end (RCP8.5, 95 <sup>th</sup> percentile)*	Kopp et al. 2017
Storm surge	100-year surge height	Wolff et al. 2018a, based on Muis et al. 2016
Mean dynamic ocean topography (MDT)	Used to reference the surge heights to the EGM96 geoid	Wolff et al. 2018a, Rio et al. 2014
<b><i>Erosion risk</i></b>		
World Heritage distance from the coastline	Mediterranean Coastal Database (MCD); Global self-consistent, hierarchical, shoreline database (GSHHS) version 2.3.7	Wolff et al. 2018a  Wessel and Smith 1996
Erodibility	Coastal material	Wolff et al. 2018a
Waves	Mean wave height	Wolff et al. 2018a
Sediment supply	Total suspended matter	Schuerch et al. 2018, based on data of the GlobColour project Doerffer and Schiller 2010
* We found the sea-level rise projections of the high-end scenario in 2100 to be lower than those of 2090 at a number of grid points, which we considered to be implausible due to the fact that the projections post-2100 continue to increase in an accelerating manner. Therefore we have calculated the mean of the sea-level rise growth rates between the years 2080-2090 and 2110-2120 and added it to the projection of 2090 to adjust the projection of 2100.		



---

**LIST OF REFERENCES**


---

- Absar SM, Preston BL (2015) Extending the Shared Socioeconomic Pathways for sub-national impacts, adaptation, and vulnerability studies. *Global Environmental Change* 33:83–96. doi: 10.1016/j.gloenvcha.2015.04.004
- Abuodha PAO, Woodroffe CD (2010) Assessing vulnerability to sea-level rise using a coastal sensitivity index. A case study from southeast Australia. *J Coast Conserv* 14(3):189–205. doi: 10.1007/s11852-010-0097-0
- Adams S, Aich V, Albrecht T, Baarsch F, Boit A, Canales Trujillo N, Carlsburg M, Coumou D, Eden A, Fader M (2014) Turn down the heat. Confronting the new climate normal. The World Bank, Washington, D.C.
- Aerts JCJH (2020) Integrating agent-based approaches with flood risk models. A review and perspective. *Water Security* 11(6183):100076. doi: 10.1016/j.wasec.2020.100076
- Aerts JCJH, Botzen WJ, Clarke KC, Cutter SL, Hall JW, Merz B, Michel-Kerjan E, Mysiak J, Surminski S, Kunreuther H (2018) Integrating human behaviour dynamics into flood disaster risk assessment. *Nature Clim Change* 8(3):193–199. doi: 10.1038/s41558-018-0085-1
- Aerts JCJH, Botzen WJW, Emanuel K, Lin N, Moel H de, Michel-Kerjan EO (2014) Climate adaptation. Evaluating flood resilience strategies for coastal megacities. *Science (New York, N.Y.)* 344(6183):473–475. doi: 10.1126/science.1248222
- Alcamo J, Henrichs T (2008) Chapter Two Towards Guidelines for Environmental Scenario Analysis. In: Alcamo J (ed) *Environmental futures. The practice of environmental scenario analysis*, 1st ed., vol 2. Elsevier, Amsterdam, Boston, pp 13–35
- Anderson DG, Bissett TG, Yerka SJ, Wells JJ, Kansa EC, Kansa SW, Myers KN, DeMuth RC, White DA (2017) Sea-level rise and archaeological site destruction: An example from the southeastern United States using DINAA (Digital Index of North American Archaeology). *PloS one* 12(11):e0188142. doi: 10.1371/journal.pone.0188142
- Anderson JE (2011) The Gravity Model. *Annu. Rev. Econ.* 3(1):133–160. doi: 10.1146/annurev-economics-111809-125114
- Antonoli F, Anzidei M, Amorosi A, Lo Presti V, Mastronuzzi G, Deiana G, Falco G de, Fontana A, Fontolan G, Lisco S, Marsico A, Moretti M, Orrù PE, Sannino GM, Serpelloni E, Vecchio A (2017) Sea-level rise and potential drowning of the Italian coastal plains. Flooding risk scenarios for 2100. *Quaternary Science Reviews* 158:29–43. doi: 10.1016/j.quascirev.2016.12.021
- Arns A, Dangendorf S, Jensen J, Talke S, Bender J, Pattiaratchi C (2017) Sea-level rise induced amplification of coastal protection design heights. *Scientific Reports* 7:40171. doi: 10.1038/srep40171
- Arthur R, Boulton CA, Shotton H, Williams HTP (2018) Social sensing of floods in the UK. *PloS one* 13(1):e0189327. doi: 10.1371/journal.pone.0189327
- Athanasiou P, van Dongeren A, Giardino A, Vousdoukas M, Gaytan-Aguilar S, Ranasinghe R (2019) Global distribution of nearshore slopes with implications for coastal retreat. *Earth Syst. Sci. Data* 11(4):1515–1529. doi: 10.5194/essd-11-1515-2019
- Athanasiou P, van Dongeren A, Giardino A, Vousdoukas MI, Ranasinghe R, Kwadijk J (2020) Uncertainties in projections of sandy beach erosion due to sea level rise. An analysis at the European scale. *Scientific Reports* 10(1):11895. doi: 10.1038/s41598-020-68576-0
- Bakker AMR, Louchard D, Keller K (2017) Sources and implications of deep uncertainties surrounding sea-level projections. *Climatic Change* 140(3-4):339–347. doi: 10.1007/s10584-016-1864-1
- Balica SF, Wright NG, van der Meulen F (2012) A flood vulnerability index for coastal cities and its use in assessing climate change impacts. *Nat Hazards* 64(1):73–105. doi: 10.1007/s11069-012-0234-1

- Balk D, Montgomery MR, McGranahan G, Kim D, Mara V, Todd M, Buettner T, Dorélie AD (2009) Mapping urban settlements and the risks of climate change in Africa, Asia and South America. In: Guzmán JM (ed) Population dynamics and climate change. UNFPA; IIED, New York, London, England, pp 80–103
- Barker JLP, Macleod CJA (2019) Development of a national-scale real-time Twitter data mining pipeline for social geodata on the potential impacts of flooding on communities. *Environmental Modelling & Software* 115(4):213–227. doi: 10.1016/j.envsoft.2018.11.013
- Bates PD, Roo APJ de (2000) A simple raster-based model for flood inundation simulation. *Journal of Hydrology* 236(1-2):54–77. doi: 10.1016/S0022-1694(00)00278-X
- Batista e Silva F, Dijkstra L, Martinez PV, Lavalle C (2016) Regionalisation of demographic and economic projections. Trend and convergence scenarios from 2015 to 2060. EUR, Scientific and technical research series, vol 27924. Publications Office, Luxembourg
- Batista e Silva F, Gallego J, Lavalle C (2013a) A high-resolution population grid map for Europe. *Journal of Maps* 9(1):16–28. doi: 10.1080/17445647.2013.764830
- Batista e Silva F, Lavalle C, Koomen E (2013b) A procedure to obtain a refined European land use/cover map. *Journal of Land Use Science* 8(3):255–283. doi: 10.1080/1747423X.2012.667450
- Bauer N, Calvin K, Emmerling J, Fricko O, Fujimori S, Hilaire J, Eom J, Krey V, Kriegler E, Mouratiadou I, Sytze de Boer H, van den Berg M, Carrara S, Daioglou V, Drouet L, Edmonds JE, Gernaat D, Havlik P, Johnson N, Klein D, Kyle P, Marangoni G, Masui T, Pietzcker RC, Strubegger M, Wise M, Riahi K, van Vuuren DP (2017) Shared Socio-Economic Pathways of the Energy Sector – Quantifying the Narratives. *Global Environmental Change* 42:316–330. doi: 10.1016/j.gloenvcha.2016.07.006
- Belle Tout lighthouse (2018). <https://www.belletout.co.uk/information/history/>. Accessed 22 Feb 2021
- Benoit G, Comeau A (2005) A sustainable future for the Mediterranean. The Blue Plan's environment and development outlook. Earthscan, London
- Benson M, O'Reilly K (2009) Migration and the search for a better way of life: a critical exploration of lifestyle migration. *The Sociological Review* 57(4):608–625
- Bernstein A, Gustafson MT, Lewis R (2019) Disaster on the horizon. The price effect of sea level rise. *Journal of Financial Economics* 134(2):253–272. doi: 10.1016/j.jfineco.2019.03.013
- Besset M, Anthony EJ, Sabatier F (2017) River delta shoreline reworking and erosion in the Mediterranean and Black Seas. The potential roles of fluvial sediment starvation and other factors. *Elem Sci Anth* 5(0):54. doi: 10.1525/elementa.139
- Bevacqua E, Vousdoukas MI, Zappa G, Hodges K, Shepherd TG, Maraun D, Mentaschi L, Feyen L (2020) More meteorological events that drive compound coastal flooding are projected under climate change. *Communications earth & environment* 1(1):47. doi: 10.1038/s43247-020-00044-z
- Birkmann J, Cutter SL, Rothman DS, Welle T, Garschagen M, van Ruijven B, O'Neill B, Preston BL, Kienberger S, Cardona OD, Siagian T, Hidayati D, Setiadi N, Binder CR, Hughes B, Pulwarty R (2015) Scenarios for vulnerability. Opportunities and constraints in the context of climate change and disaster risk. *Climatic Change* 133(1):53–68. doi: 10.1007/s10584-013-0913-2
- Black R, Adger WN, Arnell NW, Dercon S, Geddes A, Thomas D (2011) The effect of environmental change on human migration. *Global Environmental Change* 21:S3-S11. doi: 10.1016/j.gloenvcha.2011.10.001
- Blue Plan (2008) The Blue Plan's sustainable development outlook for the Mediterranean. [http://mait.camins.cat/ET2050\\_library/docs/med/blue\\_plan\\_MAP\\_2008.pdf](http://mait.camins.cat/ET2050_library/docs/med/blue_plan_MAP_2008.pdf). Accessed 22 Feb 2021
- Bock Y, Wdowinski S, Ferretti A, Novali F, Fumagalli A (2012) Recent subsidence of the Venice Lagoon from continuous GPS and interferometric synthetic aperture radar. *Geochem. Geophys. Geosyst.* 13(3):n/a-n/a. doi: 10.1029/2011GC003976

- Boke-Olén N, Abdi AM, Hall O, Lehsten V (2017) High-resolution African population projections from radiative forcing and socio-economic models, 2000 to 2100. *Scientific Data* 4:160130. doi: 10.1038/sdata.2016.130
- Boruff BJ, Emrich C, Cutter SL (2005) Erosion Hazard Vulnerability of US Coastal Counties. *Journal of Coastal Research* 215:932–942. doi: 10.2112/04-0172.1
- Bowcott O (2008) Stone by stone: Rebuilt tower open to public. <https://www.theguardian.com/artanddesign/2008/aug/29/architecture.heritage>. Accessed 22 Feb 2021
- Bright EA, Coleman PR, Rose AN, Urban ML (2012) *LandScan 2011*, 2011st edn. LandScan. Oak Ridge National Laboratory, Oak Ridge, TN
- Brown S, Nicholls RJ (2015) Subsidence and human influences in mega deltas: The case of the Ganges–Brahmaputra–Meghna. *Science of The Total Environment* 527-528:362–374. doi: 10.1016/j.scitotenv.2015.04.124
- Brown S, Nicholls RJ, Goodwin P, Haigh ID, Lincke D, Vafeidis AT, Hinkel J (2018) Quantifying Land and People Exposed to Sea-Level Rise with No Mitigation and 1.5°C and 2.0°C Rise in Global Temperatures to Year 2300. *Earth's Future* 6(3):583–600. doi: 10.1002/2017EF000738
- Brown S, Nicholls RJ, Lowe JA, Hinkel J (2016) Spatial variations of sea-level rise and impacts. An application of DIVA. *Climatic Change* 134(3):403–416. doi: 10.1007/s10584-013-0925-y
- Brown S, Nicholls RJ, Woodroffe CD, Hanson S, Hinkel J, Kebede AS, Neumann B, Vafeidis AT (2013) Sea-Level Rise Impacts and Responses: A Global Perspective. In: Finkl CW (ed) *Coastal hazards*. Springer, Dordrecht, pp 117–149
- Bruijn JA de, Moel H de, Jongman B, Wagemaker J, Aerts JCJH (2018) TAGGS. Grouping Tweets to Improve Global Geoparsing for Disaster Response. *J geovis spat anal* 2(1):48. doi: 10.1007/s41651-017-0010-6
- Bruijn JA de, Moel H de, Weerts AH, Ruiter MC de, Basar E, Eilander D, Aerts JCJH (2020) Improving the classification of flood tweets with contextual hydrological information in a multimodal neural network. *Computers & Geosciences* 140(15):104485. doi: 10.1016/j.cageo.2020.104485
- Bruun P (1962) Sea-level rise as a cause of shore erosion. *Journal of the Waterways and Harbors division* 88(1):117–132
- Bruun P (1983) Review of conditions for uses of the Bruun rule of erosion. *Coastal Engineering* 7(1):77–89. doi: 10.1016/0378-3839(83)90028-5
- Buchanan MK, Kopp RE, Oppenheimer M, Tebaldi C (2016) Allowances for evolving coastal flood risk under uncertain local sea-level rise. *Climatic Change* 137(3-4):347–362. doi: 10.1007/s10584-016-1664-7
- Cazenave A (2014) Anthropogenic global warming threatens world cultural heritage. *Environ. Res. Lett.* 9(5):51001. doi: 10.1088/1748-9326/9/5/051001
- Center for International Earth Science Information Network - CIESIN - Columbia University (2017) *Gridded Population of the World, Version 4 (GPWv4): Population Count Adjusted to Match 2015 Revision of UN WPP Country Totals, Revision 10*. NASA Socioeconomic Data and Applications Center (SEDAC), Palisades, NY
- Center for International Earth Science Information Network - Columbia University (CIESIN), International Food Policy Research Institute (IFPRI), The World Bank, Centro Internacional de Agricultura Tropical (CIAT) (2011) *Global Rural-Urban Mapping Project, Version 1 (GRUMPv1): Urban Extents Grid*. NASA Socioeconomic Data and Applications Center (SEDAC), Palisades, NY
- Chang AY, Parrales ME, Jimenez J, Sobieszczyk ME, Hammer SM, Copenhaver DJ, Kulkarni RP (2009) Combining Google Earth and GIS mapping technologies in a dengue surveillance system for developing countries. *International journal of health geographics* 8:49. doi: 10.1186/1476-072X-8-49

- Chapman S, Watson JEM, Salazar A, Thatcher M, McAlpine CA (2017) The impact of urbanization and climate change on urban temperatures. A systematic review. *Landscape Ecol* 32(10):1921–1935. doi: 10.1007/s10980-017-0561-4
- Chaussard E, Amelung F, Abidin H, Hong S-H (2013) Sinking cities in Indonesia. ALOS PALSAR detects rapid subsidence due to groundwater and gas extraction. *Remote Sensing of Environment* 128(1):150–161. doi: 10.1016/j.rse.2012.10.015
- Chen G, Li X, Liu X, Chen Y, Liang X, Leng J, Xu X, Liao W, Qiu Y'a, Wu Q, Huang K (2020a) Global projections of future urban land expansion under shared socioeconomic pathways. *Nature communications* 11(1):537. doi: 10.1038/s41467-020-14386-x
- Chen J, Liu Y, Pan T, Liu Y, Sun F, Ge Q (2017) Population exposure to droughts in China under 1.5 °C global warming target
- Chen Y, Guo F, Wang J, Cai W, Wang C, Wang K (2020b) Provincial and gridded population projection for China under shared socioeconomic pathways from 2010 to 2100. *Scientific Data* 7(1):83. doi: 10.1038/s41597-020-0421-y
- Chen Y, Li X, Huang K, Luo M, Gao M (2020c) High-Resolution Gridded Population Projections for China Under the Shared Socioeconomic Pathways. *Earth's Future* 8(6):849. doi: 10.1029/2020EF001491
- Cheng HQ, Chen JY, Chen ZJ, Ruan RL, Xu GQ, Zeng G, Zhu JR, Dai ZJ, Chen XY, Gu SH, Zhang XL, Wang HM (2018) Mapping Sea Level Rise Behavior in an Estuarine Delta System: A Case Study along the Shanghai Coast. *Cybersecurity* 4(1):156–163. doi: 10.1016/j.eng.2018.02.002
- Church JA, Clark PU, Cazenave A, Gregory JM, Jevrejeva S, Levermann A, Merrifield MA, Milne GA, Nerem RS, Nunn PD, Payne AJ, Pfeffer WT, Stammer D, Unnikrishnan AS (2013) Sea Level Change. In: IPCC (ed) *Climate change 2013. The physical science basis: Working Group I contribution to the Fifth assessment report of the Intergovernmental Panel on Climate Change / edited by Thomas F. Stocker, Working Group I co-chair, University of Bern [and nine others]*. Cambridge University Press, Cambridge, United Kingdom and New York, NY, USA
- Cigna F, Tapete D, Lee K (2018) Geological hazards in the UNESCO World Heritage sites of the UK. From the global to the local scale perspective. *Earth-Science Reviews* 176:166–194. doi: 10.1016/j.earscirev.2017.09.016
- Città di Venezia (2016) The altimetry of the historical center: percentage of flooding. <http://www.comune.venezia.it/archivio/EN/1754>. Accessed 22 Feb 2021
- Città di Venezia (2017) State of Conservation Reports by the State Party. World Heritage property Venice and its lagoon - (Italy) (C 394). <http://whc.unesco.org/en/list/394/documents/>. Accessed 22 Feb 2021
- Cooper JAG, Masselink G, Coco G, Short AD, Castelle B, Rogers K, Anthony E, Green AN, Kelley JT, Pilkey OH, Jackson DWT (2020) Sandy beaches can survive sea-level rise. *Nat. Clim. Chang.* 10(11):993–995. doi: 10.1038/s41558-020-00934-2
- Cooper JAG, Pilkey OH (2004) Sea-level rise and shoreline retreat. Time to abandon the Bruun Rule. *Global and Planetary Change* 43(3-4):157–171. doi: 10.1016/j.gloplacha.2004.07.001
- Crespo Cuaresma J (2017) Income projections for climate change research. A framework based on human capital dynamics. *Global Environmental Change* 42:226–236. doi: 10.1016/j.gloenvcha.2015.02.012
- Cutter SL, Boruff BJ, Shirley WL (2003) Social Vulnerability to Environmental Hazards \*. *Social Science Quarterly* 84(2):242–261. doi: 10.1111/1540-6237.8402002
- Daire M-Y, Lopez-Romero E, Proust J-N, Regnauld H, Pian S, Shi B (2012) Coastal Changes and Cultural Heritage (1). Assessment of the Vulnerability of the Coastal Heritage in Western France. *The Journal of Island and Coastal Archaeology* 7(2):168–182. doi: 10.1080/15564894.2011.652340



- Daly C (2011) The Potential for Indicators in the Management of Climate Change Impacts on Cultural Heritage. <http://arrow.dit.ie/cgi/viewcontent.cgi?article=1005&context=beschrecon>. Accessed 22 Feb 2021
- Daly C (2014) A Framework for Assessing the Vulnerability of Archaeological Sites to Climate Change. Theory, Development, and Application. *Conservation and Management of Archaeological Sites* 16(3):268–282. doi: 10.1179/1350503315Z.00000000086
- Dassanayake D, Burzel A, Oumeraci H (2012) Evaluation of Cultural Losses. [https://www.researchgate.net/profile/Andreas\\_Burzel/publication/266458949\\_Evaluation\\_of\\_Cultural\\_Losses/links/5525807a0cf24b822b4053ad/Evaluation-of-Cultural-Losses.pdf](https://www.researchgate.net/profile/Andreas_Burzel/publication/266458949_Evaluation_of_Cultural_Losses/links/5525807a0cf24b822b4053ad/Evaluation-of-Cultural-Losses.pdf). Accessed 22 Feb 2021
- Davidson-Arnott RGD (2005) Conceptual Model of the Effects of Sea Level Rise on Sandy Coasts. *Journal of Coastal Research* 216:1166–1172. doi: 10.2112/03-0051.1
- Dellink R, Chateau J, Lanzi E, Magné B (2017) Long-term economic growth projections in the Shared Socioeconomic Pathways. *Global Environmental Change* 42:200–214. doi: 10.1016/j.gloenvcha.2015.06.004
- Deltares (2020) DELFT3D-FLOW. Simulation of multi-dimensional hydrodynamic flows and transport phenomena, including sediments. User Manual. [https://content.oss.deltares.nl/delft3d/manuals/Delft3D-FLOW\\_User\\_Manual.pdf](https://content.oss.deltares.nl/delft3d/manuals/Delft3D-FLOW_User_Manual.pdf). Accessed 02/22/2021
- Deville P, Linard C, Martin S, Gilbert M, Stevens FR, Gaughan AE, Blondel VD, Tatem AJ (2014) Dynamic population mapping using mobile phone data. *Proceedings of the National Academy of Sciences of the United States of America* 111(45):15888–15893. doi: 10.1073/pnas.1408439111
- Di Baldassarre G, Viglione A, Carr G, Kuil L, Yan K, Brandimarte L, Blöschl G (2015) Debates-Perspectives on socio-hydrology. Capturing feedbacks between physical and social processes. *Water Resour. Res.* 51(6):4770–4781. doi: 10.1002/2014WR016416
- Diaz DB (2016) Estimating global damages from sea level rise with the Coastal Impact and Adaptation Model (CIAM). *Climatic Change* 137(1-2):143–156. doi: 10.1007/s10584-016-1675-4
- Doerffer R, Schiller H (2010) The MERIS Case 2 water algorithm. *International Journal of Remote Sensing* 28(3-4):517–535. doi: 10.1080/01431160600821127
- Dujardin S, Jacques D, Steele J, Linard C (2020) Mobile Phone Data for Urban Climate Change Adaptation. Reviewing Applications, Opportunities and Key Challenges. *Sustainability* 12(4):1501. doi: 10.3390/su12041501
- Ebi KL, Kram T, van Vuuren DP, O'Neill BC, Kriegler E (2014) A New Toolkit for Developing Scenarios for Climate Change Research and Policy Analysis. *Environment: Science and Policy for Sustainable Development* 56(2):6–16. doi: 10.1080/00139157.2014.881692
- Erban LE, Gorelick SM, Zebker HA (2014) Groundwater extraction, land subsidence, and sea-level rise in the Mekong Delta, Vietnam. *Environ. Res. Lett.* 9(8):84010. doi: 10.1088/1748-9326/9/8/084010
- ESA (2017) Land Cover CCI Product User Guide Version 2. Tech. Rep.
- European Environment Agency (EEA) (2006) The changing faces of Europe's coastal areas. [http://www.eea.europa.eu/publications/eea\\_report\\_2006\\_6](http://www.eea.europa.eu/publications/eea_report_2006_6). Accessed 22 Feb 2021
- European Environment Agency (EEA) (2014) Horizon 2020 Mediterranean report. Toward shared environmental information systems - EEA-UNEP/MAP joint report. <http://www.eea.europa.eu/publications/horizon-2020-mediterranean-report>. Accessed 22 Feb 2021
- European Union (2007) Directive 2007/60/EC of the European Parliament and of the Council of 23 October 2007 on the assessment and management of flood risks. *Official Journal of the European Union* 50(L 288):27–34
- Eurostat (2015a) Database. Maritime transport. <http://ec.europa.eu/eurostat/data/database>. Accessed 22 Feb 2021

- Eurostat (2015b) European Neighbourhood Policy countries (ENP), ENP-South Database. Maritime traffic. <http://ec.europa.eu/eurostat/web/european-neighbourhood-policy/enp-south/data/database>. Accessed 22 Feb 2021
- Eurostat (2019) European Neighbourhood Policy - South - transport statistics. [https://ec.europa.eu/eurostat/statistics-explained/index.php/European\\_Neighbourhood\\_Policy\\_-\\_South\\_-\\_transport\\_statistics#Road\\_transport](https://ec.europa.eu/eurostat/statistics-explained/index.php/European_Neighbourhood_Policy_-_South_-_transport_statistics#Road_transport). Accessed 22 Feb 2021
- Farr TG, Rosen PA, Caro E, Crippen R, Duren R, Hensley S, Kobrick M, Paller M, Rodriguez E, Roth L, Seal D, Shaffer S, Shimada J, Umland J, Werner M, Oskin M, Burbank D, Alsdorf D (2007) The Shuttle Radar Topography Mission. *Rev. Geophys.* 45(2). doi: 10.1029/2005RG000183
- Fatorić S, Seekamp E (2017) Are cultural heritage and resources threatened by climate change? A systematic literature review. *Climatic Change* 142(1-2):227–254. doi: 10.1007/s10584-017-1929-9
- Field CB (ed) (2012) *Managing the risks of extreme events and disasters to advance climate change adaptation*. Cambridge University Press, Cambridge
- Field CB, Barros VR, Dokken DJ, Mach KJ, Mastrandrea MD, Bilir TE, Chatterjee M, Ebi KL, Estrada YO, Genova RC, Girma B, Kissel ES, Levy AN, MacCracken S, Mastrandrea PR, White LL (eds) (2014) *Climate change 2014: Impacts, Adaptation and Vulnerability. Part A: Global and Sectoral Aspects. Contribution of Working Group II to the Fifth Assessment Report of the Intergovernmental Panel on Climate Change*. Cambridge University Press, Cambridge, UK and New York, NY, USA
- Flato G, Marotzke J, Abiodun B, Braconnot P, Chou SC, Collins W, Cox P, Driouech F, Emori S, Eyring V, Forest C, Gleckler P, Guilyardi E, Jakob C, Kattsov V, Reason C, Rummukainen M (2013) Evaluation of Climate Models. In: IPCC (ed) *Climate change 2013. The physical science basis: Working Group I contribution to the Fifth assessment report of the Intergovernmental Panel on Climate Change / edited by Thomas F. Stocker, Working Group I co-chair, University of Bern [and nine others]*. Cambridge University Press, Cambridge, United Kingdom and New York, NY, USA
- Florczyk AJ, Corbane C, Ehrlich D, Freire S, Kemper T, Maffenini L, Melchiorri M, Pesaresi M, Politis P, Schiavina M, Sabo F, Zanchetta L (2019) GHSL data package 2019. Public release GHS P2019. EUR, vol 29788. Publications Office of the European Union, Luxembourg
- Food and Agriculture Organization of the United Nations (FAO) (2014) *The State of World Fisheries and Aquaculture*. <http://www.fao.org/3/a-i3720e.pdf>. Accessed 22 Feb 2021
- Food and Agriculture Organization of the United Nations (FAO) (2016) *Fisheries and aquaculture software. FishStatJ - software for fishery statistical time series*. <http://www.fao.org/fishery/statistics/software/fishstatj/en>. Accessed 22 Feb 2021
- Foresight (2011) *Migration and Global Environmental Change. Final Project Report*. [https://assets.publishing.service.gov.uk/government/uploads/system/uploads/attachment\\_data/file/287717/11-1116-migration-and-global-environmental-change.pdf](https://assets.publishing.service.gov.uk/government/uploads/system/uploads/attachment_data/file/287717/11-1116-migration-and-global-environmental-change.pdf). Accessed 22 Feb 2021
- Freire S, MacManus K, Pesaresi M, Doxsey-Whitfield E, Mills J (2016) Development of new open and free multi-temporal global population grids at 250 m resolution. *Geospatial Data in a Changing World; Association of Geographic Information Laboratories in Europe (AGILE)*. AGILE 2016.
- Gao J (2017) Downscaling global spatial population projections from 1/8-degree to 1-km grid cells
- Gao J, O'Neill BC (2020) Mapping global urban land for the 21st century with data-driven simulations and Shared Socioeconomic Pathways. *Nature communications* 11(1):2302. doi: 10.1038/s41467-020-15788-7
- Garschagen M, Romero-Lankao P (2015) Exploring the relationships between urbanization trends and climate change vulnerability. *Climatic Change* 133(1):37–52. doi: 10.1007/s10584-013-0812-6
- Gesch DB (2018) Best Practices for Elevation-Based Assessments of Sea-Level Rise and Coastal Flooding Exposure. *Front. Earth Sci.* 6:344. doi: 10.3389/feart.2018.00230

- Gewin V (2016) Data sharing: An open mind on open data. *Nature* 529(7584):117–119. doi: 10.1038/nj7584-117a
- Global administrative areas (GADM) (2015). Version 2.8. [gadm.org](http://gadm.org). Accessed 22 Feb 2021
- Goodwin P, Haigh ID, Rohling EJ, Slangen A (2017) A new approach to projecting 21st century sea-level changes and extremes. *Earth's Future* 5(2):240–253. doi: 10.1002/2016EF000508
- Gornitz V (1991) Global coastal hazards from future sea level rise. *Palaeogeography, Palaeoclimatology, Palaeoecology* 89(4):379–398. doi: 10.1016/0031-0182(91)90173-O
- Gornitz VM, Daniels RC, White TW, Birdwell KR (1994) The Development of a Coastal Risk Assessment Database: Vulnerability to Sea-Level Rise in the U.S. Southeast. *Journal of Coastal Research*:327–338
- Grübler A, O'Neill B, Riahi K, Chirkov V, Goujon A, Kolp P, Prommer I, Scherbov S, Slentoe E (2007) Regional, national, and spatially explicit scenarios of demographic and economic change based on SRES. *Technological Forecasting and Social Change* 74(7):980–1029. doi: 10.1016/j.techfore.2006.05.023
- Haasnoot M, Biesbroek R, Lawrence J, Muccione V, Lempert R, Glavovic B (2020) Defining the solution space to accelerate climate change adaptation. *Reg Environ Change* 20(2):305. doi: 10.1007/s10113-020-01623-8
- Haer T, Husby TG, Botzen WW, Aerts JCJH (2020) The safe development paradox. An agent-based model for flood risk under climate change in the European Union. *Global Environmental Change* 60(2):102009. doi: 10.1016/j.gloenvcha.2019.102009
- Hallegatte S, Green C, Nicholls RJ, Corfee-Morlot J (2013) Future flood losses in major coastal cities. *Nature Climate change* 3(9):802–806. doi: 10.1038/NCLIMATE1979
- Hallegatte S, Przulski V, Vogt-Schilb A (2011) Building world narratives for climate change impact, adaptation and vulnerability analyses. *Nature Climate change* 1(3):151–155. doi: 10.1038/NCLIMATE1135
- Hambly J (2017) A review of heritage at risk from coastal processes in Scotland. Results from the Scotland's Coastal Heritage at Risk Project 2012-2016. [http://ssharp.co.uk/media/medialibrary/2018/02/Review\\_of\\_Coastal\\_Heritage\\_at\\_Risk.pdf](http://ssharp.co.uk/media/medialibrary/2018/02/Review_of_Coastal_Heritage_at_Risk.pdf). Accessed 22 Feb 2021
- Hanasaki N, Fujimori S, Yamamoto T, Yoshikawa S, Masaki Y, Hijioka Y, Kainuma M, Kanamori Y, Masui T, Takahashi K, Kanae S (2013) A global water scarcity assessment under Shared Socio-economic Pathways – Part 2. Water availability and scarcity. *Hydrol. Earth Syst. Sci.* 17(7):2393–2413. doi: 10.5194/hess-17-2393-2013
- Hanson S, Nicholls R, Ranger N, Hallegatte S, Corfee-Morlot J, Herweijer C, Chateau J (2011) A global ranking of port cities with high exposure to climate extremes. *Climatic Change* 104(1):89–111. doi: 10.1007/s10584-010-9977-4
- Hapciuc O-E, Romanescu G, Minea I, Iosub M, Enea A, Sandu I (2016) Flood susceptibility analysis of the cultural heritage in the Sucevita catchment (Romania). *International Journal of Conservation Science* 7(2):501–510
- Hastings DA, Dunbar PK (1999) Global Land One-kilometer Base Elevation (GLOBE) Digital Elevation Model. Documentation. Volume 1.0
- Hauer ME (2019) Population projections for U.S. counties by age, sex, and race controlled to shared socioeconomic pathway. *Scientific Data* 6:190005. doi: 10.1038/sdata.2019.5
- Hauer ME, Fussell E, Mueller V, Burkett M, Call M, Abel K, McLeman R, Wrathall D (2020) Sea-level rise and human migration. *Nat Rev Earth Environ* 1(1):28–39. doi: 10.1038/s43017-019-0002-9
- Hermans LM, Haasnoot M, ter Maat J, Kwakkel JH (2017) Designing monitoring arrangements for collaborative learning about adaptation pathways. *Environmental Science & Policy* 69:29–38. doi: 10.1016/j.envsci.2016.12.005

- Higgins SA (2016) Review: Advances in delta-subsidence research using satellite methods. *Hydrogeology Journal* 24(3):587–600. doi: 10.1007/s10040-015-1330-6
- Hinkel J, Lincke D, Vafeidis AT, Perrette M, Nicholls RJ, Tol RSJ, Marzeion B, Fettweis X, Ionescu C, Levermann A (2014) Coastal flood damage and adaptation costs under 21st century sea-level rise. *Proceedings of the National Academy of Sciences of the United States of America* 111(9):3292–3297. doi: 10.1073/pnas.1222469111
- Hinkel J, Nicholls RJ, Tol RSJ, Wang ZB, Hamilton JM, Boot G, Vafeidis AT, McFadden L, Ganopolski A, Klein RJT (2013a) A global analysis of erosion of sandy beaches and sea-level rise. An application of DIVA. *Global and Planetary Change* 111(8):150–158. doi: 10.1016/j.gloplacha.2013.09.002
- Hinkel J, Nicholls RJ, Vafeidis AT, Tol RSJ, Avagianou T (2010) Assessing risk of and adaptation to sea-level rise in the European Union. An application of DIVA. *Mitig Adapt Strateg Glob Change* 15(7):703–719. doi: 10.1007/s11027-010-9237-y
- Hinkel J, van Vuuren DP, Nicholls RJ, Klein RJT (2013b) The effects of adaptation and mitigation on coastal flood impacts during the 21st century. An application of the DIVA and IMAGE models. *Climatic Change* 117(4):783–794. doi: 10.1007/s10584-012-0564-8
- Hirt C (2018) Artefact detection in global digital elevation models (DEMs): The Maximum Slope Approach and its application for complete screening of the SRTM v4.1 and MERIT DEMs. *Remote Sensing of Environment* 207:27–41. doi: 10.1016/j.rse.2017.12.037
- Hoozemans FM, Marchand M, Pennekamp HA (1993) *Sea Level Rise: A Global Vulnerability Analysis. Vulnerability Assessment for Population, Coastal Wetlands and Rice Production on a Global Scale*. Delft Hydraulics, Delft
- Horton BP, Kopp RE, Garner AJ, Hay CC, Khan NS, Roy K, Shaw TA (2018) Mapping Sea-Level Change in Time, Space, and Probability. *Annu. Rev. Environ. Resour.* 43(1):481–521. doi: 10.1146/annurev-environ-102017-025826
- Howard AJ (2013) Managing global heritage in the face of future climate change. The importance of understanding geological and geomorphological processes and hazards. *International Journal of Heritage Studies* 19(7):632–658. doi: 10.1080/13527258.2012.681680
- Howard AJ, Knight D, Coulthard T, Hudson-Edwards K, Kossoff D, Malone S (2016) Assessing riverine threats to heritage assets posed by future climate change through a geomorphological approach and predictive modelling in the Derwent Valley Mills WHS, UK. *Journal of Cultural Heritage* 19:387–394. doi: 10.1016/j.culher.2015.11.007
- Huete R, Mantecón A (2012) Residential Tourism or Lifestyle Migration: Social Problems Linked to the Non-Definition of the Situation. In: Moufakkir O, Burns P (eds) *Controversies in tourism*. CABI, Wallingford, Oxfordshire, pp 160–173
- Hugo G (2011) Future demographic change and its interactions with migration and climate change. *Global Environmental Change* 21(July):S21–S33. doi: 10.1016/j.gloenvcha.2011.09.008
- Huizinga J, de Moel H, Szewczyk W (2017) *Global flood depth-damage functions. Methodology and the database with guidelines*. JRC Technical Reports. EUR 28552 EN
- Hurth F, Lückenötter J, Schonlau M (2017) *European GDP projections for 2015-2060 - 10km gridded data based on Shared Socioeconomic Pathways (SSPs)*
- Iacono M, Krizek K, El-Geneidy AM (2008) Access to destinations. How close is close enough? Estimating accurate distance decay functions for multiple modes and different purposes. [https://conservancy.umn.edu/bitstream/handle/11299/151329/1/Mn\\_DOT2008-11.pdf](https://conservancy.umn.edu/bitstream/handle/11299/151329/1/Mn_DOT2008-11.pdf). Accessed 22 Feb 2021
- International Council on Monuments and Sites (ICOMOS) (2011) *Guidance on Heritage Impact Assessments for Cultural World Heritage Properties*. [https://www.iccom.org/sites/default/files/2018-07/icomos\\_guidance\\_on\\_heritage\\_impact\\_assessments\\_for\\_cultural\\_world\\_heritage\\_properties.pdf](https://www.iccom.org/sites/default/files/2018-07/icomos_guidance_on_heritage_impact_assessments_for_cultural_world_heritage_properties.pdf). Accessed 22 Feb 2021

- International Institute for Applied Systems Analysis (IIASA) (2016) SSP Database. Version 1.1. <https://tntcat.iiasa.ac.at/SspDb>. Accessed 03 Jul 2017
- International Institute for Applied Systems Analysis (IIASA) (2018) SSP Database. Version 2.0. <https://tntcat.iiasa.ac.at/SspDb>. Accessed 22 Feb 2021
- IPCC (ed) (2013) Climate change 2013. The physical science basis: Working Group I contribution to the Fifth assessment report of the Intergovernmental Panel on Climate Change / edited by Thomas F. Stocker, Working Group I co-chair, University of Bern [and nine others]. Cambridge University Press, Cambridge, United Kingdom and New York, NY, USA
- IPCC (ed) (2019) IPCC Special Report on the Ocean and Cryosphere in a Changing Climate. Pörtner, H.-O.; Roberts, D. C.; Masson-Delmotte, V.; Zhai, P.; Tignor, M.; Poloczanska, E.; Mintenbeck, K.; Alegria, A.; Nicolai, M.; Okem, A.; Petzold, J.; Rama, B.; Weyer, N. M. (eds.), in press
- Jackson LP, Jevrejeva S (2016) A probabilistic approach to 21st century regional sea-level projections using RCP and High-end scenarios. *Global and Planetary Change* 146:179–189. doi: 10.1016/j.gloplacha.2016.10.006
- Jarvis A, Reuter HI, Nelson A, Guevara E (2008) Hole-filled SRTM for the globe Version 4, available from the CGIAR-CSI SRTM 90m Database. <http://srtm.csi.cgiar.org>
- Jiang L, O'Neill BC (2017) Global urbanization projections for the Shared Socioeconomic Pathways. *Global Environmental Change* 42:193–199. doi: 10.1016/j.gloenvcha.2015.03.008
- Jiang L, O'Neill BC, Zoraghein H, Dahlke S (2020) Population scenarios for U.S. states consistent with shared socioeconomic pathways. *Environ. Res. Lett.* 15(9):94097. doi: 10.1088/1748-9326/aba5b1
- Jones B, O'Neill BC (2013) Historically grounded spatial population projections for the continental United States. *Environ. Res. Lett.* 8(4):44021. doi: 10.1088/1748-9326/8/4/044021
- Jones B, O'Neill BC (2016) Spatially explicit global population scenarios consistent with the Shared Socioeconomic Pathways. *Environ. Res. Lett.* 11(8):84003. doi: 10.1088/1748-9326/11/8/084003
- Jones B, O'Neill BC, McDaniel L, McGinnis S, Mearns LO, Tebaldi C (2015) Future population exposure to US heat extremes. *Nature Clim Change* 5(7):652–655. doi: 10.1038/NCLIMATE2631
- Jones B, Tebaldi C, O'Neill BC, Oleson K, Gao J (2018) Avoiding population exposure to heat-related extremes. Demographic change vs climate change. *Climatic Change* 146(3-4):423–437. doi: 10.1007/s10584-017-2133-7
- Jongman B, Ward PJ, Aerts JCJH (2012) Global exposure to river and coastal flooding. Long term trends and changes. *Global Environmental Change* 22(4):823–835. doi: 10.1016/j.gloenvcha.2012.07.004
- Jongman B, Winsemius HC, Aerts JCJH, Coughlan de Perez E, van Aalst MK, Kron W, Ward PJ (2015) Declining vulnerability to river floods and the global benefits of adaptation. *Proceedings of the National Academy of Sciences of the United States of America* 112(18):E2271-80. doi: 10.1073/pnas.1414439112
- Jurgilevich A, Räsänen A, Groundstroem F, Juhola S (2017) A systematic review of dynamics in climate risk and vulnerability assessments. *Environ. Res. Lett.* 12(1):13002. doi: 10.1088/1748-9326/aa5508
- KC S, Lutz W (2017) The human core of the shared socioeconomic pathways: Population scenarios by age, sex and level of education for all countries to 2100. *Global Environmental Change* 42:181–192. doi: 10.1016/j.gloenvcha.2014.06.004
- Khakzad S, Pieters M, van Balen K (2015) Coastal cultural heritage. A resource to be included in integrated coastal zone management. *Ocean & Coastal Management* 118:110–128. doi: 10.1016/j.ocecoaman.2015.07.032
- Kirezci E, Young IR, Ranasinghe R, Muis S, Nicholls RJ, Lincke D, Hinkel J (2020) Projections of global-scale extreme sea levels and resulting episodic coastal flooding over the 21st Century. *Scientific Reports* 10(1):11629. doi: 10.1038/s41598-020-67736-6

- Klein RJT, Nicholls RJ (1998) Coastal Zones. In: Handbook on methods for climate change impacts assessment and adaptation strategies
- Klein Goldewijk K, Beusen A, Janssen P (2010) Long-term dynamic modeling of global population and built-up area in a spatially explicit way. *HYDE 3.1. The Holocene* 20(4):565–573. doi: 10.1177/0959683609356587
- Klijn F, Kreibich H, Moel H de, Penning-Rowsell E (2015) Adaptive flood risk management planning based on a comprehensive flood risk conceptualisation. *Mitig Adapt Strateg Glob Change* 20(6):845–864. doi: 10.1007/s11027-015-9638-z
- Kok K, Christensen JH, Madsen MS, Pedde S, Gramberger M, Jäger J, Carter T (2015) Evaluation of existing climate and socio-economic scenarios including a detailed descriptions of the final selection. Deliverable D2.1. [http://impressions-project.eu/documents/2020\\_9\\_0](http://impressions-project.eu/documents/2020_9_0). Accessed 22 Feb 2021
- Kok K, Rothman DS, Patel M (2006) Multi-scale narratives from an IA perspective. Part I. European and Mediterranean scenario development. *Futures* 38(3):261–284. doi: 10.1016/j.futures.2005.07.001
- Koks EE, Rozenberg J, Zorn C, Tariverdi M, Vousdoukas M, Fraser SA, Hall JW, Hallegatte S (2019) A global multi-hazard risk analysis of road and railway infrastructure assets. *Nature communications* 10(1):2677. doi: 10.1038/s41467-019-10442-3
- Koomen E, Diogo V (2017) Assessing potential future urban heat island patterns following climate scenarios, socio-economic developments and spatial planning strategies. *Mitigation and adaptation strategies for global change* 22(2):287–306. doi: 10.1007/s11027-015-9646-z
- Kopp RE, DeConto RM, Bader DA, Hay CC, Horton RM, Kulp S, Oppenheimer M, Pollard D, Strauss BH (2017) Evolving Understanding of Antarctic Ice-Sheet Physics and Ambiguity in Probabilistic Sea-Level Projections. *Earth's Future* 5(12):1217–1233. doi: 10.1002/2017EF000663
- Kopp RE, Horton RM, Little CM, Mitrovica JX, Oppenheimer M, Rasmussen DJ, Strauss BH, Tebaldi C (2014) Probabilistic 21st and 22nd century sea-level projections at a global network of tide-gauge sites. *Earth's Future* 2(8):383–406. doi: 10.1002/2014EF000239
- Koutroulis AG, Grillakis MG, Daliakopoulos IN, Tsanis IK, Jacob D (2016) Cross sectoral impacts on water availability at +2°C and +3°C for east Mediterranean island states. The case of Crete. *Journal of Hydrology* 532:16–28. doi: 10.1016/j.jhydrol.2015.11.015
- Kriegler E, Edmonds J, Hallegatte S, Ebi KL, Kram T, Riahi K, Winkler H, van Vuuren DP (2014) A new scenario framework for climate change research. The concept of shared climate policy assumptions. *Climatic Change* 122(3):401–414. doi: 10.1007/s10584-013-0971-5
- Kriegler E, O'Neill BC, Hallegatte S, Kram T, Lempert RJ, Moss RH, Wilbanks T (2012) The need for and use of socio-economic scenarios for climate change analysis. A new approach based on shared socio-economic pathways. *Global Environmental Change* 22(4):807–822. doi: 10.1016/j.gloenvcha.2012.05.005
- Kron W (2005) Flood Risk = Hazard • Values • Vulnerability. *Water International* 30(1):58–68. doi: 10.1080/02508060508691837
- Kulp S, Strauss BH (2016) Global DEM Errors Underpredict Coastal Vulnerability to Sea Level Rise and Flooding. *Front. Earth Sci.* 4:4823. doi: 10.3389/feart.2016.00036
- Kulp SA, Strauss BH (2018) CoastalDEM. A global coastal digital elevation model improved from SRTM using a neural network. *Remote Sensing of Environment* 206(2):231–239. doi: 10.1016/j.rse.2017.12.026
- Kulp SA, Strauss BH (2019) New elevation data triple estimates of global vulnerability to sea-level rise and coastal flooding. *Nature communications* 10(1):4844. doi: 10.1038/s41467-019-12808-z
- Kummu M, Moel H de, Salvucci G, Viviroli D, Ward PJ, Varis O (2016) Over the hills and further away from coast. Global geospatial patterns of human and environment over the 20th–21st centuries. *Environ. Res. Lett.* 11(3):34010. doi: 10.1088/1748-9326/11/3/034010

- Kwakkel JH, Haasnoot M, Walker WE (2016) Comparing Robust Decision-Making and Dynamic Adaptive Policy Pathways for model-based decision support under deep uncertainty. *Environmental Modelling & Software* 86:168–183. doi: 10.1016/j.envsoft.2016.09.017
- Lai S, Erbach-Schoenberg E zu, Pezzulo C, Ruktanonchai NW, Sorichetta A, Steele J, Li T, Dooley CA, Tatem AJ (2019) Exploring the use of mobile phone data for national migration statistics. *Palgrave communications* 5. doi: 10.1057/s41599-019-0242-9
- Lange MA, Llasat MC, Snoussi M, Graves A, Le Tellier J, Queralt A, Vagliasindi GM (2020) Introduction. In: Cramer W, Guiot J, Marini K (eds) *Climate and Environmental Change in the Mediterranean Basin – Current Situation and Risks for the Future*. First Mediterranean Assessment Report, in press, Marseille, France
- Lanza SG (2003) Flood hazard threat on cultural heritage in the town of Genoa (Italy). *Journal of Cultural Heritage* 4(3):159–167. doi: 10.1016/S1296-2074(03)00042-6
- Lázár AN, Nicholls RJ, Hall JW, Barbour EJ, Haque A (2020) Contrasting development trajectories for coastal Bangladesh to the end of century. *Reg Environ Change* 20(3):429. doi: 10.1007/s10113-020-01681-y
- Leimbach M, Kriegler E, Roming N, Schwanitz J (2017) Future growth patterns of world regions – A GDP scenario approach. *Global Environmental Change* 42:215–225. doi: 10.1016/j.gloenvcha.2015.02.005
- Levermann A, Clark PU, Marzeion B, Milne GA, Pollard D, Radic V, Robinson A (2013) The multimillennial sea-level commitment of global warming. *Proceedings of the National Academy of Sciences of the United States of America* 110(34):13745–13750. doi: 10.1073/pnas.1219414110
- Leyk S, Gaughan AE, Adamo SB, Sherbinin A de, Balk D, Freire S, Rose A, Stevens FR, Blankespoor B, Frye C, Comenetz J, Sorichetta A, MacManus K, Pistoletti L, Levy M, Tatem AJ, Pesaresi M (2019) The spatial allocation of population. A review of large-scale gridded population data products and their fitness for use. *Earth Syst. Sci. Data* 11(3):1385–1409. doi: 10.5194/essd-11-1385-2019
- Lichter M, Vafeidis AT, Nicholls RJ, Kaiser G (2011) Exploring Data-Related Uncertainties in Analyses of Land Area and Population in the “Low-Elevation Coastal Zone” (LECZ). *Journal of Coastal Research* 274:757–768. doi: 10.2112/JCOASTRES-D-10-00072.1
- Lincke D, Hinkel J (2018) Economically robust protection against 21st century sea-level rise. *Global Environmental Change* 51:67–73. doi: 10.1016/j.gloenvcha.2018.05.003
- Lollino G, Giordan D, Marunteanu C, Christaras B, Yoshinori I, Margottini C (eds) (2015) *Engineering Geology for Society and Territory - Volume 8*. Springer International Publishing, Cham
- López Royo M, Ranasinghe R, Jiménez JA (2016) A Rapid, Low-Cost Approach to Coastal Vulnerability Assessment at a National Level. *Journal of Coastal Research* 320:932–945. doi: 10.2112/JCOASTRES-D-14-00217.1
- Lu X, Wrathall DJ, Sundsøy PR, Nadiruzzaman M, Wetter E, Iqbal A, Qureshi T, Tatem A, Canright G, Engø-Monsen K, Bengtsson L (2016) Unveiling hidden migration and mobility patterns in climate stressed regions. A longitudinal study of six million anonymous mobile phone users in Bangladesh. *Global Environmental Change* 38(27):1–7. doi: 10.1016/j.gloenvcha.2016.02.002
- Lückenköter J, Hurth F, Schonlau M (2017) *European Population Projections for 2015–2060: 10-km Gridded Data Based on the Shared Socioeconomic Pathways (SSPs)*
- Luijendijk A, Hagenaars G, Ranasinghe R, Baart F, Donchyts G, Aarninkhof S (2018) The State of the World’s Beaches. *Scientific Reports* 8(1):6641. doi: 10.1038/s41598-018-24630-6
- Madajewicz M (2020) Who is vulnerable and who is resilient to coastal flooding? Lessons from Hurricane Sandy in New York City. *Climatic Change* 163(4):2029–2053. doi: 10.1007/s10584-020-02896-y

- Manca E, Santarossa L (2016) Tourism and sustainable development in the Mediterranean: key facts and trends, Valbonne
- Marcos M, Rohmer J, Voudoukas MI, Mentaschi L, Le Cozannet G, Amores A (2019) Increased Extreme Coastal Water Levels Due to the Combined Action of Storm Surges and Wind Waves. *Geophys. Res. Lett.* 46(8):4356–4364. doi: 10.1029/2019GL082599
- Margottini C (2015) Engineering Geology in Shaping and Preserving the Historic Urban Landscapes and Cultural Heritage: Achievements in UNESCO World Heritage Sites. In: Lollino G, Giordan D, Marunteanu C, Christaras B, Yoshinori I, Margottini C (eds) *Engineering Geology for Society and Territory - Volume 8*, vol 8. Springer International Publishing, Cham, pp 1–28
- Marsha A, Sain SR, Heaton MJ, Monaghan AJ, Wilhelmi OV (2018) Influences of climatic and population changes on heat-related mortality in Houston, Texas, USA. *Climatic Change* 146(3-4):471–485. doi: 10.1007/s10584-016-1775-1
- Marzeion B, Levermann A (2014) Loss of cultural world heritage and currently inhabited places to sea-level rise. *Environ. Res. Lett.* 9(3):34001. doi: 10.1088/1748-9326/9/3/034001
- Mavromatidi A, Briche E, Claeys C (2018) Mapping and analyzing socio-environmental vulnerability to coastal hazards induced by climate change. An application to coastal Mediterranean cities in France. *Cities* 72:189–200. doi: 10.1016/j.cities.2017.08.007
- McGranahan G, Balk D, Anderson B (2007) The rising tide. Assessing the risks of climate change and human settlements in low elevation coastal zones. *Environment and Urbanization* 19(1):17–37. doi: 10.1177/0956247807076960
- Mclaughlin S, Cooper JAG (2010) A multi-scale coastal vulnerability index. A tool for coastal managers? *Environmental Hazards* 9(3):233–248. doi: 10.3763/ehaz.2010.0052
- McLeman R (2019) International migration and climate adaptation in an era of hardening borders. *Nat. Clim. Chang.* 9(12):911–918. doi: 10.1038/s41558-019-0634-2
- McLeod E, Poulter B, Hinkel J, Reyes E, Salm R (2010) Sea-level rise impact models and environmental conservation. A review of models and their applications. *Ocean & Coastal Management* 53(9):507–517. doi: 10.1016/j.ocecoaman.2010.06.009
- McMichael C, Dasgupta S, Ayeb-Karlsson S, Kelman I (2020) A review of estimating population exposure to sea-level rise and the relevance for migration. *Environ. Res. Lett.* 15(12):123005. doi: 10.1088/1748-9326/abb398
- MedECC (2020a) *Climate and Environmental Change in the Mediterranean Basin – Current Situation and Risks for the Future. First Mediterranean Assessment Report*, in press, Marseille, France
- MedECC (2020b) *Summary for Policymakers. In: Cramer W, Guiot J, Marini K (eds) Climate and Environmental Change in the Mediterranean Basin – Current Situation and Risks for the Future. First Mediterranean Assessment Report*, in press, Marseille, France
- Mentaschi L, Voudoukas MI, Pekel J-F, Voukouvalas E, Feyen L (2018) Global long-term observations of coastal erosion and accretion. *Scientific Reports* 8(1):12876. doi: 10.1038/s41598-018-30904-w
- Merkens J-L, Lincke D, Hinkel J, Brown S, Vafeidis AT (2018) Regionalisation of population growth projections in coastal exposure analysis. *Climatic Change* 151(3):413–426. doi: 10.1007/s10584-018-2334-8
- Merkens J-L, Reimann L, Hinkel J, Vafeidis AT (2016) Gridded population projections for the coastal zone under the Shared Socioeconomic Pathways. *Global and Planetary Change* 145:57–66. doi: 10.1016/j.gloplacha.2016.08.009
- Merkens J-L, Vafeidis A (2018) Using Information on Settlement Patterns to Improve the Spatial Distribution of Population in Coastal Impact Assessments. *Sustainability* 10(9):3170. doi: 10.3390/su10093170
- Messner F, Penning-Rowsell E, Green C, Meyer V, Tunstall S, van der Veen A (2007) *Evaluating flood damages: guidance and recommendations on principles and methods.*



- [http://www.floodsite.net/html/partner\\_area/project\\_docs/T09\\_06\\_01\\_Flood\\_damage\\_guidelines\\_d9\\_1\\_v2\\_2\\_p44.pdf](http://www.floodsite.net/html/partner_area/project_docs/T09_06_01_Flood_damage_guidelines_d9_1_v2_2_p44.pdf). Accessed 22 Feb 2021
- Moel H de, Jongman B, Kreibich H, Merz B, Penning-Rowsell E, Ward PJ (2015) Flood risk assessments at different spatial scales. *Mitig Adapt Strateg Glob Change* 20(6):865–890. doi: 10.1007/s11027-015-9654-z
- Moel H de, van Alphen J, Aerts JCJH (2009) Flood maps in Europe &ndash; methods, availability and use. *Nat. Hazards Earth Syst. Sci.* 9(2):289–301. doi: 10.5194/nhess-9-289-2009
- Moftakhari HR, Salvadori G, AghaKouchak A, Sanders BF, Matthew RA (2017) Compounding effects of sea level rise and fluvial flooding. *Proceedings of the National Academy of Sciences of the United States of America*:9785–9790. doi: 10.1073/pnas.1620325114
- Monaghan AJ, Sampson KM, Steinhoff DF, Ernst KC, Ebi KL, Jones B, Hayden MH (2018) The potential impacts of 21st century climatic and population changes on human exposure to the virus vector mosquito *Aedes aegypti*. *Climatic Change* 146(3-4):487–500. doi: 10.1007/s10584-016-1679-0
- Mondal P, Tatem AJ (2012) Uncertainties in measuring populations potentially impacted by sea level rise and coastal flooding. *PLoS ONE* 7(10):e48191. doi: 10.1371/journal.pone.0048191
- Moss RH, Edmonds JA, Hibbard KA, Manning MR, Rose SK, van Vuuren DP, Carter TR, Emori S, Kainuma M, Kram T, Meehl GA, Mitchell JFB, Nakicenovic N, Riahi K, Smith SJ, Stouffer RJ, Thomson AM, Weyant JP, Wilbanks TJ (2010) The next generation of scenarios for climate change research and assessment. *Nature* 463(7282):747–756. doi: 10.1038/nature08823
- Muis S, Apecechea MI, Dullaart J, Lima Rego J de, Madsen KS, Su J, Yan K, Verlaan M (2020) A High-Resolution Global Dataset of Extreme Sea Levels, Tides, and Storm Surges, Including Future Projections. *Front. Mar. Sci.* 7:831. doi: 10.3389/fmars.2020.00263
- Muis S, Guneralp B, Jongman B, Aerts JCJH, Ward PJ (2015) Flood risk and adaptation strategies under climate change and urban expansion: A probabilistic analysis using global data. *The Science of the total environment* 538:445–457. doi: 10.1016/j.scitotenv.2015.08.068
- Muis S, Verlaan M, Nicholls RJ, Brown S, Hinkel J, Lincke D, Vafeidis AT, Scussolini P, Winsemius HC, Ward PJ (2017) A comparison of two global datasets of extreme sea levels and resulting flood exposure. *Earth's Future*. doi: 10.1002/2016EF000430
- Muis S, Verlaan M, Winsemius HC, Aerts JCJH, Ward PJ (2016) A global reanalysis of storm surges and extreme sea levels. *Nature communications* 7:11969. doi: 10.1038/ncomms11969
- Murakami D, Yamagata Y (2019) Estimation of Gridded Population and GDP Scenarios with Spatially Explicit Statistical Downscaling. *Sustainability* 11(7):2106. doi: 10.3390/su11072106
- Nakićenović N (2000) Special report on emissions scenarios. A special report of Working Group III of the Intergovernmental Panel on Climate Change. Cambridge University Press, Cambridge
- Neumann B, Vafeidis AT, Zimmermann J, Nicholls RJ (2015) Future coastal population growth and exposure to sea-level rise and coastal flooding--a global assessment. *PloS one* 10(3):e0118571. doi: 10.1371/journal.pone.0118571
- Neverre N, Dumas P (2015) Projecting and valuing domestic water use at regional scale. A generic method applied to the Mediterranean at the 2060 horizon. *Water Resources and Economics* 11:33–46. doi: 10.1016/j.wre.2015.06.001
- Nicholls RJ (1995) Coastal megacities and climate change. *GeoJournal* 37(3):369–379. doi: 10.1007/BF00814018
- Nicholls RJ (2004) Coastal flooding and wetland loss in the 21st century. Changes under the SRES climate and socio-economic scenarios. *Global Environmental Change* 14(1):69–86. doi: 10.1016/j.gloenvcha.2003.10.007
- Nicholls RJ (2010) Impacts of and Responses to Sea-Level Rise. In: Church J (ed) *Understanding sea-level rise and variability*. Blackwell Pub, Hoboken, NJ, pp 17–51
- Nicholls RJ, Brown S, Goodwin P, Wahl T, Lowe J, Solan M, Godbold JA, Haigh ID, Lincke D, Hinkel J, Wolff C, Merckens J-L (2018) Stabilization of global temperature at 1.5°C and 2.0°C.

- Implications for coastal areas. *Philosophical transactions. Series A, Mathematical, physical, and engineering sciences* 376(2119). doi: 10.1098/rsta.2016.0448
- Nicholls RJ, Hanson S, Herweijer C, Patmore N, Hallegatte S, Corfee-Morlot J, Château J, Muir-Wood R (2008a) Ranking Port Cities with High Exposure and Vulnerability to Climate Extremes: Exposure Estimates. *OECD Environment Working Papers* 1. doi: 10.1787/011766488208
- Nicholls RJ, Marinova N, Lowe JA, Brown S, Vellinga P, Gusmao D de, Hinkel J, Tol RSJ (2011) Sea-level rise and its possible impacts given a 'beyond 4 degrees C world' in the twenty-first century. *Philosophical transactions. Series A, Mathematical, physical, and engineering sciences* 369(1934):161–181. doi: 10.1098/rsta.2010.0291
- Nicholls RJ, Wong PP, Burkett V, Woodroffe CD, Hay J (2008b) Climate change and coastal vulnerability assessment. *Scenarios for integrated assessment. Sustain Sci* 3(1):89–102. doi: 10.1007/s11625-008-0050-4
- Ninno A, Ciavola P, Billi P (2018) The Po Delta is restarting progradation: geomorphological evolution based on a 47-years Earth Observation dataset. *Scientific Reports* 8(1):3457. doi: 10.1038/s41598-018-21928-3
- O'Neill BC, Kriegler E, Ebi KL, Kemp-Benedict E, Riahi K, Rothman DS, van Ruijven BJ, van Vuuren DP, Birkmann J, Kok K, Levy M, Solecki W (2017) The roads ahead. Narratives for shared socioeconomic pathways describing world futures in the 21st century. *Global Environmental Change* 42:169–180. doi: 10.1016/j.gloenvcha.2015.01.004
- O'Neill BC, Kriegler E, Riahi K, Ebi KL, Hallegatte S, Carter TR, Mathur R, van Vuuren DP (2014) A new scenario framework for climate change research. The concept of shared socioeconomic pathways. *Climatic Change* 122(3):387–400. doi: 10.1007/s10584-013-0905-2
- O'Neill BC, Carter TR, Ebi K, Harrison PA, Kemp-Benedict E, Kok K, Kriegler E, Preston BL, Riahi K, Sillmann J, van Ruijven BJ, van Vuuren D, Carlisle D, Conde C, Fuglestedt J, Green C, Hasegawa T, Leininger J, Monteith S, Pichs-Madruga R (2020) Achievements and needs for the climate change scenario framework. *Nature climate change*:1–11. doi: 10.1038/s41558-020-00952-0
- Oppenheimer M, Campos M, Warren R, Birkmann J, Luber G, O'Neill B, Takahashi K (2014) Emergent risks and key vulnerabilities. In: Field CB, Barros VR, Dokken DJ, Mach KJ, Mastrandrea MD, Bilir TE, Chatterjee M, Ebi KL, Estrada YO, Genova RC, Girma B, Kissel ES, Levy AN, MacCracken S, Mastrandrea PR, White LL (eds) *Climate change 2014: Impacts, Adaptation and Vulnerability. Part A: Global and Sectoral Aspects. Contribution of Working Group II to the Fifth Assessment Report of the Intergovernmental Panel on Climate Change*. Cambridge University Press, Cambridge, UK and New York, NY, USA, pp 1039–1099
- Oppenheimer M, Glavovic BC, Hinkel J, van de Wal R, Magnan AK, Abd-Elgawad A, Cai R, Cifuentes-Jara M, DeConto RM, Ghosh T, Hay J, Isla F, Marzeion B, Meyssignac B, Sebesvari Z (2019) Sea Level Rise and Implications for Low-Lying Islands, Coasts and Communities. In: IPCC (ed) *IPCC Special Report on the Ocean and Cryosphere in a Changing Climate*. Pörtner, H.-O.; Roberts, D. C.; Masson-Delmotte, V.; Zhai, P.; Tignor, M.; Poloczanska, E.; Mintenbeck, K.; Alegria, A.; Nicolai, M.; Okem, A.; Petzold, J.; Rama, B.; Weyer, N. M. (eds.), in press
- Özhan E (2002) Coastal erosion management in the Mediterranean: an overview. <https://wedocs.unep.org/handle/20.500.11822/1749?show=full>. Accessed 22 Feb 2021
- Özkaynak B, Rodríguez-Labajos B (2010) Multi-scale interaction in local scenario-building. A methodological framework. *Futures* 42(9):995–1006. doi: 10.1016/j.futures.2010.08.022
- Paprotny D, Morales-Nápoles O, Vousdoukas MI, Jonkman SN, Nikulin G (2018) Accuracy of pan-European coastal flood mapping. *J Flood Risk Management* 12(2):e12459. doi: 10.1111/jfr3.12459
- Peduzzi P, Dao H, Herold C, Mouton F (2009) Assessing global exposure and vulnerability towards natural hazards. *The Disaster Risk Index. Nat. Hazards Earth Syst. Sci.* 9(4):1149–1159. doi: 10.5194/nhess-9-1149-2009

- Pekel J-F, Cottam A, Gorelick N, Belward AS (2016) High-resolution mapping of global surface water and its long-term changes. *Nature* 540(7633):418–422. doi: 10.1038/nature20584
- Pendleton EA, Thieler RE, Williams JS (2004) Coastal Vulnerability Assessment of Cape Hatteras National Seashore (CAHA) to Sea-Level Rise. <https://pubs.usgs.gov/of/2004/1064/images/pdf/caha.pdf>. Accessed 22 Feb 2021
- Perry J (2011) World Heritage hot spots. A global model identifies the 16 natural heritage properties on the World Heritage List most at risk from climate change. *International Journal of Heritage Studies* 17(5):426–441. doi: 10.1080/13527258.2011.568064
- Pesaresi M, Florczyk A, Schiavina M, Melchiorri M, Maffenini L (2019) GHS settlement grid, updated and refined REGIO model 2014 in application to GHS-BUILT R2018A and GHS-POP R2019A, multitemporal (1975-1990-2000-2015), R2019A. <http://data.europa.eu/89h/42e8be89-54ff-464e-be7b-bf9e64da5218>. Accessed 22 Feb 2021
- Pesaresi M, Melchiorri M, Alice S, Kemper T (2016) Atlas of the human planet 2016. Mapping human presence on earth with the global human settlement layer. EUR, Scientific and technical research series, vol 28116. Publications Office, Luxembourg
- Pezzulo C, Hornby GM, Sorichetta A, Gaughan AE, Linard C, Bird TJ, Kerr D, Lloyd CT, Tatem AJ (2017) Sub-national mapping of population pyramids and dependency ratios in Africa and Asia. *Scientific Data* 4:170089. doi: 10.1038/sdata.2017.89
- Phillips H (2014) Adaptation to Climate Change at UK World Heritage Sites. *Progress and Challenges. The Historic Environment: Policy & Practice* 5(3):288–299. doi: 10.1179/1756750514Z.00000000062
- Phillips H (2015) The capacity to adapt to climate change at heritage sites—The development of a conceptual framework. *Environmental Science & Policy* 47:118–125. doi: 10.1016/j.envsci.2014.11.003
- Piante C, Ody D (2015) Blue Growth in the Mediterranean Sea: the Challenge of Good Environmental Status. [http://www.medtrends.org/reports/MEDTRENDS\\_REGIONAL.pdf](http://www.medtrends.org/reports/MEDTRENDS_REGIONAL.pdf). Accessed 22 Feb 2021
- POPGRID Data Collaborative (2020) Leaving No One Off The Map. A guide for gridded population data for sustainable development
- Pörtner H-O, D.C. Roberts, V. Masson-Delmotte, P. Zhai, E. Poloczanska, K. Mintenbeck, M. Tignor, A. Alegria, M. Nicolai, A. Okem, J. Petzold, B. Rama, N.M. Weyer (2019) Technical Summary. In: IPCC (ed) IPCC Special Report on the Ocean and Cryosphere in a Changing Climate. Pörtner, H.-O.; Roberts, D. C.; Masson-Delmotte, V.; Zhai, P.; Tignor, M.; Poloczanska, E.; Mintenbeck, K.; Alegria, A.; Nicolai, M.; Okem, A.; Petzold, J.; Rama, B.; Weyer, N. M. (eds.), in press
- Poulter B, Halpin PN (2008) Raster modelling of coastal flooding from sea-level rise. *International Journal of Geographical Information Science* 22(2):167–182. doi: 10.1080/13658810701371858
- Preston BL, Yuen EJ, Westaway RM (2011) Putting vulnerability to climate change on the map. A review of approaches, benefits, and risks. *Sustain Sci* 6(2):177–202. doi: 10.1007/s11625-011-0129-1
- PROTHEGO project (2018) Map viewer. <http://mapapps2.bgs.ac.uk/prothego/index.html>. Accessed 22 Feb 2021
- R Core Team (2020) R: A language and environment for statistical computing, R Foundation for Statistical Computing, Vienna, Austria
- Ramieri E, Hartley A, Barbanti A, Duarte Santos F, Gomes A, Hilden M, Laihonon P, Marinova N, Santini M (2011) Methods for assessing coastal vulnerability to climate change. ETC CCA Technical Paper 1/2011. [ftp://sitelftp.unine.ch/bouzelboudjen/Guelat\\_Jeremie\\_2013\\_UniNE\\_Geog/BD\\_risques\\_%20cotiers/doc/Methods%20for%20assessing%20coastal.pdf](ftp://sitelftp.unine.ch/bouzelboudjen/Guelat_Jeremie_2013_UniNE_Geog/BD_risques_%20cotiers/doc/Methods%20for%20assessing%20coastal.pdf). Accessed 22 Feb 2021

- Ramirez JA, Lichter M, Coulthard TJ, Skinner C (2016) Hyper-resolution mapping of regional storm surge and tide flooding. Comparison of static and dynamic models. *Nat Hazards* 82(1):571–590. doi: 10.1007/s11069-016-2198-z
- Ranasinghe R (2016) Assessing climate change impacts on open sandy coasts. A review. *Earth-Science Reviews* 160(4):320–332. doi: 10.1016/j.earscirev.2016.07.011
- Ranasinghe R, Stive MJF (2009) Rising seas and retreating coastlines. *Climatic Change* 97(3-4):465–468. doi: 10.1007/s10584-009-9593-3
- Reeder LA, Rick TC, Erlandson JM (2012) Our disappearing past. A GIS analysis of the vulnerability of coastal archaeological resources in California’s Santa Barbara Channel region. *J Coast Conserv* 16(2):187–197. doi: 10.1007/s11852-010-0131-2
- Reeder-Myers LA (2015) Cultural Heritage at Risk in the Twenty-First Century. A Vulnerability Assessment of Coastal Archaeological Sites in the United States. *The Journal of Island and Coastal Archaeology* 10(3):436–445. doi: 10.1080/15564894.2015.1008074
- Reimann L, Merkens J-L, Vafeidis AT (2018a) Regionalized Shared Socioeconomic Pathways: narratives and spatial population projections for the Mediterranean coastal zone. *Regional Environmental Change* 18:235–245. doi: 10.1007/s10113-017-1189-2
- Reimann L, Vafeidis AT, Brown S, Hinkel J, Tol RSJ (2018b) UNESCO cultural World Heritage in the Mediterranean coastal zone. <https://doi.org/10.6084/m9.figshare.5759538>
- Reimann L, Vollstedt B, Koerth J, Tsakiris M, Beer M, Vafeidis AT (2021) Extending the Shared Socioeconomic Pathways (SSPs) to support local adaptation planning – A climate service for Flensburg, Germany. *Futures* 127. doi: 10.1016/j.futures.2020.102691
- Riahi K, van Vuuren DP, Kriegler E, Edmonds J, O’Neill BC, Fujimori S, Bauer N, Calvin K, Dellink R, Fricko O, Lutz W, Popp A, Cuaresma JC, KC S, Leimbach M, Jiang L, Kram T, Rao S, Emmerling J, Ebi K, Hasegawa T, Havlik P, Humpenöder F, Da Silva LA, Smith S, Stehfest E, Bosetti V, Eom J, Gernaat D, Masui T, Rogelj J, Strefler J, Drouet L, Krey V, Luderer G, Harmsen M, Takahashi K, Baumstark L, Doelman JC, Kainuma M, Klimont Z, Marangoni G, Lotze-Campen H, Obersteiner M, Tabeau A, Tavoni M (2017) The Shared Socioeconomic Pathways and their energy, land use, and greenhouse gas emissions implications: An overview. *Global Environmental Change* 42:153–168. doi: 10.1016/j.gloenvcha.2016.05.009
- Rich DC (1980) Potential models in human geography. Concepts and techniques in modern geography, vol 26. *Geo Abstracts*, Norwich
- Rigaud KK, de Sherbinin A, Jones B, Bergmann J, Clement V, Ober K, Schewe J, Adamo S, McCusker B, Heuser S, Midgley A (2018) *Groundswell: Preparing for Internal Climate Migration.*, Washington, DC
- Rio M-H, Mulet S, Picot N (2014) Beyond GOCE for the ocean circulation estimate. Synergetic use of altimetry, gravimetry, and in situ data provides new insight into geostrophic and Ekman currents. *Geophys. Res. Lett.* 41(24):8918–8925. doi: 10.1002/2014GL061773
- Rockström J, Schellnhuber HJ, Hoskins B, Ramanathan V, Schlosser P, Brasseur GP, Gaffney O, Nobre C, Meinshausen M, Rogelj J, Lucht W (2016) The world's biggest gamble. *Earth’s Future* 4(10):465–470. doi: 10.1002/2016EF000392
- Rogelj J, den Elzen M, Höhne N, Fransen T, Fekete H, Winkler H, Schaeffer R, Sha F, Riahi K, Meinshausen M (2016) Paris Agreement climate proposals need a boost to keep warming well below 2 degrees C. *Nature* 534(7609):631–639. doi: 10.1038/nature18307
- Rohat G (2018) Projecting Drivers of Human Vulnerability under the Shared Socioeconomic Pathways. *International journal of environmental research and public health* 15(3). doi: 10.3390/ijerph15030554
- Rohat G, Flacke J, Dosio A, Dao H, Maarseveen M (2019a) Projections of Human Exposure to Dangerous Heat in African Cities Under Multiple Socioeconomic and Climate Scenarios. *Earth’s Future* 7(5):528–546. doi: 10.1029/2018EF001020

- Rohat G, Flacke J, Dosio A, Pedde S, Dao H, van Maarseveen M (2019b) Influence of changes in socioeconomic and climatic conditions on future heat-related health challenges in Europe. *Global and Planetary Change* 172:45–59. doi: 10.1016/j.gloplacha.2018.09.013
- Rohat G, Wilhelmi O, Flacke J, Monaghan A, Gao J, Dao H, van Maarseveen M (2019c) Characterizing the role of socioeconomic pathways in shaping future urban heat-related challenges. *The Science of the total environment* 695:133941. doi: 10.1016/j.scitotenv.2019.133941
- Roy KC, Hasan S, Mozumder P (2020) A multilabel classification approach to identify hurricane-induced infrastructure disruptions using social media data. *Computer-Aided Civil and Infrastructure Engineering* 35(12):1387–1402. doi: 10.1111/mice.12573
- Sabbioni C, Cassar M, Brimblecombe P, Lefevre RA (2008) Vulnerability of cultural heritage to climate change. [https://www.coe.int/t/dg4/majorhazards/activites/2009/Ravello15-16may09/Ravello\\_APCAT2008\\_44\\_Sabbioni-Jan09\\_EN.pdf](https://www.coe.int/t/dg4/majorhazards/activites/2009/Ravello15-16may09/Ravello_APCAT2008_44_Sabbioni-Jan09_EN.pdf). Accessed 22 Feb 2021
- Sampson CC, Smith AM, Bates PD, Neal JC, Alfieri L, Freer JE (2015) A high-resolution global flood hazard model. *Water resources research* 51(9):7358–7381. doi: 10.1002/2015WR016954
- Sanna S, Le Tellier J (2013) Building on the Mediterranean scenario experiences. Cross-cutting approaches between regional foresight analysis and participatory prospective, Valbonne
- Satta A, Venturini S, Puddu M, Firth J, Lafitte A (2015) Strengthening the Knowledge Base on Regional Climate Variability and Change: Application of a Multi-Scale Coastal Risk Index at Regional and Local Scale in the Mediterranean. <https://planbleu.org/en/publications/strengthening-the-knowledge-base-on-regional-climate-variability-and-change-application-of-a-multi-scale-coastal-risk-index-at-regional-and-local-scale-in-the-mediterranean/>. Accessed 22 Feb 2021
- Sauzade D, Rousset N (2013) Greening the Mediterranean fisheries: tentative assessment of the economic leeway, Valbonne
- Schiavina M, Freire S, MacManus K (2019) GHS population grid multitemporal (1975, 1990, 2000, 2015) R2019A. <http://data.europa.eu/89h/0c6b9751-a71f-4062-830b-43c9f432370f>. Accessed 22 Feb 2021
- Schleussner C-F, Rogelj J, Schaeffer M, Lissner T, Licker R, Fischer EM, Knutti R, Levermann A, Frieler K, Hare W (2016) Science and policy characteristics of the Paris Agreement temperature goal. *Nature Climate change* 6(9):827–835. doi: 10.1038/NCLIMATE3096
- Schmidt M, Rudolf B (2013) Climate Change and Cultural Heritage: Findings of a rapid Vulnerability Assessment of Cultural Heritage in the Republic of Macedonia and Recommendations towards National Strategies for Cultural Heritage Protection in the context of Climate Change. Project report. <http://docshare04.docshare.tips/files/24286/242864272.pdf>. Accessed 22 Feb 2021
- Schneider A, Friedl MA, Potere D (2009) A new map of global urban extent from MODIS satellite data. *Environ. Res. Lett.* 4(4):44003. doi: 10.1088/1748-9326/4/4/044003
- Schuerch M, Spencer T, Temmerman S, Kirwan ML, Wolff C, Lincke D, Mcowen CJ, Pickering MD, Reef R, Vafeidis AT, Hinkel J, Nicholls RJ, Brown S (2018) Future response of global coastal wetlands to sea-level rise. *Nature* 561(7722):231–234. doi: 10.1038/s41586-018-0476-5
- Schweizer VJ, Kurniawan JH (2016) Systematically linking qualitative elements of scenarios across levels, scales, and sectors. *Environmental Modelling & Software* 79:322–333. doi: 10.1016/j.envsoft.2015.12.014
- Scussolini P, Aerts JCJH, Jongman B, Bouwer LM, Winsemius HC, de Moel H, Ward PJ (2016) FLOPROS. An evolving global database of flood protection standards. *Nat. Hazards Earth Syst. Sci.* 16(5):1049–1061. doi: 10.5194/nhess-16-1049-2016
- Seenath A, Wilson M, Miller K (2016) Hydrodynamic versus GIS modelling for coastal flood vulnerability assessment. Which is better for guiding coastal management? *Ocean & Coastal Management* 120(10):99–109. doi: 10.1016/j.ocecoaman.2015.11.019

- Seto KC, Fragkias M, Güneralp B, Reilly MK (2011) A meta-analysis of global urban land expansion. *PloS one* 6(8):e23777. doi: 10.1371/journal.pone.0023777
- Seto KC, Güneralp B, Hutyrá LR (2012) Global forecasts of urban expansion to 2030 and direct impacts on biodiversity and carbon pools. *Proceedings of the National Academy of Sciences of the United States of America* 109(40):16083–16088. doi: 10.1073/pnas.1211658109
- Shaw J, Taylor RB, Forbes DL, Ruz MH, Solomon S (1998) Sensitivity of the coasts of Canada to sea-level rise (No. 505). Ottawa, Ontario: Geological Survey of Canada
- Sherbinin A de, Bukvic A, Rohat G, Gall M, McCusker B, Preston B, Apotsos A, Fish C, Kienberger S, Muhonda P, Wilhelmi O, Macharia D, Shubert W, Sliuzas R, Tomaszewski B, Zhang S (2019) Climate vulnerability mapping. A systematic review and future prospects. *WIREs Clim Change* 35(1):515. doi: 10.1002/wcc.600
- Shirzaei M, Freymueller J, Törnqvist TE, Galloway DL, Dura T, Minderhoud PSJ (2021) Measuring, modelling and projecting coastal land subsidence. *Nature Reviews Earth & Environment* 2(1):40–58. doi: 10.1038/s43017-020-00115-x
- Skov-Petersen H (2001) Estimation of distance-decay parameters. GIS-based indicators of recreational accessibility. *ScanGIS*:237–258
- Slangen ABA, Carson M, Katsman CA, van de Wal RSW, Köhl A, Vermeersen LLA, Stammer D (2014) Projecting twenty-first century regional sea-level changes. *Climatic Change* 124(1):317–332. doi: 10.1007/s10584-014-1080-9
- Small C, Nicholls RJ (2003) A Global Analysis of Human Settlement in Coastal Zones. *Journal of Coastal Research* 19(3):584–599
- Syvitski JPM, Kettner AJ, Overeem I, Hutton EWH, Hannon MT, Brakenridge GR, Day J, Vörösmarty C, Saito Y, Giosan L, Nicholls RJ (2009) Sinking deltas due to human activities. *Nature Geosci* 2(10):681–686. doi: 10.1038/ngeo629
- Taherkhani M, Vitousek S, Barnard PL, Frazer N, Anderson TR, Fletcher CH (2020) Sea-level rise exponentially increases coastal flood frequency. *Scientific Reports* 10(1):6466. doi: 10.1038/s41598-020-62188-4
- Taramelli A, Di Matteo L, Ciavola P, Guadagnano F, Tolomei C (2015) Temporal evolution of patterns and processes related to subsidence of the coastal area surrounding the Bevano River mouth (Northern Adriatic) – Italy. *Ocean & Coastal Management* 108:74–88. doi: 10.1016/j.ocecoaman.2014.06.021
- Tatem AJ (2017) WorldPop, open data for spatial demography. *Scientific Data* 4:170004. doi: 10.1038/sdata.2017.4
- Taylor T, Hunt A, Cassar M, Wainwright I (2007) Quantifying the costs of climate change impacts on the built environment. In: Cassar M, Hawkings C (eds) *Engineering historic futures. Stakeholders dissemination and scientific research report*. UCL Centre for Sustainable Heritage, London, pp 124–144
- Temmerman S, Meire P, Bouma TJ, Herman PMJ, Ysebaert T, Vriend HJ de (2013) Ecosystem-based coastal defence in the face of global change. *Nature* 504(7478):79–83. doi: 10.1038/nature12859
- Terama E, Clarke E, Rounsevell MDA, Fronzek S, Carter TR (2019) Modelling population structure in the context of urban land use change in Europe. *Reg Environ Change* 19(3):667–677. doi: 10.1007/s10113-017-1194-5
- Terrill G (2008) Climate Change. How Should the World Heritage Convention Respond? *International Journal of Heritage Studies* 14(5):388–404. doi: 10.1080/13527250802284388
- Tessler ZD, Vörösmarty CJ, Overeem I, Syvitski JPM (2018) A model of water and sediment balance as determinants of relative sea level rise in contemporary and future deltas. *Resilience and Bio-Geomorphic Systems – Proceedings of the 48th Binghamton Geomorphology Symposium* 305:209–220. doi: 10.1016/j.geomorph.2017.09.040

- The World Bank (2016) World Development Indicators.  
<http://databank.worldbank.org/data/reports.aspx?source=world-development-indicators#>.  
Accessed 22 Feb 2021
- Thieler ER, Hammar-Klose ES (1999) National Assessment of Coastal Vulnerability to Sea-Level Rise: Preliminary Results for the U.S. Atlantic Coast. U.S. Geological Survey Open-File Report 99-593
- Tiggeloven T, Moel H de, Winsemius HC, Eilander D, Erkens G, Gebremedhin E, Diaz Loaiza A, Kuzma S, Luo T, Iceland C, Bouwman A, van Huijstee J, Ligtoet W, Ward PJ (2020) Global-scale benefit–cost analysis of coastal flood adaptation to different flood risk drivers using structural measures. *Nat. Hazards Earth Syst. Sci.* 20(4):1025–1044. doi: 10.5194/nhess-20-1025-2020
- Toimil A, Losada IJ, Nicholls RJ, Dalrymple RA, Stive MJF (2020) Addressing the challenges of climate change risks and adaptation in coastal areas. A review. *Coastal Engineering* 156:103611. doi: 10.1016/j.coastaleng.2019.103611
- Torresan S, Critto A, Rizzi J, Marcomini A (2012) Assessment of coastal vulnerability to climate change hazards at the regional scale. The case study of the North Adriatic Sea. *Nat. Hazards Earth Syst. Sci.* 12(7):2347–2368. doi: 10.5194/nhess-12-2347-2012
- Turner BL, Kasperson RE, Matson PA, McCarthy JJ, Corell RW, Christensen L, Eckley N, Kasperson JX, Luers A, Martello ML, Polsky C, Pulsipher A, Schiller A (2003) A framework for vulnerability analysis in sustainability science. *Proceedings of the National Academy of Sciences of the United States of America* 100(14):8074–8079. doi: 10.1073/pnas.1231335100
- U.S. National Park Service (2015) Moving the Cape Hatteras Lighthouse.  
<https://www.nps.gov/caha/learn/historyculture/movingthelighthouse.htm>
- UNDRR (2015) Sendai Framework for Disaster Risk Reduction 2015-2030.  
<https://www.undrr.org/publication/sendai-framework-disaster-risk-reduction-2015-2030>.  
Accessed 22 Feb 2021
- UNEP/MAP (2008) Protocol on integrated coastal zone management in the Mediterranean. *Protocole relatif à la gestion intégrée des zones côtières de la Méditerranée = Protocolo relativo a la gestion integrada de las zonas costeras del Mediterraneo. Priority Actions Programme, Split*
- UNEP/MAP (2012) State of the Mediterranean marine and coastal environment.  
[https://wedocs.unep.org/bitstream/handle/20.500.11822/364/sommcer\\_eng.pdf?sequence=4&isAllowed=y](https://wedocs.unep.org/bitstream/handle/20.500.11822/364/sommcer_eng.pdf?sequence=4&isAllowed=y). Accessed 22 Feb 2021
- UNEP/MAP (2016) Mediterranean strategy for sustainable development 2016-2025. Investing in environmental sustainability to achieve social and economic development. Plan Bleu, Regional Activity Centre, Valbonne
- UNEP/MAP (2017) Regional Climate Change Adaptation Framework for the Mediterranean Marine and Coastal Areas. UNEP/MAP, Athens, Greece
- UNEP-WCMC and IUCN (2019) Protected Planet: The World Database on Protected Areas (WDPA). January 2019. <https://www.protectedplanet.net/en>. Accessed 22 Feb 2021
- UNESCO (1972) Convention concerning the protection of the world cultural and natural heritage.  
<http://whc.unesco.org/archive/convention-en.pdf>. Accessed 22 Feb 2021
- UNESCO World Heritage Centre (2007) Climate Change and World Heritage. World Heritage reports 22
- UNESCO World Heritage Centre (2008) Policy Document on the Impacts of Climate Change on World Heritage Properties. <https://whc.unesco.org/uploads/activities/documents/activity-397-2.pdf>. Accessed 22 Feb 2021
- UNESCO World Heritage Centre (2015a) Operational Guidelines for the Implementation of the World Heritage Convention. <http://whc.unesco.org/en/guidelines/>. Accessed 22 Feb 2021
- UNESCO World Heritage Centre (2015b) World Heritage Review.  
<http://unesdoc.unesco.org/images/0023/002355/235561e.pdf>. Accessed 22 Feb 2021

- UNESCO World Heritage Centre (2018) World Heritage List. <http://whc.unesco.org/en/list/>. Accessed 07 Nov 2018
- UNFCCC (2016) Paris Agreement. As contained in the report of the Conference of the Parties on its twenty-first session, FCCC/CP/2015/10/Add.1. [https://unfccc.int/files/meetings/paris\\_nov\\_2015/application/pdf/paris\\_agreement\\_english\\_.pdf](https://unfccc.int/files/meetings/paris_nov_2015/application/pdf/paris_agreement_english_.pdf). Accessed 22 Feb 2021
- United Nations, Department of Economic and Social Affairs, Population Division (2019) World urbanization prospects. The 2018 revision. United Nations, New York
- Vafeidis AT, Nicholls RJ, McFadden L, Tol RSJ, Hinkel J, Spencer T, Grashoff PS, Boot G, Klein RJT (2008) A New Global Coastal Database for Impact and Vulnerability Analysis to Sea-Level Rise. *Journal of Coastal Research* 244:917–924. doi: 10.2112/06-0725.1
- Vafeidis AT, Schuerch M, Wolff C, Spencer T, Merkens JL, Hinkel J, Lincke D, Brown S, Nicholls RJ (2019) Water-level attenuation in global-scale assessments of exposure to coastal flooding. A sensitivity analysis. *Nat. Hazards Earth Syst. Sci.* 19(5):973–984. doi: 10.5194/nhess-19-973-2019
- van Huijstee J, van Bommel B, Bouwman A, van Rijn F (2018) Towards an Urban Preview: Modelling future urban growth with 2UP, PBL Netherlands Environmental Assessment Agency, The Hague
- van Ruijven BJ, Levy MA, Agrawal A, Biermann F, Birkmann J, Carter TR, Ebi KL, Garschagen M, Jones B, Jones R, Kemp-Benedict E, Kok M, Kok K, Lemos MC, Lucas PL, Orlove B, Pachauri S, Parris TM, Patwardhan A, Petersen A, Preston BL, Ribot J, Rothman DS, Schweizer VJ (2014) Enhancing the relevance of Shared Socioeconomic Pathways for climate change impacts, adaptation and vulnerability research. *Climatic Change* 122(3):481–494. doi: 10.1007/s10584-013-0931-0
- van Vuuren DP, Edmonds J, Kainuma M, Riahi K, Thomson A, Hibbard K, Hurtt GC, Kram T, Krey V, Lamarque J-F, Masui T, Meinshausen M, Nakicenovic N, Smith SJ, Rose SK (2011a) The representative concentration pathways. An overview. *Climatic Change* 109(1-2):5–31. doi: 10.1007/s10584-011-0148-z
- van Vuuren DP, Kriegler E, O’Neill BC, Ebi KL, Riahi K, Carter TR, Edmonds J, Hallegatte S, Kram T, Mathur R, Winkler H (2014) A new scenario framework for Climate Change Research. Scenario matrix architecture. *Climatic Change* 122(3):373–386. doi: 10.1007/s10584-013-0906-1
- van Vuuren DP, Smith SJ, Riahi K (2010) Downscaling socioeconomic and emissions scenarios for global environmental change research. A review. *WIREs Clim Change* 1(3):393–404. doi: 10.1002/wcc.50
- van Vuuren DP, Stehfest E, den Elzen MGJ, Kram T, van Vliet J, Deetman S, Isaac M, Klein Goldewijk K, Hof A, Mendoza Beltran A, Oostenrijk R, van Ruijven B (2011b) RCP2.6: exploring the possibility to keep global mean temperature increase below 2°C. *Climatic Change* 109(1):95. doi: 10.1007/s10584-011-0152-3
- van Wesenbeeck BK, Boer W de, Narayan S, van der Star WRL, Vries MB de (2017) Coastal and riverine ecosystems as adaptive flood defenses under a changing climate. *Mitig Adapt Strateg Glob Change* 22(7):1087–1094. doi: 10.1007/s11027-016-9714-z
- Vanos JK, Baldwin JW, Jay O, Ebi KL (2020) Simplicity lacks robustness when projecting heat-health outcomes in a changing climate. *Nature communications* 11(1):6079. doi: 10.1038/s41467-020-19994-1
- Veldkamp TIE, Wada Y, Aerts, J C J H, Ward PJ (2016) Towards a global water scarcity risk assessment framework. Incorporation of probability distributions and hydro-climatic variability. *Environ. Res. Lett.* 11(2):24006. doi: 10.1088/1748-9326/11/2/024006
- Vitousek S, Barnard PL, Fletcher CH, Frazer N, Erikson L, Storlazzi CD (2017) Doubling of coastal flooding frequency within decades due to sea-level rise. *Scientific Reports* 7(1):1399. doi: 10.1038/s41598-017-01362-7



- Vojinovic Z, Hammond M, Golub D, Hirunsalee S, Weesakul S, Meesuk V, Medina N, Sanchez A, Kumara S, Abbott M (2016) Holistic approach to flood risk assessment in areas with cultural heritage. A practical application in Ayutthaya, Thailand. *Nat Hazards* 81(1):589–616. doi: 10.1007/s11069-015-2098-7
- Vousdoukas MI, Bouziotas D, Giardino A, Bouwer LM, Mentaschi L, Voukouvalas E, Feyen L (2018a) Understanding epistemic uncertainty in large-scale coastal flood risk assessment for present and future climates. *Nat. Hazards Earth Syst. Sci.* 18(8):2127–2142. doi: 10.5194/nhess-18-2127-2018
- Vousdoukas MI, Mentaschi L, Hinkel J, Ward PJ, Mongelli I, Ciscar J-C, Feyen L (2020a) Economic motivation for raising coastal flood defenses in Europe. *Nature communications* 11(1):2119. doi: 10.1038/s41467-020-15665-3
- Vousdoukas MI, Mentaschi L, Voukouvalas E, Bianchi A, Dottori F, Feyen L (2018b) Climatic and socioeconomic controls of future coastal flood risk in Europe. *Nature Clim Change* 8(9):776–780. doi: 10.1038/s41558-018-0260-4
- Vousdoukas MI, Mentaschi L, Voukouvalas E, Verlaan M, Feyen L (2017) Extreme sea levels on the rise along Europe's coasts. *Earth's Future* 5(3):304–323. doi: 10.1002/2016EF000505
- Vousdoukas MI, Mentaschi L, Voukouvalas E, Verlaan M, Jevrejeva S, Jackson LP, Feyen L (2018c) Global probabilistic projections of extreme sea levels show intensification of coastal flood hazard. *Nature communications* 9(1):2360. doi: 10.1038/s41467-018-04692-w
- Vousdoukas MI, Ranasinghe R, Mentaschi L, Plomaritis TA, Athanasiou P, Luijendijk A, Feyen L (2020b) Reply to. Sandy beaches can survive sea-level rise. *Nat. Clim. Chang.* 10(11):996–997. doi: 10.1038/s41558-020-00935-1
- Vousdoukas MI, Ranasinghe R, Mentaschi L, Plomaritis TA, Athanasiou P, Luijendijk A, Feyen L (2020c) Sandy coastlines under threat of erosion. *Nat. Clim. Chang.* 10(3):260–263. doi: 10.1038/s41558-020-0697-0
- Vousdoukas MI, Voukouvalas E, Mentaschi L, Dottori F, Giardino A, Bouziotas D, Bianchi A, Salamon P, Feyen L (2016) Developments in large-scale coastal flood hazard mapping. *Nat. Hazards Earth Syst. Sci.* 16(8):1841–1853. doi: 10.5194/nhess-16-1841-2016
- Wada Y, van Beek, Ludovicus P. H., Sperna Weiland FC, Chao BF, Wu Y-H, Bierkens MFP (2012) Past and future contribution of global groundwater depletion to sea-level rise. *Geophys. Res. Lett.* 39(9):n/a-n/a. doi: 10.1029/2012GL051230
- Wahl T (2017) Sea-level rise and storm surges, relationship status. Complicated! *Environ. Res. Lett.* 12(11):111001. doi: 10.1088/1748-9326/aa8eba
- Wahl T, Haigh ID, Nicholls RJ, Arns A, Dangendorf S, Hinkel J, Slangen ABA (2017) Understanding extreme sea levels for broad-scale coastal impact and adaptation analysis. *Nature communications* 8:16075. doi: 10.1038/ncomms16075
- Walker W, Haasnoot M, Kwakkel J (2013) Adapt or Perish. A Review of Planning Approaches for Adaptation under Deep Uncertainty. *Sustainability* 5(3):955–979. doi: 10.3390/su5030955
- Wang J-J (2015) Flood risk maps to cultural heritage. Measures and process. *Journal of Cultural Heritage* 16(2):210–220. doi: 10.1016/j.culher.2014.03.002
- Wang T, Sun F (2021) Spatially explicit global gross domestic product (GDP) data set consistent with the Shared Socioeconomic Pathways
- Ward PJ, Blauhut V, Bloemendaal N, Daniell JE, Ruiter MC de, Duncan MJ, Emberson R, Jenkins SF, Kirschbaum D, Kunz M, Mohr S, Muis S, Riddell GA, Schäfer A, Stanley T, Veldkamp TIE, Winsemius HC (2020) Review article. Natural hazard risk assessments at the global scale. *Nat. Hazards Earth Syst. Sci.* 20(4):1069–1096. doi: 10.5194/nhess-20-1069-2020
- Ward PJ, Couasnon A, Eilander D, Haigh ID, Hendry A, Muis S, Veldkamp TIE, Winsemius HC, Wahl T (2018) Dependence between high sea-level and high river discharge increases flood hazard in global deltas and estuaries. *Environ. Res. Lett.* 13(8):84012. doi: 10.1088/1748-9326/aad400

- Ward PJ, Jongman B, Aerts JCJH, Bates PD, Botzen WJW, Diaz Loaiza A, Hallegatte S, Kind JM, Kwadijk J, Scussolini P, Winsemius HC (2017) A global framework for future costs and benefits of river-flood protection in urban areas. *Nature Climate change* 7(9):642–646. doi: 10.1038/NCLIMATE3350
- Ward PJ, Jongman B, Salamon P, Simpson A, Bates P, Groeve T de, Muis S, Perez EC de, Rudari R, Trigg MA, Winsemius HC (2015) Usefulness and limitations of global flood risk models. *Nature Clim. Change* 5(8):712–715
- Ward PJ, Jongman B, Weiland FS, Bouwman A, van Beek R, Bierkens MFP, Ligtvoet W, Winsemius HC (2013) Assessing flood risk at the global scale. Model setup, results, and sensitivity. *Environ. Res. Lett.* 8(4):44019. doi: 10.1088/1748-9326/8/4/044019
- Wessel P, Smith WHF (1996) A global, self-consistent, hierarchical, high-resolution shoreline database. *J. Geophys. Res.* 101(B4):8741–8743. doi: 10.1029/96JB00104
- Wilkinson MD, Dumontier M, Aalbersberg IJ, Appleton G, Axton M, Baak A, Blomberg N, Boiten J-W, da Silva Santos, Luiz Bonino, Bourne PE, Bouwman J, Brookes AJ, Clark T, Crosas M, Dillo I, Dumon O, Edmunds S, Evelo CT, Finkers R, Gonzalez-Beltran A, Gray AJG, Groth P, Goble C, Grethe JS, Heringa J, 't Hoen, Peter A C, Hooft R, Kuhn T, Kok R, Kok J, Lusher SJ, Martone ME, Mons A, Packer AL, Persson B, Rocca-Serra P, Roos M, van Schaik R, Sansone S-A, Schultes E, Sengstag T, Slater T, Strawn G, Swertz MA, Thompson M, van der Lei J, van Mulligen E, Velterop J, Waagmeester A, Wittenburg P, Wolstencroft K, Zhao J, Mons B (2016) The FAIR Guiding Principles for scientific data management and stewardship. *Scientific Data* 3:160018. doi: 10.1038/sdata.2016.18
- Winsemius HC, Aerts JCJH, van Beek, Ludovicus P. H., Bierkens MFP, Bouwman A, Jongman B, Kwadijk J, Ligtvoet W, Lucas PL, van Vuuren DP, Ward PJ (2016) Global drivers of future river flood risk. *Nature Clim Change* 6(4):381–385. doi: 10.1038/NCLIMATE2893
- Wolff C, Nikolettopoulos T, Hinkel J, Vafeidis AT (2020) Future urban development exacerbates coastal exposure in the Mediterranean. *Scientific Reports* 10(1):14420. doi: 10.1038/s41598-020-70928-9
- Wolff C, Vafeidis AT, Lincke D, Marasmi C, Hinkel J (2016) Effects of Scale and Input Data on Assessing the Future Impacts of Coastal Flooding. An Application of DIVA for the Emilia-Romagna Coast. *Front. Mar. Sci.* 3(32):34. doi: 10.3389/fmars.2016.00041
- Wolff C, Vafeidis AT, Muis S, Lincke D, Satta A, Lionello P, Jimenez JA, Conte D, Hinkel J (2018a) A Mediterranean coastal database for assessing the impacts of sea-level rise and associated hazards. *Scientific Data* 5:180044. doi: 10.1038/sdata.2018.44
- Wolff C, Vafeidis AT, Muis S, Lincke D, Satta A, Lionello P, Jimenez JA, Conte D, Hinkel J (2018b) Mediterranean coastal database (MCD). <https://doi.org/10.6084/m9.figshare.c.3145426.v1>
- Wong PP, Losada IJ, Gattuso J-P, Hinkel J, Khattabi A, McInnes KL, Saito Y, Sallenger A (2014) Coastal systems and low-lying areas. In: Intergovernmental Panel on Climate Change (IPCC) (ed) *Climate change 2014. Impacts, adaptation and vulnerability / edited by Christopher B. Field, Working Group II Co-Chair, Department of Global Ecology, Carnegie Institution for Science, Vicente R. Barros, Working Group II Co-Chair, Centro de Investigaciones del Mar y la Atmósfera, Universidad de Buenos Aires [and 14 others]. Cambridge University Press, Cambridge, United Kingdom and New York, NY, USA*
- World Economic Forum (WEF) (2011) Scenarios for the Mediterranean Region. [http://www3.weforum.org/docs/WEF\\_Scenario\\_MediterraneanRegion\\_Report\\_2011.pdf](http://www3.weforum.org/docs/WEF_Scenario_MediterraneanRegion_Report_2011.pdf). Accessed 03 Jul 2017
- Wrathall DJ, Mueller V, Clark PU, Bell A, Oppenheimer M, Hauer M, Kulp S, Gilmore E, Adams H, Kopp R, Abel K, Call M, Chen J, deSherbinin A, Fussell E, Hay C, Jones B, Magliocca N, Marino E, Slangen A, Warner K (2019) Meeting the looming policy challenge of sea-level change and human migration. *Nat. Clim. Chang.* 9(12):898–901. doi: 10.1038/s41558-019-0640-4

- Yamazaki D, Ikeshima D, Tawatari R, Yamaguchi T, O'Loughlin F, Neal JC, Sampson CC, Kanae S, Bates PD (2017) A high-accuracy map of global terrain elevations. *Geophys. Res. Lett.* 44(11):5844–5853. doi: 10.1002/2017GL072874
- Yesudian AN, Dawson RJ (2021) Global analysis of sea level rise risk to airports. *Climate Risk Management* 31(1):100266. doi: 10.1016/j.crm.2020.100266
- Zhou Q, Leng G, Feng L (2017) Predictability of state-level flood damage in the conterminous United States: the role of hazard, exposure and vulnerability. *Scientific Reports* 7(1):5354. doi: 10.1038/s41598-017-05773-4
- Zoraghein H, O'Neill BC (2020a) U.S. State-level Projections of the Spatial Distribution of Population Consistent with Shared Socioeconomic Pathways. *Sustainability* 12(8):3374. doi: 10.3390/su12083374
- Zoraghein H, O'Neill B (2020b) A spatial population downscaling model for integrated human-environment analysis in the United States. *DemRes* 43:1483–1526. doi: 10.4054/DemRes.2020.43.54
- Zscheischler J, Martius O, Westra S, Bevacqua E, Raymond C, Horton RM, van den Hurk B, AghaKouchak A, Jézéquel A, Mahecha MD, Maraun D, Ramos AM, Ridder NN, Thiery W, Vignotto E (2020) A typology of compound weather and climate events. *Nat Rev Earth Environ* 1(7):333–347. doi: 10.1038/s43017-020-0060-z
- Zscheischler J, Westra S, van den Hurk BJJM, Seneviratne SI, Ward PJ, Pitman A, AghaKouchak A, Bresch DN, Leonard M, Wahl T, Zhang X (2018) Future climate risk from compound events. *Nat. Clim. Chang.* 8(6):469–477. doi: 10.1038/s41558-018-0156-3



---

**ERKLÄRUNG**

---

Hiermit erkläre ich, dass ich die vorliegende Dissertation, abgesehen von der Beratung durch meine Betreuer, nach Inhalt und Form selbständig verfasst habe und keine weiteren Quellen und Hilfsmittel als die hier angegebenen verwendet habe. Diese Arbeit hat weder ganz noch in Teilen bereits an anderer Stelle im Rahmen eines Prüfungsverfahrens vorgelegen. Als kumulative Dissertation sind Kapitel 2 bis 4, wie zu Beginn der Kapitel vermerkt, in den genannten Zeitschriften veröffentlicht bzw. im Peer-Review Prozess. Ich erkläre, dass die vorliegende Arbeit unter Einhaltung der Regeln guter wissenschaftlicher Praxis der Deutschen Forschungsgemeinschaft entstanden ist. Weiterhin versichere ich hiermit, dass mir bisher kein akademischer Grad entzogen wurde.

Kiel, 2021